Universidad de Valladolid

Escuela de Doctorado Universidad de Valladolid

PhD PROGRAM IN BIOMEDICAL RESEARCH

DOCTORAL THESIS

Role of insulin-degrading enzyme (IDE) in pancreatic beta-cell function: relevance in health and diabetes mellitus

By Cristina María Fernández Díaz

to apply for PhD degree at the

University of Valladolid

Supervised by:

Irene Cózar Castellano, PhD

Germán Perdomo Hernández, PhD

This work was conducted within the Institute of Biology and Molecular Genetic (IBGM) in cooperation with University of Valladolid (UVa). It has been possible thanks to the following funding:

- Grant I+D+I “Retos Investigación” - Call 2014 - (SAF2014-58702-C2-1-R & SAF2014-58702-C2-2-R).

- Grant I+D+I “Retos Investigación” - Call 2016 - (SAF2016-77871-C2-1-R & SAF2016-77871-C2-2-R).

- Contrato predoctoral de la Universidad de Valladolid (Convocatoria 2016).

- European Molecular Biology Organization (EMBO) Short-Term Fellowships (2018).

- Becas de movilidad ERASMUS+ Prácticas de la Universidad de Valladolid (Convocatoria 2018/2019).

INDEX

INDEX

ABBREVIATIONS

1. ABBREVIATIONS

%	Percentage
1,10-Ph	1,10-fenantrolina
a.m.	After meridian
ADP	Adenosine diphosphate
ANOVA	Analysis of variance
Aß	Amyloid ß-protein
ATP	Adenosine triphosphate
AU	Arbitrary units
AUC	Area under the curve
cDNA	Complementary deoxyribonucleic acid
DAPI	4', 6-diamidino-2-fenilindol
DNA	Deoxyribonucleic Acid
DNA	Deoxyribonucleic acid
DPP-4	Dipeptidyl peptidase-4
DTT	Dithiothreitol
ELISA	Enzyme-linked immunosorbent assay
g	Gravitational forces
GAPDH	Glyceraldehyde-3-phosphatedehydrogenase
GCK	Glucokinase
GK	Goto-Kakizaki diabetic rats
GLP-1	Glucagon-like peptide-1
GLUT1	Glucose transporter 1
GLUT2	Glucose transporter 2
GLUT4	Glucose transporter 4
GSIS	Glucose-stimulated insulin secretion
IDE	Insulin-degrading enzyme
IEq	Islet equivalents

IF	Immunofluorescence
Ins-Cre	Insulin-Cre
INSR	Insulin receptor
IP-GTT	Intraperitoneal glucose tolerance test
IP-ITT	Intraperitoneal insulin tolerance test
K_{ATP}	ATP-sensitive potassium channel
Km	Michaelis–Menten constant
KO	Knock-out
L-IDE-KO	Liver-IDE knock-out
LSB	Laemmli sample buffer
mRNA	Messenger ribonucleic acid
ºC	Centigrade
OHAs	Oral hypoglycemic agents
PCR	Polymerase chain reaction
RNA	Ribonucleic acid
RT-qPCR	Real-time reverse transcription-quantitative polymerase chain reaction
SDS	Sodium dodecyl sulfate
SEM	Standard error of the mean
SGLT-2	Sodium-glucose cotransporter type 2 inhibitors
shRNA	Short hairpin RNA
T1DM	Type 1 diabetes mellitus
T2DM	Type 2 diabetes Mellitus
TBE	Tris-borate-EDTA
TCA	Tricarboxylic acid cycle
TMB	3, 3', 5, 5'- tetramethylbenzidine
VLDL	Very low density lipoprotein
WAT	White adipose tissue
WHO	World health organization
WT	Wild type

SUMMARY

2. SUMMARY

Insulin-degrading enzyme (IDE) is a zinc metalloprotease proposed as the main responsible for degrading insulin, in addition to degrading other peptides such as glucagon, amylin, and amyloid peptide. The association of genetic polymorphisms within the *Ide* locus and susceptibility to suffer type 2 diabetes (T2DM) is well known, but its therapeutic potential remains unclear. Some investigations have spurred the notion that transient and/or partial inhibition of IDE may help to develop a new pharmacological treatment for T2DM. However, there is a paucity of data in the literature regarding IDE role in insulin producing cells (pancreatic beta-cells) and its potential relationship with pathophysiological conditions, such as T2DM.

The aim of the present study is to understand the physiological role of IDE in pancreatic beta-cells. For this purpose, we have performed a wide variety of *in vivo* and *in vitro* studies. To determine IDE protein expression in physiological and pathophysiological conditions in pancreatic islets, we have performed histological studies and protein analysis techniques in T2DM patient's pancreas and in several T2DM preclinical models. To elucidate the role of IDE in pancreatic beta-cells, we have performed IDE activity inhibition both *in vitro*, by using of pharmacological inhibitors and shRNA silencing; and *in vivo*, by generating a mouse colony with specific *Ide* ablation in pancreatic beta-cells: B-IDE-KO mouse line. In these models, we have analyzed beta-cell function, as well as the metabolic impact of IDE ablation on pancreatic beta-cells in the B-IDE-KO mouse.

Our studies show that IDE is expressed in beta- and alpha-cells of the pancreatic islet, both in humans and rodents, with increased expression in alpha- than in beta-cells. Additionally, in pathophysiological conditions that are accompanied by hyperinsulinemia, IDE is increased in pancreatic beta-cells, pointing out that IDE is involved in adaptive cellular mechanisms of beta-cells to the hyperinsulinemic environment.

Regarding the role of IDE in pancreatic beta-cells, we observe that both acute and chronic inhibition of IDE in mature beta-cells leads to impaired glucose-stimulated insulin secretion, revealing that IDE plays a key role in beta-cell function. Surprisingly, genetic ablation of *Ide* in beta-cells in embryonic life leads to constitutive insulin secretion and beta-cell immaturity, suggesting a new role of IDE in beta-cell development.

In light of our results, we can conclude that IDE has an important role on beta-cell function, thus, IDE inhibition is not a good therapeutic approach for the T2DM treatment.

INTRODUCTION

3. INTRODUCTION

3.1 GLUCOSE HOMEOSTASIS: A HIGHLY SOPHISTICATED NETWORK

Glucose is the principal source of energy in all organisms, necessary to ensure the proper functioning of cellular metabolism. In vertebrates and other higher organisms, tighly regulated control of blood glucose levels (glycemia), is essential to maintain glucose homeostasis. Glycemic control is a highly sophisticated process that involves numerous organs and hormones working in concert. Among these, the pancreas plays a key role due to the secretion of two primary hormones: insulin and glucagon. These two pancreatic hormones collaborate to maintain blood glucose levels within a very narrow range (4-6 mM) [1].

Blood glucose levels are regulated by the opposing actions of these hormones as illustrated schematically in **Figure 1**.

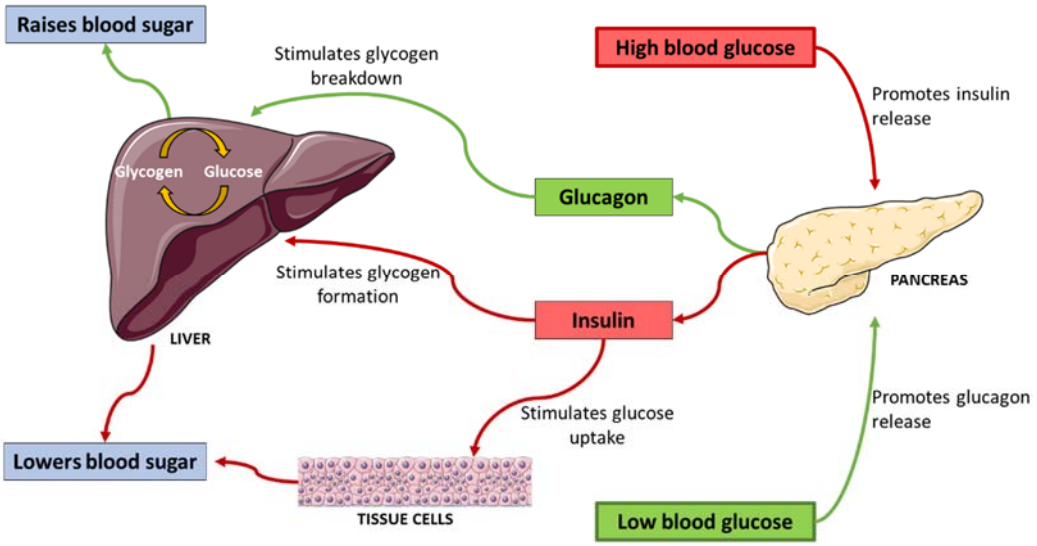

Figure 1: Maintenance of glucose homeostasis by insulin and glucagon.

Under fasting conditions, for example during the nighttime fasting period or between meals, plasma glucose levels decrease. In response, pancreatic alpha-cells to secrete glucagon, a hyperglycemic hormone which stimulates hepatic glycogenolysis and gluconeogenesis [2], thus restoring blood glucose levels. In addition, during prolonged fasting, glucagon promotes renal gluconeogenesis in order to raises blood glucose [3].

In contrast, after a rise in blood glucose levels, as happens after meals, elevated glucose promotes insulin secretion by pancreatic beta-cells. This hormone promotes insulin-dependent glucose uptake by various tissues, mainly skeletal muscle, liver and white adipose tissue, thus removing exogenous glucose from the blood stream and restoring normoglycemia [4-6]. Moreover, insulin promotes anabolic processes, such as glycogenesis [7, 8], lipogenesis [9], and the incorporation of amino acids into proteins [10].

As is obvious, the continuous supply of glucose to the organism is indispensable. In this regard, the opposing action of these two hormones, insulin and glucagon, form the central core of glucose metabolism regulation. However, disturbances of this metabolic framework may lead to serious metabolic disorders such as diabetes mellitus, whose prevalence, comorbidities and medical costs have been dangerously increasing over the past few decades [11].

3.2 DIABETES MELLITUS: THE EPIDEMIC OF OUR TIME

According to World Health Organization, diabetes is defined as a chronic disease that occurs either when the pancreas does not produce enough insulin or when the body cannot effectively use the insulin that produces [12].

More than 20 years ago, in 1997, it was projected that in 2010 there would be 221 million people with diabetes in the world [13]. Those expectations have been vastly exceeded: in 2017 more than 425 million people in the world had diabetes mellitus [14]. (**Figure 2**).

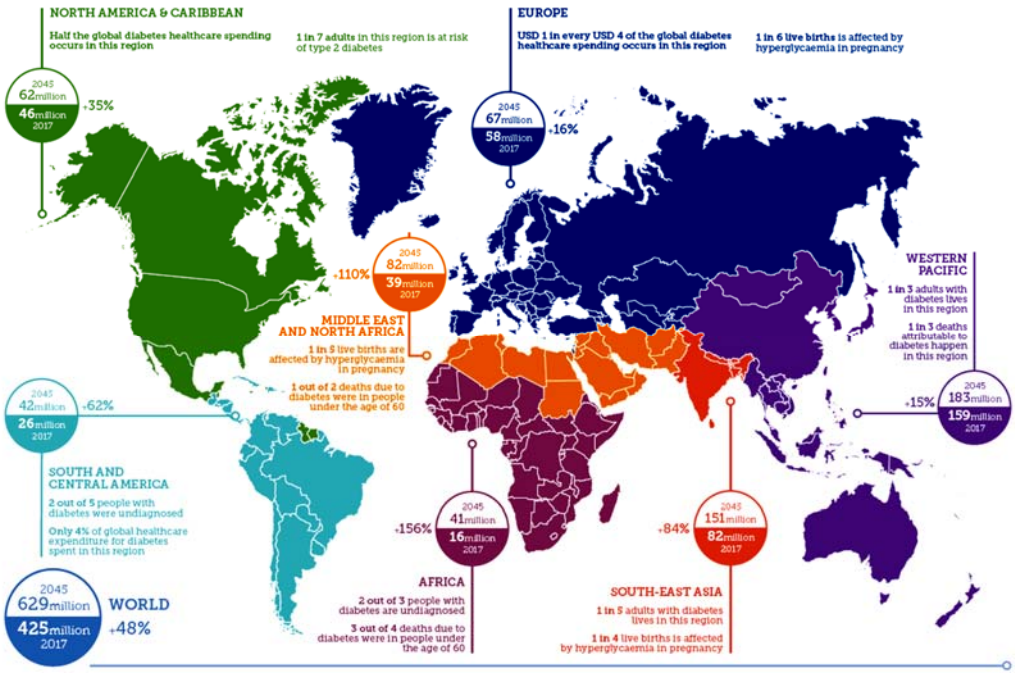

Figure 2: Prevalence and worldwide distribution of diabetes in 2017 and estimated prevalence for the year 2045 [14].

The number of people in the world with diabetes has quadrupled since 1980, with an alarming increase in this last century [15] as depicted in **Figure 3**. In Spain, there were 3,584,500 cases of diabetes in 2017, approximately 10% of adult Spanish population [14].

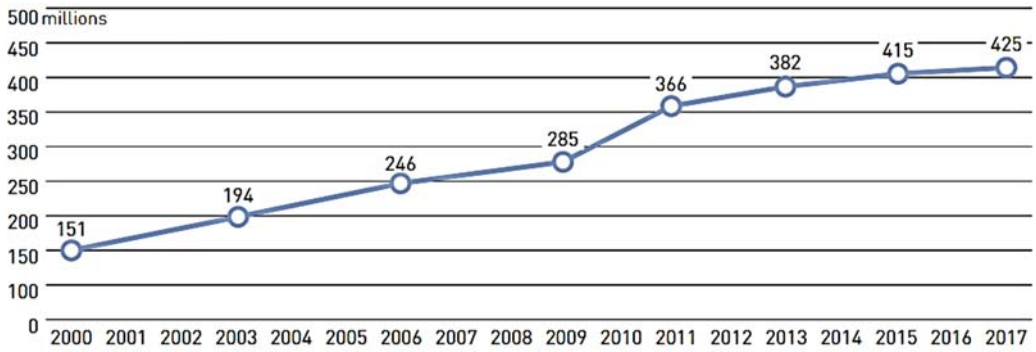

Figure 3: Worldwide total number of adults with diabetes (20-79 years) in XXI century [14].

In addition to this, it should be taken into account that approximately 30% of the population has prediabetes: glucose levels above the normal range and below the diagnostic threshold of diabetes [16]. People with prediabetes have a high risk of developing type 2 diabetes in the next 3 to 5 years [14].

This dramatic rise in prevalence reflects an increase in incidence of many risk factors associated with this disease, especially overweight and obesity [17], a reflection of unhealthy diets and the sedentary lifestyle of today's society.

Diabetes can result in several serious consequences, including blindness, kidney failure, increased risk of heart attacks and stroke, as well as lower limb amputation [18]. In 2016, 1.6 million deaths in the world were directly caused by diabetes mellitus, making the disease one of the top 10 causes of death in the world. Moreover, impaired fasting glucose caused an additional 2.2 million deaths

[19]. Premature death and comorbidities due to diabetes represent a large economic burden to countries health systems, something often called the indirect cost of diabetes [20]. In 2017, the International Foundation of Diabetes estimated that the total healthcare expenditure on diabetes reached 637 billion euros [14].

These alarming data reveal the urgent need to mitigate risk factors, improve diagnosis and treatments, as well as promote high-quality research to increase understanding of the disease, focusing efforts on the goal of improving the quality of life of patients with diabetes mellitus.

3.2.1 TYPES OF DIABETES AND THERAPEUTIC APPROACH

There are two main types of diabetes: Type 1 and Type 2.

Type 1 diabetes mellitus (T1DM) is an autoimmune disease that causes specific destruction of insulin-producing cells: the pancreatic beta-cells. This destruction leads to low or no insulin secretion into the bloodstream, with the consequent increase in blood glucose levels [21, 22] (**Figure 4**).

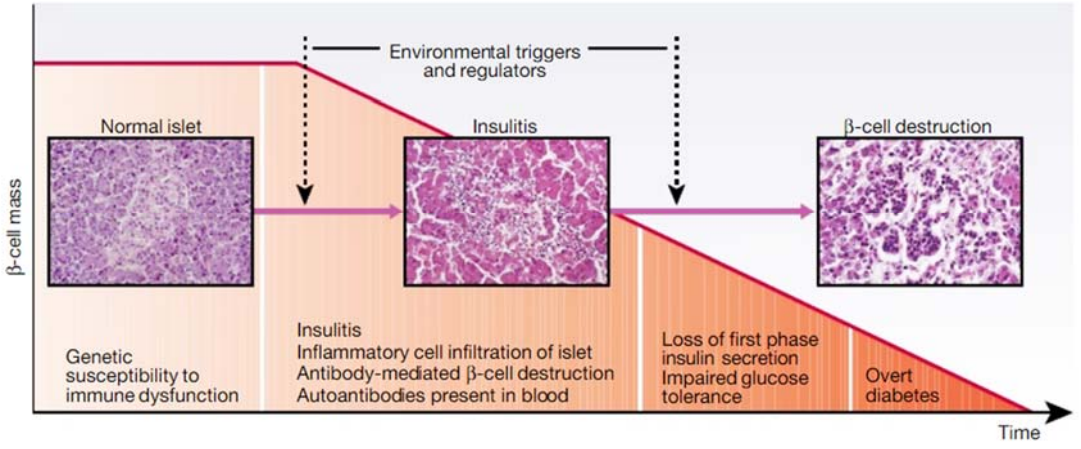

Figure 4: Pathogenesis of type 1 diabetes. Sequence of events in the development of type 1 diabetes [23].

This type of diabetes represents 5-10% of the total cases of the disease [24]. The onset of type 1 diabetes is influenced by a combination of hereditary and environmental factors, but the main cause of this destructive process is still unknown and thus currently not preventable [25, 26]. Patients with type 1 diabetes need daily exogenous insulin administration to maintain stable glucose levels and to avoid deleterious consequences associated with elevated blood sugar.

Type 2 diabetes mellitus (T2DM) is characterized by an insufficient response of insulin by the peripheral tissues of the body (insulin resistance). There is feedback between insulin-sensitive tissues and beta-cells: insulin resistance leads to increased insulin requirements, leading to an exaggerated response by the beta-cells [27]. Increased demand for insulin secretion and beta-cell hyperfunction in turn results in a decreased functional beta-cell mass causing impaired insulin secretion and hyperglycemia [28] (**Figure 5**).

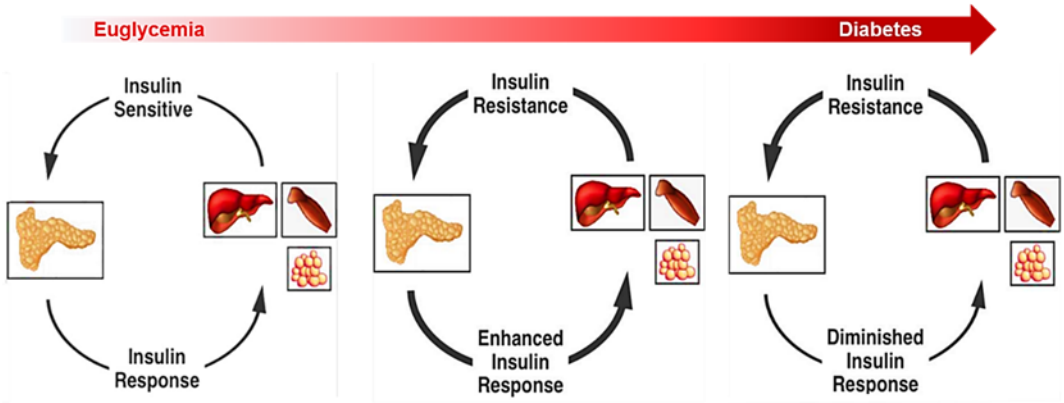

Figure 5: Pathogenesis of type 2 diabetes. Proposed sequence of events in the development of type 2 diabetes [27].

This decrease in functional beta-cell mass has a complex and multifactorial nature. Among multiple factors, it has been described that glucotoxicity [29, 30] and lipotoxicity [31], which cause increased oxidative stress [32, 33], as well as increased proinflammatory cytokines [34, 35], amyloid deposits [36, 37], together

with the stress of endoplasmic reticulum caused by beta-cell exhaustion [38, 39], leads to beta-cell dysfunction and death.

T2DM is the most common type of diabetes, representing around 90-95% of the total cases of diabetes. Regarding the pathogenesis, there is a strong link between T2DM and obesity and physical inactivity. There are also other risk factors, such as increasing age, sedentary lifestyle and multiple genetic factors [40].

The first recommended therapeutic intervention for T2DM patients is the change of lifestyle: adoption of a healthy diet, increased physical activity and maintenance of a healthy body weight. If these changes in lifestyle are not enough to manage glucose levels, oral hypoglycemic medication is usually initiated. Metformin is indisputably the most commonly used oral antidiabetic agent worldwide [41]. The hypoglycemic effects of metformin are mainly due to decreased hepatic gluconeogenesis [42], and to a lesser extent, to delayed intestinal nutrient absorption [43]. It also induces insulin-mediated glucose uptake in the skeletal muscle [44]. If this drug fails, another therapeutic approach is the combination of different drugs, such as sulphonylureas, glucagon-like peptide 1 (GLP-1) receptor agonists, dipeptidyl peptidase 4 (DPP-4) inhibitors, thiazolidinediones or sodium-glucose cotransporter 2 (SGLT2) inhibitors [45]. When oral hypoglycemic agents (OHAs) are unable to maintain normoglycemia, exogenous insulin administration must be prescribed in order to make a good management of blood glucose and to avoid health complications [14, 40].

There are also some less common types of diabetes:

- Gestational Diabetes: Any degree of glucose intolerance that was first recognized during pregnancy, regardless of whether the condition may have predated the pregnancy or persisted after the pregnancy [46].

- Latent Autoimmune Diabetes of Adults (LADA): Also called slowly progressive insulin-dependent diabetes, is a form of type 1 diabetes that develops later into adulthood characterized by patients with clinical type 2 diabetes that have immunogenic characteristics of type 1 diabetes [47].

- Maturity-Onset Diabetes of the Young (MODY): Also known as monogenic diabetes, is inherited disease resulting from a single genetic mutation in an autosomal dominant gene. At least 13 genes involved in MODY are identified to date, but the most commonly reported forms are involving glucokinase gene (MODY2) and the transcription factors HNF1A (MODY3) and HNF4A (MODY1) [47, 48].

- Neonatal diabetes: Monogenic diabetes occurring under 6 months of age that could be transient (most often due to overexpression of genes on chromosome 6q24) or permanent (most commonly due to autosomal dominant mutations in the genes encoding the Kir6.2 subunit (KCNJ11) and SUR1 subunit (ABCC8) of the β-cell K_{ATP} channel) [48, 49].

- Secondary diabetes: Diabetes arose as a complication of other diseases such as hormone disturbances, diseases of the pancreas or as a result of drugs [14].

Clearly, the pancreas plays a pivotal role in the regulation of glucose homeostasis, and therefore is one of the main organs involved in the pathogenesis of diabetes mellitus.

3.3 ENDOCRINE PANCREAS: MORPHOLOGY AND PHYSIOLOGY

In humans, the pancreas is an organ that lies in the upper abdomen behind the stomach. It is considered a mixed gland: it has endocrine and exocrine function. The exocrine pancreas is composed of acinar and ductal cells whose function is to synthesize and release digestive enzymes (pancreatic lipase and amylase, phospholipase, nucleases…) and bicarbonate from ductal cells into the duodenum [50]. It represents 96–99% of total pancreas volume [51] (**Figure 6**).

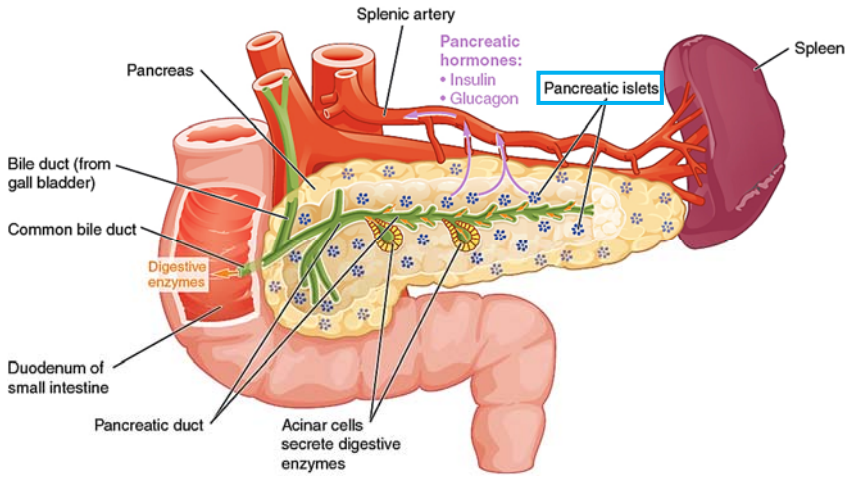

Figure 6: Overview of human pancreas localization and anatomy. The image is adapted from [52].

On the other hand, the endocrine pancreas has metabolic functions, secreting into the bloodstream different types of hormones responsible for nutrient metabolism and the maintenance of blood glucose homeostasis in the body. The functional units of the endocrine pancreas are the pancreatic islets, also called islets of Langerhans, which are embedded within the exocrine pancreas.

3.3.1 ISLETS OF LANGERHANS

In 1869, Paul Langerhans, through his exhaustive histological studies, discovered that the pancreas was a heterogeneous organ composed of different structures. Some of them were small clusters of cells scattered throughout the organ with a well-defined structure, now called islets of Langerhans. They represent only 1-4 % of total pancreas volume [51, 53].

Pancreatic islets are highly vascularized multicellular mini-organs composed of 5 different cell types, each one responsible for the release of a specific hormone. The coordinated action of all of them guarantees a correct maintenance of glucose homeostasis:

- *Beta-cells (β)*: Insulin-secreting cells. Insulin is a hypoglycemic hormone, responsible for lowering blood glucose levels mediating glucose uptake into cells [54]. They comprise 50-70% of the islet cells in humans and up to 80% in rodents.

- *Alpha-cells (α):* Glucagon-secreting cells. Glucagon is a hyperglycemic hormone, preventing low blood glucose in fasting periods promoting hepatic gluconeogenesis [54, 55]. They are the second largest cell population of the islet, around 40% in humans and 20% in rodents.

- *Delta-cells (δ):* Somatostatin-secreting cells. Somatostatin is a hormone that indirectly modulates glucose homeostasis, negatively regulating in a paracrine way insulin, glucagon and pancreatic polypeptide secretion [56, 57]. They represent 3-10% of the total number of cells of the islets.

- *PP-cells*: Pancreatic polypeptide-secreting cells. Its main functions are the regulation of satiety, in addition to inhibiting the secretion of glucagon by alpha-cells [58, 59]. They comprise around 3-5% of the islet.

- *Epsilon-cells (ε):* Ghrelin-secreting cells. Ghrelin has orexigenic properties, as well as ability of manage insulin, glucagon, pancreatic polypeptide and somatostatin release [60]. They are around 1% of the total islets cells.

As shown in **Figure 7**, there is a remarkable difference between the architecture of the human and mouse pancreatic islets. In rodents α, δ, PP and ε cells are found in the periphery and the beta-cell makes up the central body of the islet.

In contrast, in humans the different cell types seem to be randomly distributed in the islet [51, 61, 62]. This different distribution has implications at the paracrine regulation and functional level. Mouse beta-cells will be surrounded mostly by other beta-cells meanwhile human beta-cells will be surrounded by other non-beta-cells.

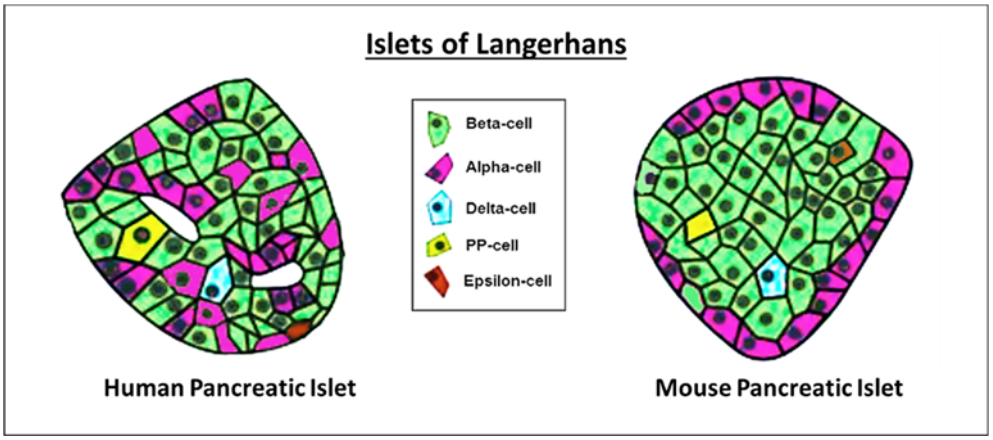

Figure 7: Architecture of human and mouse pancreatic islet. The image is adapted from [51].

Islets are exposed to the systemic glucose concentration, since the pancreas receives a rich vascular supply originating from the splenic artery. Although, as mentioned before, the islets only represent 1-4% of the total pancreas, they receive up to 20% of the pancreatic blood supply [63]. This high vascularization explains how small fluctuations in blood glucose lead to rapid and large changes in the secretion of pancreatic regulatory hormones.

3.4 PANCREATIC BETA-CELL AND INSULIN HOMEOSTASIS

Pancreatic beta-cells are the most important cell type in the pathogenesis of diabetes mellitus. Its destruction leads to type 1 diabetes, and its dysfunction is part of the process of development of type 2 diabetes.

Pancreatic beta-cells act as a glucose sensor: its main function is the secretion of insulin in response to high glucose in order to maintain optimal blood glucose levels in the body. Insulin synthesis, secretion and clearance are highly regulated processes, whose abnormalities are closely related to the pathogenesis of diabetes mellitus.

3.4.1 BETA-CELL DEVELOPMENT AND IDENTITY

Pancreas originates from the endodermal gut tube epithelium [64]. Subsequently, during pancreas development, a subset of epithelial cells starts to express the pro-endocrine progenitor factor *Ngn3*, giving rise to all types of pancreatic endocrine cells [65-67].

Then, activation of different patterns of transcription factors leads to the differentiation into distinct endocrine pancreas lineages. Insulin expressing beta-cells are the first endocrine cells to appear at 7.5–8 weeks of gestation in the human pancreas [68] (**Figure 8**).

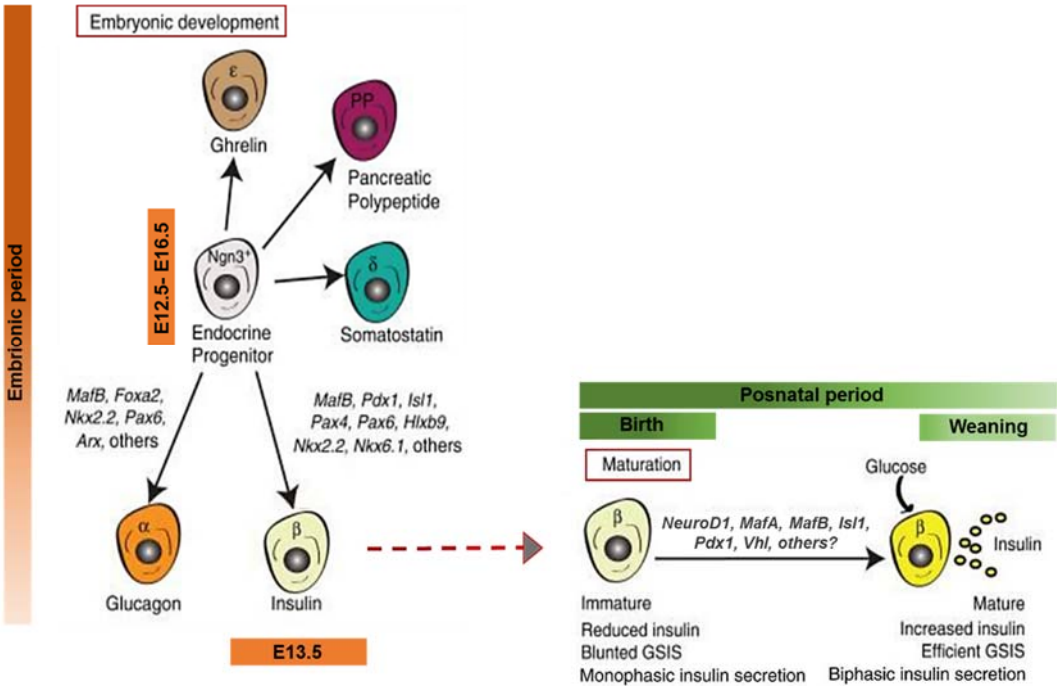

Figure 8: Embryonic development of pancreatic endocrine cells and beta-cell maturation. The image is adapted from [69].

After this differentiation process, the beta-cell must undergo a maturation process carried out by transcriptional regulators, which allows it to acquire physiological characteristics commonly known as beta-cell identity. Some of these factors include the expression of genes such as *Nkx2-2*, *Nkx6-1*, *Mafa*, *Mafb*, *Pax6*, *Pdx1*, *Neurod1*, *Urocortin3* and *Syt4* [70-72].

Recent studies suggest that genetic deletion of key beta-cell genes, may induce aberrant patterns of these transcription factors, affecting its differentiation state, leading the beta-cell to lose its insulin secretory properties and therefore, its identity [73].

The most critical aspect of beta-cell identity is glucose-stimulated insulin secretion (GSIS) and the mechanism through which beta-cells control glucose metabolism [74, 75]. Insulin secretion is a tightly regulated mechanism, where all the many components of cellular machinery of the beta-cell secretory pathway, including intracellular mechanisms and transcription factors must be highly orchestrated. Some of these components, such as the glucose transporter 2 (GLUT2), glucokinase and ATP-sensitive potassium channels (K_{ATP}) are key defining contributors to the establishment and maintenance of beta-cell identity.

Disturbances in these critical components inevitably lead to beta-cell dysfunction [74, 76]. Loss of mature beta-cell identity is a common feature found in different forms of diabetes, from monogenic to type 2 diabetes [77]. An immature beta-cell is characterized, among others, by impaired GSIS accompanied by high basal insulin secretion at low glucose levels [71, 72, 78, 79], secretion of immature insulin granules with increased proinsulin content [79] and abnormal pattern of GLUT2 in the plasma membrane [72, 79-81]. Loss of maturation in beta-cell is due to both, downregulation of genes required for GSIS and upregulation of genes permitting activation of glycolytic flux at lower extracellular glucose thresholds (Hk1, Hk2, Ldha, AldoB...). These are glucose-secretion decoupling genes or beta cell disallowed genes [82, 83].

3.4.2 INSULIN BIOSYNTHESIS

Glucose is the principal physiological regulator of insulin in beta-cells, generating intracellular signals that stimulate insulin secretion, insulin mRNA translation, and insulin transcription [84]. Humans have a single insulin gene, *Ins*. However, rodents have two, *Ins1* and *Ins2*. Transcription of *Ins* is largely regulated by key transcription factors including *Pdx*1, *Pax6*, *Mafa*, and *Neurod1* along with numerous coregulators [85].

These several factors also contribute to the regulation of insulin transcription in response to glucose and autocrine insulin signaling [76], but it is simplistic to assume that these are the only transcription factors contributing to this process, since our knowledge is currently incomplete [85]. The use of tissue-specific knockouts animal models will help to identify and analyze the function of candidate genes that may contribute in this process.

In 1923, and after numerous findings by previous researchers, F. Banting and J.J.R. Macleod were awarded with the Nobel Prize for insulin discovery [86, 87]. Insulin is translated initially as preproinsulin, then transported into the secretory pathway via signal peptide, which is removed after entry into the lumen of the endoplasmic reticulum, resulting in proinsulin [88] (**Figure 9**). Subsequent to proinsulin maturation and stabilization, proinsulin is transported from the endoplasmic reticulum to the Golgi apparatus, where it is efficiently sorted into secretory immature vesicles [89]. Only 1–2% of the protein is remaining as proinsulin and will be secreted within mature secretory granules [90, 91].

Proinsulin is processed via the prohormone convertases 1/3 (PC1/3) and 2 (PC2), which cleave the C-peptide connections to A- and B-chain. Thereby, mature insulin and detached C-peptide are stored together in the same secretion granule until the beta-cell receives stimuli triggering exocytosis [90, 92].

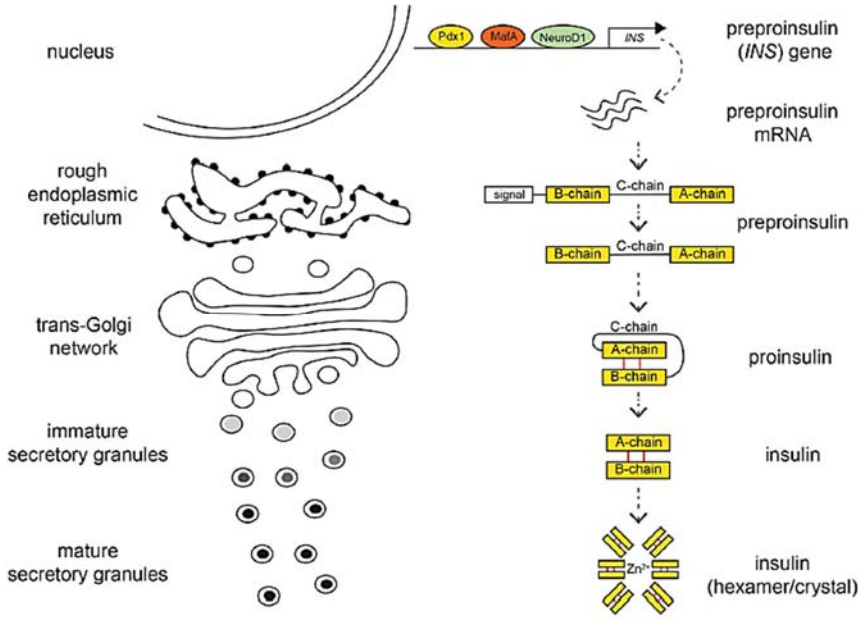

Figure 9: **Insulin biosynthesis**. Insulin maturation along the granule secretory pathway. The image is adapted from [90].

C-peptide is secreted at a 1:1 molar ratio to insulin, thus representing a direct measure of endogenous insulin [93]. Mature insulin is then stored as hexameric insulin/Zn^{2+} crystals in the secretory granules and is released by regulated exocytosis.

3.4.3 INSULIN SECRETION: STIMULUS-DEPENDENT EXOCYTOSIS

Pancreatic beta-cells secrete insulin in response to elevated blood glucose levels. This kind of molecular process, wherein a stimulus is translated into hormone release, is called stimulus-secretion coupling. In particular, this process in beta-cells is known as glucose-stimulated insulin secretion (GSIS) [94].

Pancreatic beta-cells act as a glucose sensor due to presence of glucose transporters in their plasma membranes. In the case of human beta-cells, the main glucose transporter is the glucose transporter 1 (GLUT1), while in mice it is GLUT2. In rodent alpha-cells, GLUT1 is the main transporter [95, 96]. Both transporters located on the cell surface of the beta-cells have very different Km values: GLUT1 is operative at glucose concentrations between 1-3 mM glucose and GLUT2 is operative between 15 and 20 mM [97]. These differences in glucose transporters between rodents and humans are due to the lower threshold for glucose stimulated insulin secretion in human beta-cells compared to rodents, so GLUT1 properties are more compatible with the dose-response curve for GSIS in humans (Km 6.5 mM) [95, 98]. Therefore, mutations in these transporters can lead to pronounced dysregulation of pancreatic endocrine cells function.

In presence of increased glucose levels, glucose enters into the beta-cells through the glucose transporters, GLUT2 in rodents and GLUT1 in humans [95], where it is rapidly phosphorylated to glucose-6-phosphate by glucokinase (GCK) and incorporated into the glycolytic pathway generating downstream metabolites, such as pyruvate. Pyruvate is catabolized at the mitochondrial level in the tricarboxylic acid cycle (TCA), producing an increase in ATP levels and thus a rise in the ATP:ADP ratio within the cell.

This increased ATP:ADP ratio in turn leads to the closure of ATP-sensitive potassium channels (K_{ATP}) [99]. K_{ATP} channels in beta-cell are formed by two subunits: Sur1 and Kir6.2. The closure of these channels causes potassium ions (K^+) accumulation inside the cell, making the inside of the cell less negative than the outside. This difference leads to a depolarization of the plasma membrane (**Figure 10)**.

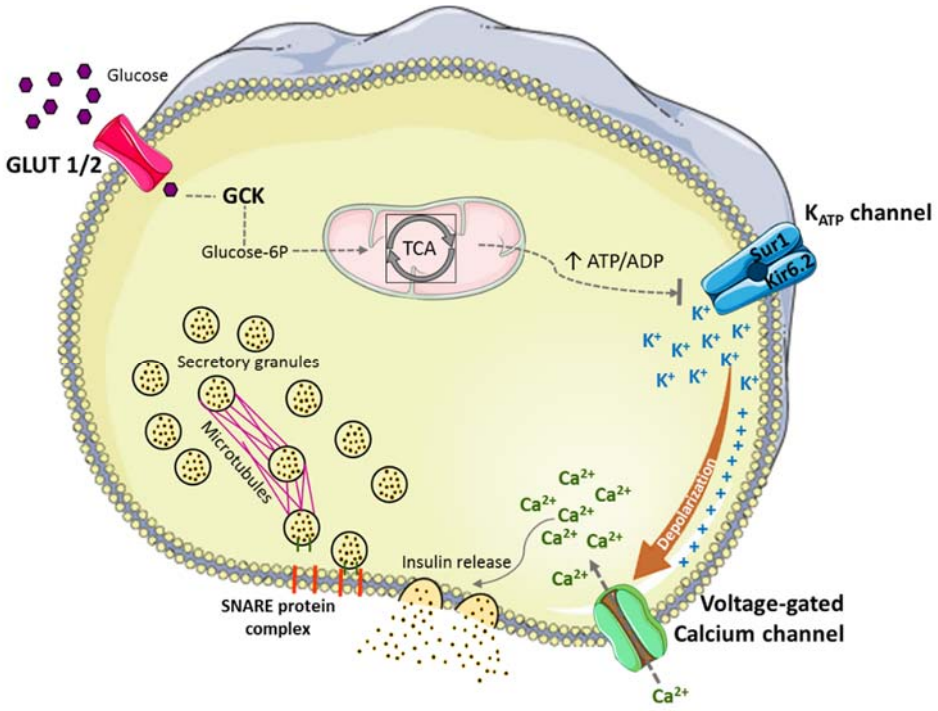

Figure 10: Mechanism of glucose-stimulated insulin secretion in pancreatic beta-cell.

When the membrane potential depolarizes sufficiently (approximately −50 mV), it causes oscillating electrical activity that leads to the opening of voltage-gated L-type calcium channels [100], allowing calcium entry into the cell by facilitated diffusion. The increase of intracellular calcium then triggers the exocytosis of insulin granules [92, 101]. Each pancreatic beta-cell contains more than 10,000 secretory granules of insulin, but only a small fraction is secreted: ~2% per hour at maximal glucose concentrations [102, 103].

Secretory granules are stored within the beta-cell cytoplasm at some distance away from the cell membrane [102]. To reach the plasma membrane, these granules must travel a relatively long distance along the cell cytoskeleton from the site of granule synthesis in the trans-Golgi network to the cell periphery [104]. The

beta-cell cytoskeleton is composed of a microtubule network that occupies most of the cell with the exception of the region next to the plasma membrane, which is occupied by the cortical actin network [105, 106]. These cytoskeleton microtubules, polymers of α/β tubulin dimers, play an essential role in insulin granule positioning [107-110].

In beta-cells, microtubules originate at the Golgi and form a dense non-radial meshwork [111]. Transport along these microtubules limits granule dwelling at the cell periphery, restricting granule availability for secretion. High glucose causes depolymerization of these microtubules, decreasing their density and thus allowing the movement of secretory granules to the cell periphery to promote insulin release [111, 112] (**Figure 11**).

Once at the periphery, granules are retained within the actin-rich cell cortex adjacent to the plasma membrane. Actin reorganization is then necessary to allow insulin granules access to the plasma membrane for subsequent docking and fusion [104, 106, 113].

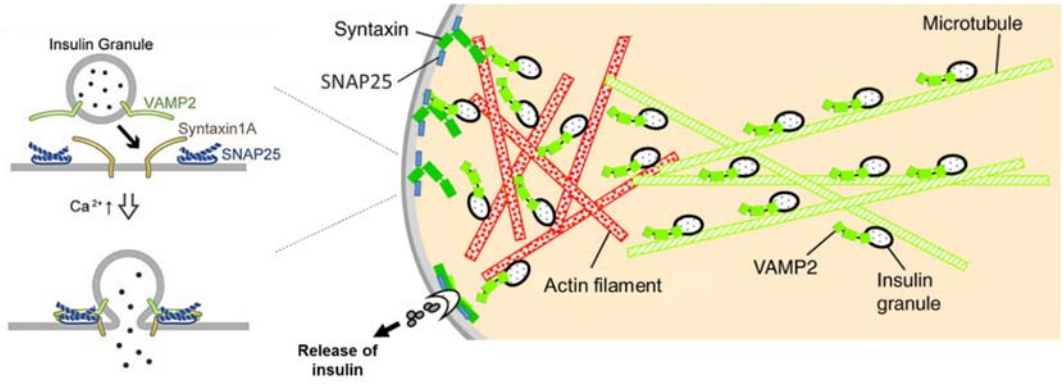

Figure 11: Insulin granule mobilization during GSIS and the formation of SNARE proteins complex. The image is adapted from [110, 114].

This membrane fusion process is mediated by SNARE (soluble N-ethylmaleimide-sensitive factor attachment protein receptor) proteins [115, 116]. SNAREs are divided into two groups: a vesicle-attached membrane protein (VAMP2), and two plasma membrane proteins, syntaxin-1A and the 25-kDa synaptosomal-associated protein (SNAP-25) [115, 117]. The fusion of insulin granules with the plasma membrane requires the assembly of a complex between the granule membrane VAMP2 and the integral plasma membrane syntaxin-1A, as well as membrane-associated SNAP-25, thus creating the SNARE-complex [118].

Actin acts as a barrier to block SNARE-complex formation. Glucose stimulation triggers transient actin reorganization, thereby allowing the granules access to the plasma membrane for subsequent interactions between VAMP2/syntaxin-1A/SNAP-25 proteins [110]. This specific interaction docks the secretory granules at the correct membrane site, with subsequent membrane fusion and insulin release (**Figure 11**).

Insulin from beta-cells is secreted following a characteristic biphasic pattern [119-121]: a rapid but transient first phase during which the readily releasable pool (RRP) of granules previously docked to the plasma membrane undergo exocytosis [102]. This first phase is followed by a slowly developing and sustained second phase during which secretion continues at a lower rate since newcomer granules must first approach the plasma membrane before being able to fuse and exocytose, resulting in a lower rate at which new granules can be supplied for release [102, 122]. (**Figure 12**).

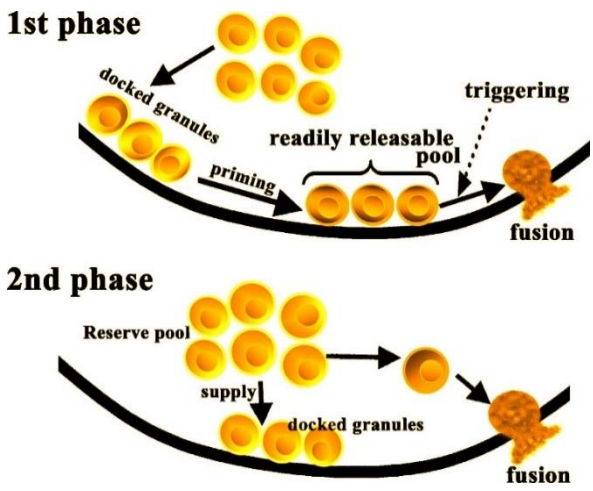

Figure 12: Model of biphasic insulin exocytosis mechanism in pancreatic beta-cells. The image is adapted from [122].

Once insulin leaves the beta-cell and reaches the bloodstream is ready to exert its actions on insulin-sensitive tissues.

3.4.4 INSULIN ACTION

Insulin action in glucose homeostasis is usually typified by its direct effects on three principal tissues: skeletal muscle, liver, and white adipocytes [123]. Insulin binds to the insulin receptor (INSR) on the plasma membrane of target cells [124]. The best studied functional effect of insulin signaling cascade is the increased glucose transport activity. Activated INSR initiates a downstream metabolic signaling, which finally stimulates the translocation of the glucose transporter 4 (GLUT4) storage vesicles from intracellular pools to the surface cell membrane, thus increasing the rate of glucose uptake [125, 126].

- *Skeletal muscle*

Muscle insulin action is a tightly coordinated process whereby insulin promotes glucose utilization and storage by increasing glucose uptake and regulating the rate of glycogen synthesis and glycolysis [127, 128]. Regarding to protein metabolism, insulin increases the rate of protein synthesis and decreases the rate of protein degradation [127, 129].

- *Liver*

In liver, insulin rapidly and potently reduces hepatic glucose production [130]. It activates glycogen synthesis [131, 132], and decreases gluconeogenic gene expression, thus inhibiting the rate of hepatic glycogenolysis and gluconeogenesis [133, 134]. Regarding lipids, insulin promotes lipid esterification [135], transcriptionally regulates de novo lipogenesis [136], decreases the rate of fatty acid oxidation [127] and increases very-low-density lipoprotein (VLDL) formation [136].

- *Adipocytes*

In white adipocyte tissue (WAT), insulin increases the rate of glucose transport across the cell membrane [137]. One of the most important roles of insulin in WAT is lipolysis suppression in order to maintain euglycemia [127, 128]. Insulin is a potent antilipolytic hormone capable to decrease rapidly plasma non-esterified fatty acid [138, 139]. It also increases the uptake of free fatty acids from blood and it promotes triglyceride esterification and storage [135, 139].

As observed, these insulin effects encourage the synthesis of carbohydrates, lipids and proteins; therefore, insulin is considered to be an anabolic hormone. A summary of its actions in the main target tissues is shown in **Figure 13**.

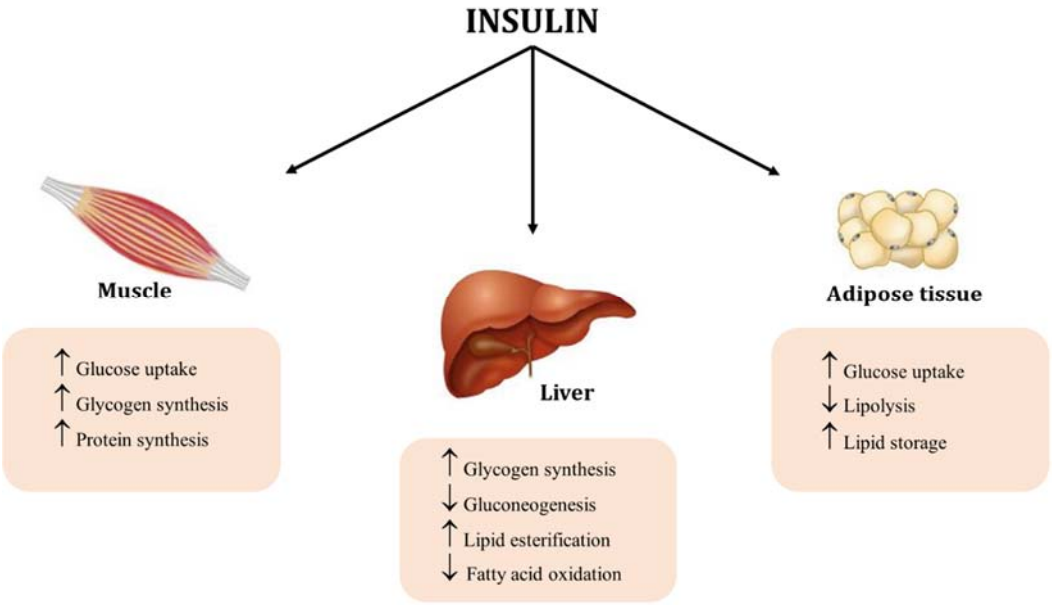

Figure 13: Insulin actions in main insulin-sensitive tissues.

3.4.5 INSULIN CLEARANCE

Insulin from pancreas is secreted directly into the portal circulation [140, 141], reaching the liver, where the "first pass" of insulin clearance occurs. In this step, between 50-80% of the insulin released by the pancreas is degraded, so that only about a third of the total secreted reaches the bloodstream [142, 143]. In contrast, C-peptide is not degraded by liver, so it goes directly to the systemic circulation [144, 145]. This is the reason why C-peptide is used as a biomarker of beta-cell function instead of insulin circulating levels.

The liver is thus responsible for regulating the flow of insulin to the systemic circulation, thereby acting as a gatekeeper regulating this process [143]. In pathological situations, the liver can modulate the clearance ratio to attempt to maintain adequate plasma insulin levels [146, 147]. After this first pass, remaining

insulin exits the liver via the hepatic vein, reaching the heart (**Figure 14**). Insulin is then distributed to the rest of the body through the systemic circulation.

After circulation, insulin returns to the liver via the hepatic artery, and the hormone is subject to a second round of insulin clearance ("second pass") within hepatocytes. In addition to the liver, remaining circulating insulin is finally degraded by the kidney and other tissues to a limited extent [148, 149].

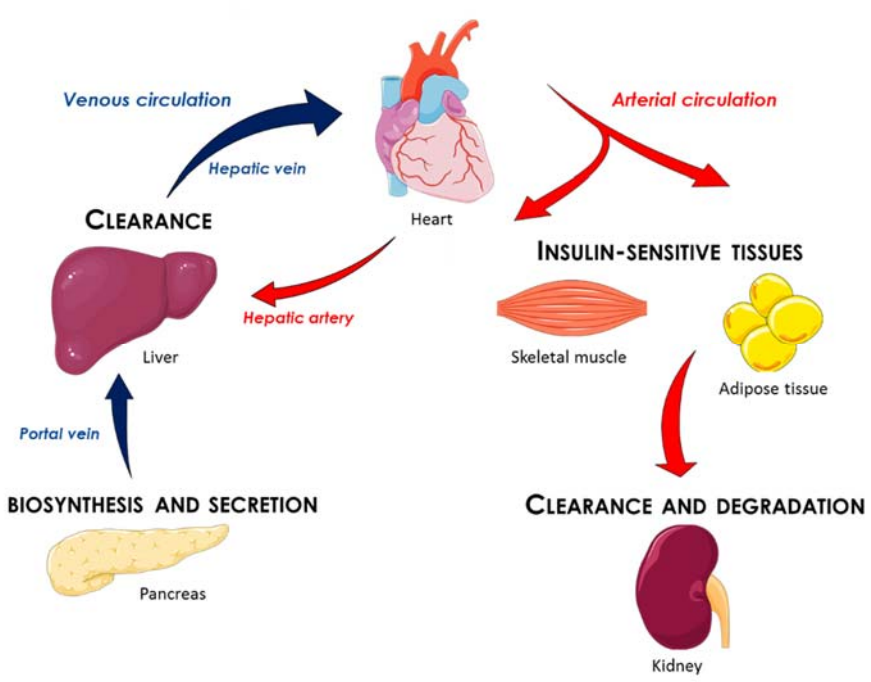

Figure 14: Journey of insulin from synthesis to degradation in the body.

Independent evidence, beginning in 1949 [150], showed that insulin is rapidly degraded by a protease called IDE (insulin-degrading enzyme). By virtue of its unusually rigid structure, being comprised of two separate chains attached by disulfide bonds at multiple locations, insulin is not readily degraded by most proteases. Given that IDE degrades insulin so efficiently, it was widely assumed

that insulin clearance *in vivo* must involve IDE at some level, most likely at the level of the liver [151, 152]. However, this idea was not directly tested until recently. A recent study in liver-specific IDE knockout mice showed that IDE is not the rate-limiting factor controlling insulin clearance by the liver, since deleting it in liver caused no difference in the rate of exogenous insulin clearance [153]. This study highlights how critical it is to study the tissue-specific role of this protein, as it is an ubiquitous and multifunctional enzyme.

3.5 INSULIN-DEGRADING ENZYME

IDE (insulin-degrading enzyme) is an evolutionarily conserved 110-kDa zinc-metalloendopeptidase (**Figure 15**). IDE derived its name based on its ability to strongly bind and degrade insulin, the property for which it was initially discovered more than 70 years ago [150].

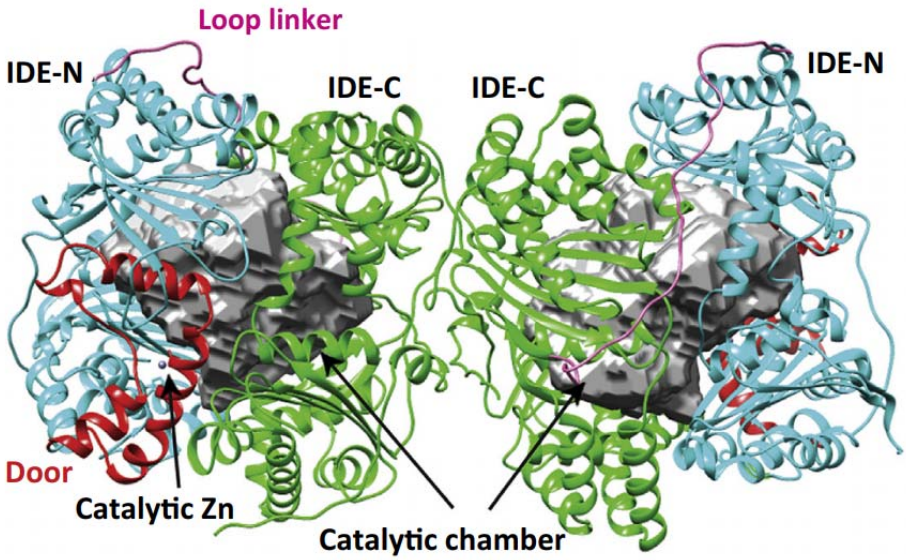

Figure 15: IDE structure: IDE-N (cyan) and IDE-C (green) terminal units of IDE form two halves of a catalytic chamber (grey), including the catalytic zinc ion and the door subdomain (red) [154].

IDE is a homodimeric protein, with each monomer being composed of two ~55 kDa homologous N- and C-terminal bowl-shaped domains (IDE-N and IDE-C) that are connected by a short linker to form the final 110 kDa protein [155]. Overall each monomer of IDE resembles a clamshell that can adopt "open" and "closed" conformation, with IDE-N and IDE-C forming each of the two halves. When in the closed conformation, the two halves form a large internal chamber that completely encapsulates and entraps insulin and other substrates. In the open conformation, substrates can enter into the catalytic chamber, and proteolyzed fragments can exit. The active site of IDE is bipartite, comprised of regions within both IDE-N (which contains the active-site Zn atom) and IDE-C that is fully formed only when the protease is in the closed position [156]. As a consequence, IDE can only process substrates that are small enough and appropriately shaped to fit inside its internal chamber. These features prohibit IDE from engulfing peptides greater than ~80 amino acids in length [154, 155].

New electron microscopy data suggests IDE passes also through open-closed transition during its catalytic cycle allowing the unfolding of its substrates prior to the cleavage reaction. Therefore, IDE could be found with five different conformations: completely closed with substrate bound, partially closed with substrate bound, partially open with substrate unbound, and open without substrate [157, 158].

3.5.1 IDE LOCATION, SUBSTRATES AND FUNCTIONS

IDE has a high affinity for insulin (Km = 10-100 nM), but processes it relatively slowly compared to most proteases (Kcat = 0.5-2/s^{-1}) by virtue of its complicated catalytic cycle involving the opening and closing of the protease [159]. Nevertheless, as mentioned, insulin is an unusually rigid peptide that is highly resistant to proteolytic degradation by most other proteases, making IDE the most

efficient known insulin protease. In addition to insulin, another intermediate-sized peptide substrate of IDE is glucagon [155, 160]. In 1985, glucagon was reported to be degraded with an apparent Km of 3.46 μM and Kcat 0.641 s^{-1} by a semi-purified protease that has been inferred to be IDE [161]. Recently, these data have been questioned with the use of new quantitative glucagon degradation assays, pointing to Km values between 380-800 nM and Kcat values between 1.16 and 1.76 s^{-1} [162]. IDE also degrades other small peptides such as somatostatin, amylin and peptide amyloid (Aβ) [149, 155] turning it into a protein of interest in the study of diseases such as diabetes mellitus and Alzheimer's disease [163]. Other substrates of IDE include various hormones, growth factors, and neuropeptides, including growth factors and endorphins [164, 165]. Some authors claim that IDE also has regulatory functions for proteasome activity, for steroid receptors, for the oxidation of fatty acids in peroxisomes, or for non-proteolytic processes mediating in growth and development [166-172].

Regarding its location, IDE has a ubiquitous tissue and cell type distribution. Within cells, it is located principally within the cytoplasm, but it has been reported to localize in various subcellular compartments, including intracellular vesicles, plasma membrane, mitochondria, peroxisomes, as well as being secreted by a non-classical protein export pathway [154, 164, 173, 174]. This wide distribution suggests a multifunctional role of this protein. Despite decades of study, there remains a lack of knowledge about its presence and role in the cells responsible for insulin production: pancreatic beta-cells.

3.5.2 IDE AND DIABETES MELLITUS

Several single nucleotide polymorphisms in noncoding regions of the human IDE gene on chromosome 10q are associated with the development of type 2 diabetes mellitus [175-177]. Furthermore, non-sense and frameshift mutations have been found in the IDE gene in patients with T2DM [178]. In Goto-Kakizaki (GK) rats, a preclinical model of type 2 diabetes, an partial loss-of-function mutation in the *Ide* gene was found to be at least partially responsible for the diabetic phenotype in this rodent model [179]. These data elucidate the importance of the role of IDE in the pathogenesis of diabetes, and its possible therapeutic potential.

The literature contains many conflicting reports on IDE´s roles in different tissues of diabetic patients, apparently due to diverse criteria for inclusion of patients in studies, and variability in the type of diabetes and the stage in which the disease is developed [163]. For instance, in human erythrocytes, IDE activity was increased in T2DM patients taking sulphonylureas, but it was unmodified in type 1 diabetic patients under good glycemic control [180]. In a different study, an increase of IDE activity in plasma and erythrocytes was demonstrated both in insulin-dependent and in non-insulin-dependent diabetic patients [181].

On the other hand, decreased IDE activity in adipocytes of pre-diabetic and diabetic subjects was demonstrated [182]. Regarding pancreatic tissue, Steneberg et al showed for the first time in human islets that IDE levels were decreased (by ~40%) in human T2DM islets compared with nondiabetic controls, but without providing information about the pharmacological therapy of such patients [183]. Likewise, other authors found a decrease of *Ide* mRNA expression in the liver of diabetic subjects [184].

Interestingly, insulin treatment causes an increase of IDE activity in HepG2 cells, abolished in highly glucose conditions, suggesting that insulin and glucose levels may provoke disturbances of IDE activity in T2DM [185].

These controversial data corroborate the idea that IDE may be a multifunctional enzyme, with several tissue-specific functions, highlighting the need to decipher the specific role that IDE plays in each tissue. In addition, they reflect the importance that pharmacological treatments may modulate IDE activity.

3.5.3 IDE INHIBITORS AND THEIR THERAPEUTIC POTENTIAL

The assumed role of IDE in insulin clearance led to the idea that transient IDE inhibition could be used to modulate insulin levels in patients suffering T2DM. More than six decades ago, it was reported that an endogenous inhibitor of IDE could enhance the hypoglycemic action of insulin in rats and rabbits, highlighting the potential use of IDE inhibitors to modulate the action of insulin [186]. Attempts to further confirm or refute IDE's role in insulin degradation have been attempted using several very crude inhibitors of IDE *in vitro*, including bacitracin, N-ethylmaleimide, and 1,10-phenanthraline [149, 187]. However, these inhibitors are all non-specific and of very low potency, so the relevance of these studies is difficult to assess.

Taking advance of IDE tertiary structure, new IDE inhibitors with better potency, improved selectivity, and structurally defined binding sites have been developed [155, 165, 188-191]. Only a very limited number of *in vivo* studies have so far been conducted using these newer inhibitors with some conflicting results [165, 190, 191], due to differences in the IDE binding site (**Figure 16**), pharmacokinetics and pharmacodynamics of the compounds, differences in selectivity for different

substrates, as well as preclinical models have been used to study the pharmacological action of these inhibitors.

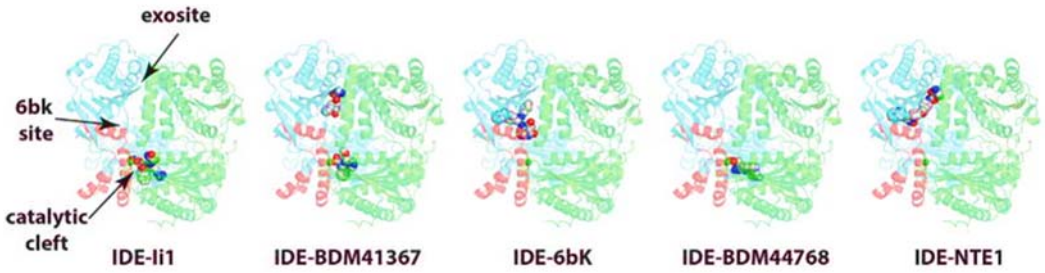

Figure 16: Co-crystal structures comparing the binding sites of different IDE inhibitors [154].

IDE inhibitor 1 (Ii1), was the first reported high-affinity inhibitor for IDE. It is a peptide hydroxamate designed by determining the subsite specificity of IDE, and it interacts with the active-site Zn atom in IDE-N, as well as with the active-site portion of IDE-C [188]. Ii1 was reported to effectively reduce the clearance of insulin in CHO-IR cultured cells.

Another recently developed IDE inhibitor is BDM41367, which binds to both the catalytic site of IDE and to an “exosite” region distal to the active site that has an innate affinity to peptides [155]. This compound was found to be a partially active, substrate-selective modulator of IDE that inhibits Aβ degradation but promotes insulin degradation when tested in human recombinant IDE [189].

BDM44768 is proposed to inhibit IDE in part by locking IDE in the closed conformation, thus preventing substrates from accessing the catalytic chamber. This compound prevents insulin degradation *in vitro*, but when tested in preclinical mouse models of diabetes, BDM44768 induced glucose intolerance [190].

6bK is a promising IDE inhibitor that binds a unique exosite outside both the catalytic cleft and N-terminal exosite [165]. 6bK was reported to improve oral glucose tolerance in high fat diet-induced obese mice and enhanced insulin-induced hypoglycemia. Interestingly, the administration of 6bK induces glucose intolerance when glucose is injected intraperitoneally, probably to the elevated glucagon levels consequence of IDE inhibition.

Few years ago, a research team at Eli Lilly reported the characterization of two novel IDE inhibitors, NTE-1 and NTE-2 [191]. These compounds binds to the N-terminal substrate anchoring site and the 6bK-binding exosite. Consistent with 6bK, NTE-1 improved oral glucose tolerance in diet-induced obese mice, but without effects on insulin-induced hypoglycemia. Interestingly, treated animals show normal levels of glucagon. Moreover, in insulin-tolerance tests and euglycemic clamping experiments, NTE-1 exerted no detectible effect on insulin action or plasma insulin levels.

Together, these studies highlighted the controversy surrounding the potential therapeutic utility of IDE inhibitors, as well as the importance of identifying substrate-selective IDE inhibitors, so that effects on insulin, glucagon and amylin, among other substrates, can be separated. In the same way, it strengthens the need to search for IDE inhibitors specifically targeted to a cell type in order to obtain the desired therapeutic results. However, currently IDE´s tissue-specific role remains poorly defined. Hopefully, progress in knowledge of IDE´s role in specific tissues will promote the development of IDE-based therapies to treat T2DM.

3.5.4 GENETIC ABLATION OF *Ide*: A COMPLEX STUDY MODEL

Many authors have proposed IDE inhibition as a therapeutic treatment for T2DM. This reasoning is based on the assumption that IDE inhibition will lead to reduced insulin clearance, allowing a given amount of insulin released by the

pancreas to be more effective by increasing time in the bloodstream. Given that glucose homeostasis is dependent on a complex interplay between many hormones, such as insulin, amylin, and glucagon, the effects of an IDE defect *in vivo* are expected to be complex.

In order to elucidate the physiological function of IDE and the pathogenesis of T2DM, numerous authors have described the metabolic phenotype that causes total IDE ablation in rodents [183, 192, 193]. All of them show a common phenotype: *Ide* ablation creates disturbances in the management of insulin, which causes associated deleterious comorbidities.

Farris and colleagues were the first group to describe the phenotype resulting from global genetic deletion of IDE. At 6 months of age, IDE knockout mice, presented a metabolic phenotype characterized by normal baseline glucose levels, but pronounced glucose and insulin intolerance, together with hyperinsulinemia [192]**.** These authors proposed that hyperinsulinemia is a consequence of a deficiency in the capacity for insulin clearance.

In 2011, Abdul-Hay and colleagues reported on a longitudinal study of IDE knockout mice, conducted at 2, 4 and 6 months of age to investigate the emergence of the metabolic phenotype. Consistent with the phenotype described by Farris et al., these mice showed hyperinsulinemia at 2, 4 and 6 months of age. Surprisingly, at 2 months of age, the mice showed a modest but significant improvement in glucose tolerance and insulin sensitivity. However, at 6 months of age, these mice showed severe glucose intolerance and insulin resistance [193].

In 2013, Steneberg et al. studied the phenotype of IDE knockout mice at 2 months of age. They described a metabolic phenotype consisting of severe glucose intolerance, accompanied by a decrease in insulin secretion [183]. These results are in contrast to those previously observed by other authors. In addition,

Steneberg et al. highlight the importance of IDE in the regulation of insulin secretion, since they observed an increase in intracellular insulin of pancreatic islets, pointing to a secretory defect in beta-cells. Mechanistically, they attributed the observed effects to the fact that IDE can associate irreversibly with alpha-synuclein protein, preventing the correct reorganization of the cellular microtubules, and therefore, the correct secretion of insulin.

Since all animal models used so far are global IDE knockout mouse, it is very difficult to separate the mechanistic components that underlie the observed phenotypes. In addition, it should be noted that none of the global IDE knockout studies, except for Steneberg et al., have focused on islet insulin secretion. Moreover, it must be taken into account that in these models, IDE is knocked out in all cells of the pancreatic islet, so the paracrine action of the rest of cell types with pancreatic beta-cells could directly compromise the function of this cell type.

Recently, Villa-Perez et al. reported the first tissue-specific IDE knockout mouse. They generated mice with liver-specific ablation of IDE (L-IDE-KO) using Cre-loxP system. In this technique, desired DNA segments are flanked by two loxP DNA motifs (often referred to as "floxed" loci) and Cre-mediated recombination results in excision of floxed DNA. The cell specificity of recombination is controlled by promoter and enhancer sequences that drive Cre expression in the cell or tissue type of interest, thus ablating the floxed genetic locus in the entire lineage [194]. In L-IDE-KO loxP sites are positioned flanking IDE gene and Cre recombinase expression is driven exclusively in liver using the albumin promoter [153]. L-IDE-KO mice exhibited glucose intolerance and insulin resistance due to decreased insulin receptor levels in hepatocytes. However, these mice showed similar plasma insulin levels and hepatic insulin clearance as control mice, revealing that IDE is not the principal or rate-limiting hormone involved in hepatic insulin clearance, but that it plays a fundamental role in the etiology of hepatic insulin resistance.

In conclusion, these animal models of study highlight the importance of IDE in the regulation of glucose metabolism, and its impact on the etiology of hyperinsulinemia and insulin resistance. However, it is impossible to decipher from them the role played by IDE in insulin-producing cells. Thus, IDE needs to be studied in beta-cell models to unravel the specific role of IDE in pancreatic beta-cell function.

HYPOTHESES AND AIMS

4. HYPOTHESES AND AIMS

4.1 HYPOTHESES

Based on previous publications and our group´s preliminary results we hypothesize that:

- IDE is expressed in pancreatic beta- and alpha-cells of humans and rodents.
- Diabetes-related conditions can lead to changes in IDE expression levels in pancreatic beta- and alpha-cells.
- IDE plays a key role in the function of the pancreatic beta-cells, and its loss-of-function affects glucose-stimulated insulin secretion.
- The modulation of IDE activity in pancreatic beta-cells could be a therapeutic approach in the treatment of type 2 diabetes mellitus.

4.2 AIMS

The main aim of this study is to understand the physiological role of IDE on the pancreatic beta-cell *in vitro* and *in vivo*. This general aim can be split in the following specific objectives:

- To study IDE expression pattern in beta- and alpha-cells of the pancreatic islets.
- To investigate IDE expression regulation in different diabetes-related models, both in humans and rodents.
- To assess the effect of transient pharmacological IDE inhibition in pancreatic beta-cells *in vitro*.
- To generate and analyze the phenotype of an *in vitro* model of *Ide* permanent ablation: INS1-E shRNA-IDE cells.
- To generate and characterize a beta-cell specific *Ide* knockout mouse model (B-IDE-KO).

MATERIAL AND METHODS

5. MATERIAL AND METHODS

5.1 EXPERIMENTAL ANIMALS

5.1.1 ANIMAL FACILITIES

Experimental procedures were approved by University of Valladolid Research Animal Ethical Committee and JCyL authorities (Protocol number #5003931) in accordance with the European Guidelines for Care and Use of Mammals in Research (European Commission Directive 86/609/CEE and Spanish Royal Decree 1201/2005).

Rodents were housed in ventilated cages on a 14-hours light, 10-hours dark schedule at the animal facility of the University of Valladolid (UVa, Spain). Cage enrichment included cotton bedding. Water and food (standard rodent chow diet) were available ad libitum.

5.1.2 RODENT MODELS

- ***db/db* MICE**

Leptin receptor heterozygous mice BKS.Cg-+Leprdb/+ Lepr +/OlaHsd (db/+) were purchased (Harlan, UK) and then they were bred in our animal facility to obtain +/+ or db/db mice.

- **SD/HFD MICE**

8 week old C57Bl6/J male mice were bought (Charles River, France) and they were fed standard (SD) or high fat diet (HFD: 60% kcal% fat) (Research Diets, USA) for 18 weeks.

– **SPRAGUE DAWLEY RATS**

Three-month-old male Sprague Dawley rats were provided by Animal Research and Welfare Service (SIBA) of the University of Valladolid; they were fed SD and water ad libitum.

5.1.3 B-IDE-KO MICE

5.1.3.1 BREADING STRATEGIES OF BETA-CELL SPECIFIC IDE KNOCKOUT MICE

Cre – LoxP recombination system was used for generating our tissue specific knockout. *Ide*$^{flox/flox}$ mice were kindly provided by Dr. Malcom Leissring [193] from University of California, Irvine, USA. These mice have *loxP* sites flanking *exon 3* of *Ide* gene. *Exon 3* contains the catalytic site sequence, critical for the proteolytic activity of the enzyme. *Insulin-Cre* mice kindly provided by Dr. Herrera [195] from University of Geneva, Switzerland. This transgene expresses *Cre* recombinase under the control of the insulin promoter, which is active in pancreatic beta-cells.

To generate beta-cell specific IDE knockout mice, *Insulin-Cre* mice were crossed with *Ide*$^{flox/flox}$ mice. Cre-LoxP recombination results in the deletion of *exon 3* of the IDE gene, causing a frameshift with two stop codons in *exon 4* and therefore, an early termination of translation. Thus, we obtained our experimental litter *Ide*$^{flox/flox;}$*Ins-Cre/*+, named hereafter B-IDE-KO, and their controls *Ide*$^{flox/flox;}$ +/+ or *Ide*$^{flox/+;}$ +/+. (**Figure 17**).

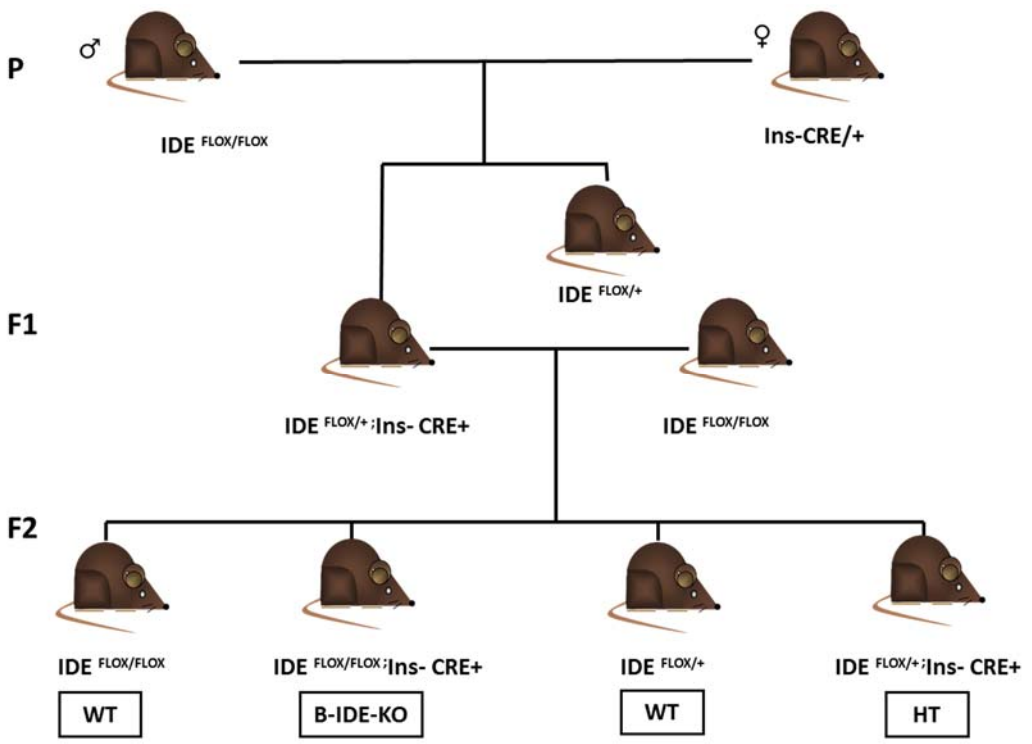

Figure 17. Breading strategy for generating B-IDE-KO mice colony.

5.1.3.2 MOUSE GENOTYPING

To genotype B-IDE-KO mice colony, PCRs were performed with genomic DNA extracted from mice tail snips of ~0.2 cm using QuickExtract™ DNA Extraction Solution (Epicentre, EEUU). Tails were incubated in 50 µL of QuickExtract™ solution at 65ºC for 8 min, followed by 2 min incubation at 98 ºC in a thermoblock. The PCR reaction master mix components are listed in **Table 1**.

Component	Volume (µl)
Buffer Reaction Mix (Bioline, UK) 5x	8
Primer Forward (Metabion, Germany) 100 µM	0,20
Primer Reverse (Metabion, Germany) 100 µM	0,20
My Taq DNA Polymerase (Bioline, UK) 5 u/µl	0,25
Nuclease Free Water	30,35
DNA Sample	1
Final Volume	40

Table 1. PCR reaction master mix components per reaction.

Genes analyzed by PCR were: *GAPDH*, used as control for the quality of DNA extraction, *Ide*$^{flox/flox}$ and *Ins-Cre*. Primer sequences and the sizes of resulted amplicons were detailed in **Table 2**.

Gen	Sequence	pb
GAPDH	*5'-GATG GCAT GGA CTG TGG TCA T-3'* *5'-CGT GGA GTC TAC TGG TGT CTT-3'*	250
IDE$^{flox/flox}$	*5'-AAC TGC CAC CTG TCC AAT CC-3'* *5'-CTC AGG GAT ACA ATG CGT GC-3'*	WT IDE: 480 IDE$^{flox/flox}$: 650
Ins-Cre	*5'-TAA GGC TAA GTA GAG GTG T-3'* *5'-TCC ATG GTG ATA CAA GGG AC-3'*	473

Table 2. Primer sequences used for mice genotyping.

PCR products were mixed with loading buffer for DNA (Bioline, UK), loaded into 2% agarose gel and electrophoresed in TBE buffer (89 mM Tris-HCl, pH 7.6, 89 mM boric acid and 2 mM EDTA). The gel was stained with RedSafe (Invitrogen, USA) and the bands were visualized by an ultraviolet transilluminator showing the three kind of genotypes obtained in our mouse colony **(Figure 18)**.

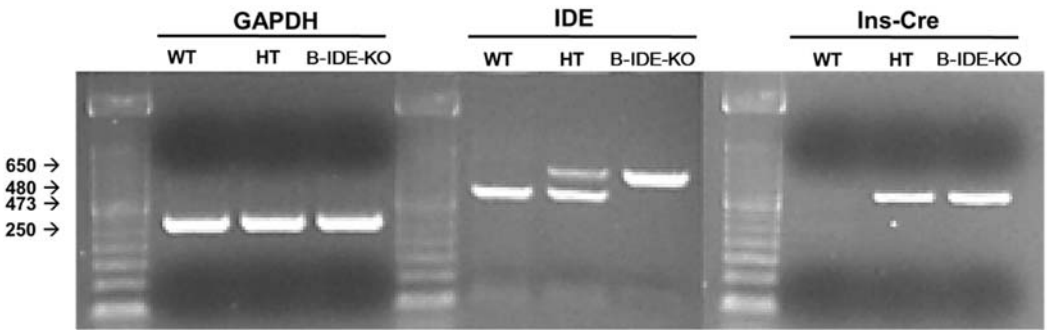

Figure 18. Representative image of PCRs results for mice genotyping. WT (wild type); HT (heterozygous); B-IDE-KO (beta-cell specific IDE-knockout mouse)

5.1.3.3 METABOLIC CHARACTERIZATION

Male mice were metabolically studied at 2 months and 6 months of age.

- **BODY WEIGHT**

Body weight was monitored at 2 and 6 months old using a digital weight scale (Adam Equipment, USA).

- **BLOOD GLUCOSE**

Blood glucose levels were measured directly from cut tails tips using the Breeze2 Glucometer (Bayer, Germany). Blood glucose measurements were performed in mice under fasting (6 or 16 hours without food) or non-fasting conditions (after dark schedule), after a glucose overload (IP-GTT) and after an insulin tolerance test (IP-ITT).

– **BLOOD SAMPLING AND PLASMA COLLECTION**

Plasma samples were obtained by direct blood flow from tail tip collecting the blood with Microvette®, a capillary tube coated with potassium-EDTA (Stardest, Germany). Then, blood samples were centrifuged at 1,200 X *g* for 10 min at 4ºC to obtain plasma fraction.

Plasma measurements were performed in mice under fasting (6 hours without food) or non-fasting conditions (after dark schedule) or after a glucose challenge. Plasma C-peptide levels were measured using Mouse Ultrasensitive C-peptide ELISA (ALPCO, USA). Plasma insulin levels were measured using Mouse Ultrasensitive Insulin ELISA (Mercodia AB, Sweden).

– **INTRA-PERITONEAL GLUCOSE TOLERANCE TEST (IP-GTT)**

For the assessment of glucose tolerance, we performed intra-peritoneal glucose tolerance test (IP-GTT). Mice were fasted for 6 hours from 8 a.m. to 2 p.m. 2 g/kg Glucose body weight was injected into the intraperitoneal cavity. Blood glucose levels were measured at different time points: 0, 15, 30, 60 and 120 min after glucose injection.

– **INTRA-PERITONEAL INSULIN TOLERANCE TEST (IP-ITT)**

For the evaluation of insulin sensitivity tolerance, we performed intra-peritoneal insulin tolerance test (IP-ITT). Mice in non-fasting conditions were injected with a dose of 0.75 U Humulin (Lilly, USA)/kg body weight. Blood glucose levels were measured at different time points: 0, 5, 15 and 30 min after glucose injection.

5.2 HUMAN PANCREAS AND PANCREATIC ISLETS

5.2.1 HUMAN PANCREAS

Human pancreas samples were obtained from the biobank of the San Carlos Clinical Hospital in Madrid (protocol authorized by the Ethics Committee for Clinical Research #12/202 and accordingly to the Declaration of Helsinki). Human pancreas samples were obtained from cadaveric donors using ultrasound imaging to collect tissue samples with minimum impact on the deceased body. Human pancreata were classified into three groups: non-diabetic population (control), T2DM patients treated with oral hypoglycemic agents (T2DM+OHAs) and T2DM patients undergoing insulin treatment (T2DM+Insulin). Cases were categorized by sex and age. Controls without T2DM diagnosis were matched by age and sex. Control, n=9; T2DM+OHAs, n=9; T2DM+insulin, n=8.

Pancreas were fixed with 4% formaldehyde for 48-72 hours and then they were embedded into paraffin blocks. 5 µm sections were cut with a microtome. Tissue samples were selected using the following inclusion criteria:

- Patients aged between 40 and 80 years.
- Control pancreas in which morphologically normal islets are observed, with adequate suitable structure and without evidence of deteriorated tissue when observed after hematoxylin-eosine staining.
- Samples must have a minimum number of pancreatic islets by microscopic examination (n ≥ 5 per slide).

A description of each subject included in the study is shown in **Table 12** in results section.

5.2.2 HUMAN ISLETS

Human islets were obtained and isolated by Dr. Olle Körsgren lab at the University of Uppsala (Sweeden) through the JDRF award 31-2008-416 (ECIT Islet for Basic Research program). Human islets were shipped to our laboratory and after their arrival, islets were cultured in petri dishes in RPMI 1640 medium supplemented with 2 mM L-glutamine, 5.5 mM D-glucose, 10% FBS, 100 U/ml penicillin, and 100 µg/ml streptomycin. The islets were maintained at 37 °C with 5% CO_2 in a humidified atmosphere. Detailed information about human islet donors are shown in **Table 3**.

ID	Sex	Age	BMI	HbA1c	Cause of death	Cold ischaemia time (h)	Isolation centre
H2210	F	55	24	5.6	Unknown	05:37	Uppsala University
H2235	M	70	23.4	5.8	Intracerebral hemorrhage	07:21	Uppsala University

Table 3. Demographic data of human islet donors included in the study.

5.3 RODENT PANCREATIC ISLET ISOLATION AND CULTURE

Islet isolation is a process through which pancreas is digested using collagenase and islets are separated out of exocrine tissue. Isolation method depends on the technique that islets are going to be used for:

- Ficoll (Histopaque®) gradient technique allows to recover most of digested islets but the cells will be more stressed out. This method is mainly used for obtaining enough islets for western-blot and RT-qPCR.

- Handpicking method requires picking up islets one by one using pipets after collagenase digestion. Only part of the islets are recovered, but this technique is useful to have islets with optimal function, as for glucose-stimulated insulin secretion.

5.3.1 ISLET ISOLATION FOR WESTERN-BLOT AND RT-QPCR

Rodents were euthanized by inhaled isoflurane. The connection of the pancreatic duct to the intestine was clamped and their pancreata were perfused through the pancreatic duct with 3 mL per mouse or 10 mL per rat of a solution of 1000 IU/ml of Collagenase P (Roche Diagnostics, USA) in cold Hanks solution (Sigma-Aldrich, USA). Once perfused, the pancreas was dissected and kept cold until digestion. The enzymatic digestion of the tissue was carried out at 37 °C for 15 minutes in a 50 ml tube. The digestion process was stopped by the addition of 10 mL of cold Hanks-10% FBS, followed by 3 cycles of agitations and centrifugations for 2 minutes at 330 X *g* in a centrifuge, discarding the supernatants with collagenase residues. The sediment was resuspended in the same solution and was filtered with a 500 µm steel strainer to eliminate possible remains of undigested tissues. The sediment was resuspended in 10 mL of Histopaque® 1077 (Sigma Aldrich, USA). A density gradient was formed with 10 mL of Hanks solution, followed by a centrifugation at 1500 X *g* for 20 minutes at 10 °C. After this, pancreatic islets were located at the interface between the two densities. Islets were collected with a micro-pipette and mixed with 30 mL of Hanks solution. The remains of Histopaque® were washed by 3 cycles of 30 mL of Hanks solution centrifuging 2 minutes at 330 X *g*. Afterwards islets were cultured in RPMI 1640 medium supplemented with 2 mM L-glutamine, 5.5 mM D-glucose, 10% FBS, 100 U/ml penicillin, and 100 µg/ml streptomycin. The islets were maintained at 37 °C with 5% CO_2 in a humidified atmosphere.

5.3.2 ISLET ISOLATION FOR GLUCOSE-STIMULATED INSULIN SECRETION

Rodents were euthanized by inhaled isoflurane. The connection of the pancreatic duct to the intestine was clamped and their pancreata were perfused with 3 mL of a solution of Collagenase IV (Sigma-Aldrich, USA) in cold isolation medium (115 mM NaCl, 5 mM KCl, 10 mM $NaHCO_3$, 1.1 mM $MgCl_2$, 1.2 mM NaH_2CO_4, 2.5 mM $CaCl_2$, 25 mM HEPES, 1% BSA and 5 mM Glucose, pH 7.4) at a concentration of 1000 UI / mouse through the pancreatic duct. Once perfused, the pancreas was dissected and kept cold until digestion. The enzymatic digestion of the tissue was carried out at 37 °C for 10 minutes. The digestion process was stopped by the addition of cold isolation medium. After this, supernatants are deposited in petri dishes and islets are collected under a microscope by handpicking method. Afterwards islets were grown in RPMI 1640 medium supplemented with 2 mM L-glutamine, 5.5 mM D-glucose, 10% FBS, 100 U/ml penicillin, and 100 µg/ml streptomycin. The islets were maintained at 37 °C with 5% CO_2 in a humidified atmosphere.

5.4 CELL CULTURES

5.4.1 INS-1 E CELL CULTURE

The rat insulinoma cell line, INS-1E derived from the parental cell line INS-1, were a gift of Dr. Pierre Maechler (University of Geneva, Switzerland). This cell type has the ability to secrete insulin in response to glucose overload. Cells were grown in RPMI 1640 Glutamax (GIBCO, USA), 11 mM Glucose, 10 mM Hepes (Invitrogen Ltd, Europe), 0.05 mM β-Mercaptoethanol (Sigma-Aldrich, USA) 1 mM Sodium Pyruvate (Invitrogen Ltd, Europe), 5% FBS and 1% Penicillin-Streptomycin (Invitrogen Ltd, Europe). Cells were cultured at 37 °C with 5% CO_2 in a humid atmosphere.

5.4.2 INS1-E SHRNA-IDE

5.4.2.1 GENERATION OF INS1-E SHRNA-IDE CELL LINE

To study the effect of stable IDE silencing on the cellular phenotype of pancreatic beta-cells, we subjected the INS1-E line to transduction with short hairpin RNA (shRNA) lentiviral vectors and we generated two INS1-E shRNA-IDE lines.

The vector used was pGreenPuro™ shRNA Cloning and Expression Lentivector (System Biosciences, USA). The pGreenPuro™ vector is an improved third generation of HIV-based expression lentivector. It contains a puromycin resistance gene to enable drug selection of target cells stably expressing the shRNA, and a copGFP gene, that works as a fluorescent reporter for the transduced cells. A map of the pGreenPuro™ vector is shown in **Figure 19.**

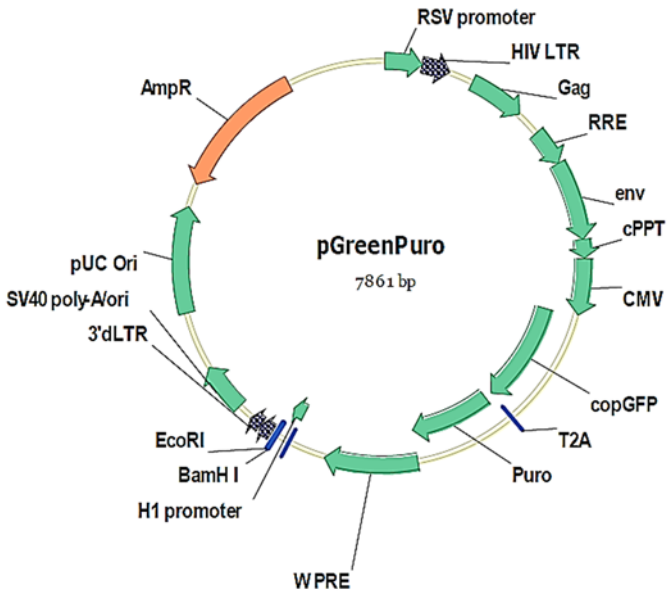

Figure 19. Map and features of pGreenPuro™ Vector [196].

First, the design of the target sequences within the coding regions of the IDE gene was carried out. These sequences containing both sense and anti-sense strand were designed according to manufacturer´s template to form a stem-loop structure when transcribed. The sequences of oligonucleotides finally selected are shown in **Table 4**. Sequences were called *p18* and *p25* since this sequences are located in exon 18 and 25 of the rat *Ide* gen respectively.

p18 Forward sequence
5´- GATCCCGGCTGCATATTGAAGCCCTTCTTCCTGTCAGAAAGGGCTTCAATATGCAGCCGTTTTTG-3´
p18 Reverse sequence
5´- AATTCAAAAACGGCTGCATATTGAAGCCCTTTCTGACAGGAAGAAGGGCTTCAATATGCAGCCGG-3´

p25 Forward sequence
5´- GATCCCCCTTGTGAAGCCACACATTACTTCCTGTCAGATAATGTGTGGCTTCACAAGGGTTTTTG -3´
p25 Reverse sequence
5´- AATTCAAAAACCCTTGTGAAGCCACACATTATCTGACAGGAAGTAATGTGTGGCTTCACAAGGGG-3´

Table 4. Oligonucleotides sequences designed for the lentiviral vector with initiator, sense, loop, antisense and terminator sequences highlighted.

Once oligonucleotides sequences were obtained, second step was cloning these sequences into the BamHI/EcoRI sites of the shRNA lentiviral vector pGreenPuro™ Vector and the resultant plasmids were screened for insert by PCR. Afterwards, we proceeded to the transfection and selection of *E. coli* DH10α with the target shRNA, followed by a purification of shRNA viral vector.

At this point, our plasmids were sequenced by Sanger Sequencing Service (Complutense University of Madrid) in order to verify that our sequences were the

desired ones. Once the sequences were verified, lentiviral stocks were produced by transient cotransfection into the human 293FT cell line. Afterwards, INS1-E cells were transduced and subsequently subjected to puromycin selection of stably infected cells and after that cultured as mentioned above.

Gene silencing efficiency was assessed by RT-qPCR and western blotting procedures as previously described.

5.4.2.2 ELECTRON MICROSCOPY

To analyze vesicle density in INS1-E shRNA-IDE cells, cells were scraped from the flask with PBS (137 mM NaCl, 2.7 mM KCl, 10 mM Na_2HPO_4, 2 mM KH_2PO_4) immediately after performing GSIS and centrifuged for 5 min at 300 X *g* for pellet formation. Pellets were fixed in 2% formaldehyde plus 2% glutaraldehyde in PBS for 30 min at 4ºC. Samples were then embedded in 2% agar, post-fixed with 1% osmium tetroxide in water, dehydrated through a graded series of ethanol and embedded in Epoxy EMbed-812 resin (EMS, Electron Microscopy Sciences). Ultrathin sections were obtained with a Leica EM UC7 ultramicrotome, contrasted with uranyl acetate and lead citrate, and analyzed using a Tecnai Spirit Twin 120 kv electron microscope with a CCD Gatan Orius SC200D camera with Digital Micrograph™ software. Electron microscopy was performed with the assistance of Electron Microscopy Service-NUCLEUS (University of Salamanca). Insulin vesicle density was quantified using ImageJ software.

5.5 PANCREATIC BETA-CELL TREATMENTS

5.5.1 INSULIN TREATMENT

INS-1 E cells were seeded at a confluence of 200,000 cells per well in 24-well plates. Next day, cells were treated in serum-free medium 24 hours before the experiment. 24 hours later, they were treated with serum free medium containing 500 nM human insulin (#I9278, Sigma-Aldrich, USA) at indicated time points: 0, 1, 2 and 4 hours respectively.

Rat and human islets were plated in cell culture inserts into 24-well plates at a density of 400 IEq (islet equivalents) in serum-free medium overnight. 24 hours later, islets were treated with serum-free medium containing 500 nM insulin at indicated time points: 0, 1, 4 and 8 hours respectively.

5.5.2 1,10-PHENANTROLINE

INS-1 E were treated for 30 min with 2 mM 1,10-Phenantroline (#131377, Sigma-Aldrich, USA) previously to the GSIS (glucose-stimulated insulin secretion). This product is a metalloprotease inhibitor (**Figure 20**) which markedly inhibits IDE activity [167].

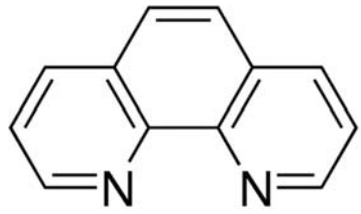

Figure 20. Structure of 1,10-Phenanthroline [167, 197].

5.5.3 NTE-2

Human and rat islets were treated with NTE-2 (0.1 μM), an IDE inhibitor provided by Lilly Research Laboratories (**Figure 21**). Islets were treated with this compound for 1h at 37ºC in complete medium before the GSIS [191].

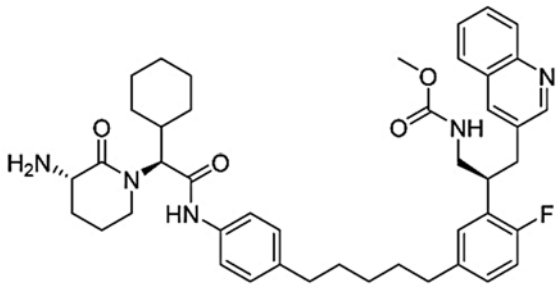

Figure 21. Structure of NTE-2 [191].

5.6 HISTOLOGICAL STUDIES

5.6.1 PANCREAS DISSECTION, FIXATION AND PARAFFIN EMBEDDING

For the extraction of pancreas, mice were euthanized by inhaled isoflurane. We accessed by latero-longitudinal incision to the abdominal cavity of the animal and proceeded to the extraction of the pancreas. Once the pancreas was dissected, it was washed with PBS and weighed on a precision scale. After that, it was introduced in a histological cassette and immersed in 10% neutral buffer formalin solution (Bio-Optica, Milano, Italy) overnight. After this fixation time, tissue was dehydrated, immersed in successive solutions of ethanol (Dávila Villalobos S.L., Spain) of increasing concentration from 70% to 100% dilution and finally to absolute xylol (PanReac AppliChem, Germany) and then embedded into paraffin

blocks. Once hardened, five- micrometers pancreas serial sections were obtained from these blocks. Sections were incubated at 56 °C overnight to favor the adherence of the sample to the slides. Polysine treated slides were preferably used to guarantee tissue adhesion.

5.6.2 PANCREATIC ISLET FIXATION AND PARAFFIN EMBEDDING

After specific treatments, pancreatic islets were fixed with 10% neutral buffer formalin for 1 h. Small blocks of islets were prepared with Histogel (Thermo Scientific, USA) together with small spheres of Affigel (BIO-RAD, USA) to better identify where the islets are in the paraffin blocks. Islets blocks were treated in a gradient of alcohols to be subsequently embedded in paraffin. 5 µm sections were obtained. Sections were incubated at 56 °C overnight to favor the adherence of the sample to the slide. Polysine treated slides were preferably used to guarantee tissue adhesion.

5.6.3 IMMUNOFLUORESCENCE AND IMMUNOHISTOCHEMISTRY

To study the expression of specific proteins in pancreatic cells, paraffin was removed from pancreas and islets paraffin slides by immersing them in xylol and then in a battery of ethanol solutions of decreasing concentration from 100% to 70% in H_20. After several washes with PBS, the antigen was unmasked with sodium citrate solution (10 mM citric acid – pH 6) in a vegetable steamer at maximum power for 20 min. Once they reached room temperature, they were washed with PBS for 5 minutes, three times. Then, to avoid non-specific binding of the antibody, samples were blocked for one hour with a blocking solution (PBS, 2% normal goat serum (Dako, Germany), 1% BSA (Sigma-Aldrich, USA) and incubated overnight at 4 °C with the corresponding primary antibodies in blocking solution. Primary antibodies used are summarized in **Table 5**.

Antibody	Supplier	Reference	Dilution	Species
Insulin	Abcam	#7842	1:2000	Guinea Pig
Glucagon	Abcam	#10988	1:2000	Mouse
IDE	Millipore	#9210	1:2000	Rabbit
GLUT1	Millipore	#07-1401	1:500	Rabbit
GLUT2	Millipore	#07-1402	1:500	Rabbit

Table 5. List of primary antibodies used for immunofluorescence.

The next day, after washing three times with PBS, it was blocked for 10 minutes at room temperature. The block was then removed and incubated for 30 minutes with the corresponding secondary antibodies, according to **Table 6**.

Antibody	Supplier	Reference	Dilution	Species
Anti-Guinea Pig Alexa 488	Invitrogen	#A11073	1:200	Goat
Anti-Mouse Alexa 647	Invitrogen	#A21236	1:300	Goat
Anti-Rabbit Alexa 594	Invitrogen	#A11012	1:200	Goat
Anti-Rabbit Ig-G HRP	Jackson Inmuno	#711-035-152	1:12000	Rabbit
Anti-Mouse Ig-G HRP	GE Healthcare	#NA9310	1:2000	Mouse

Table 6. List of secondary antibodies used for immunofluorescence.

Once washed three times with PBS, the sample was mounted with a coverslip and with histology mounting medium Fluoroshield with DAPI (Sigma-Aldrich, USA).

Fluorescence images of pancreas sections and INS1-E cells were acquired using a NIKON Eclipse 90i microscope associated with CCD NIKON camera 161 (DSRi1), using a 20X or 40X objective. Fluorescence images of islets sections were acquired in non-saturated conditions using Confocal Leica TCS SP5 microscope, using a 63X oil immersion objective.

The number and area of pancreatic beta- or alpha-cells and/or IDE-positive cells; and fluorescence intensity were quantified using ImageJ software (NIH, USA).

5.6.4 BETA- AND ALPHA-CELL AREA

For the evaluation of the pancreatic beta- and alpha-cell area, paraffin-embedded pancreas from 6 months old mice were sectioned into 5-µm-thick slices. Slices were collected from 4 different areas of the pancreas, separated by at least 100 µm. All the islets located in each section of pancreas were analyzed, representing about 100 islets analyzed per mouse. To observe alpha and beta-cells, immunohistochemistry was performed as mentioned above. HRP-linked secondary antibodies were used and diaminobenzidine (DAB) (Sigma-Aldrich, USA) was the reagent for antigen detection. Finally, sections were counterstained with hematoxylin (Bio-Optica, Italy). Images of the sections were acquired using a NIKON Eclipse 90i microscope associated with CCD NIKON camera (DSRi1), using a 20X objective. Beta- and alpha-cell area were calculated using ImageJ software (NIH, USA).

5.7 BETA-CELL FUNCTION

5.7.1 GLUCOSE-STIMULATED INSULIN SECRETION

Beta-cell function from our models were evaluated in-vitro by glucose stimulated insulin secretion technique.

- INS1-E cell line

INS1-E cells were seeded on cell culture 24-well plates at a density of 200,000 cells per well for 72 hours. Cells were changed to glucose-free culture medium 2 hours before glucose challenge. Cells were then washed twice and preincubated for 30 min at 37ºC in glucose-free HEPES balanced salt solution (HBSS) (114 mM NaCl, 4.7 mM KCl, 1.2 mM KH_2PO_4, 1.16 mM $MgSO_4$, 20 mM HEPES, 2.5 mM $CaCl_2$, 25.5 mM $NaHCO_3$, and 0.2% bovine serum albumin [essentially fatty acid free], pH 7.2). Next, cells were washed once with glucose-free HBSS and then, insulin secretion was stimulated by using static incubation for 30 min period in 1 ml of the same buffer containing 2 or 16 mM glucose respectively. These experiments were always performed in triplicates. 6 wells were used per condition, 3 wells were treated with 2 mM glucose and 3 wells treated with 16 mM glucose. Secreted insulin was measured by Rat Insulin ELISA (Mercodia AB, Sweden) **(Table 7)**.

- Human islets

Human islets were plated on cell culture inserts (#PIXP01250, Millipore, USA) onto 24-well plates at a density of 20 IEq (islet equivalent: a pancreatic islet with a diameter of 150 µm) groups in HBSS. Islets were washed twice in 1 ml HBSS with 2.2 mM glucose followed by 10 minutes of preincubation in 2 ml of the same buffer. Insulin secretion was stimulated by using static incubation for 30 minutes in 1 ml

of the same buffer, followed by 30 minutes of incubation in HBSS containing 22 mM glucose. Cell culture supernatants were used to measure secreted insulin, proinsulin using Insulin/Proinsulin ELISA (Mercodia AB, Sweden) **(Table 7)**.

- Rodent islets

Rodent islets were isolated by hand-picking method. Once isolated, islets were allowed to recover for 2 hours at 37 °C and 5% CO_2 in a humidified atmosphere. To promote insulin secretion, groups of 5 IEq plated on cell culture inserts were incubated for one hour in 500 µl of 3 mM glucose Krebs-Ringer buffer (140 mM NaCl, 4.5 mM KCl, 1 mM $MgCl_2$, 25 mM HEPES, 2.5 mM $CaCl_2$, 0.1% BSA) for one hour, followed by 500 µl of 16 mM glucose Krebs-Ringer buffer for one hour. After this, hormone secretion in cell culture medium was analyzed by Insulin/Proinsulin ELISA (Mercodia AB, Sweden) **(Table 7)**.

5.7.2 INTRACELLULAR INSULIN CONTENT

To analyze the INS1-E cell line intracellular insulin content, cells were treated with 1 ml of acid ethanol (1.5% HCl in 70% EtOH) per 200,000 cells for 1 hour at 4ºC prior to collection.

To analyze islets intracellular content, 100 µl of acid ethanol was added per IEq. They were incubated for 1 hour at 4 ºC prior to intracellular content collection.

Afterwards, samples were analyzed by ELISA for the determination of hormones content as previously explained **(Table 7)**.

5.8 ENZYME-LINKED IMMUNOSORBENT ASSAY (ELISA)

To determine hormone levels in plasma, cell culture supernatants from GSIS or intracellular hormone concentration, we used enzyme-linked immunosorbent assay (ELISA). ELISA kits used in this study are "sandwich" type, which means that this assay is composed by two highly specific antibodies that recognize two different epitopes in the same protein, providing high effectiveness and sensitivity in the recognition of the desired protein.

In our assays, wells are pre-coated with a first anti-antigen antibody. The sample containing the antigen is deposited inside these wells together with peroxidase-conjugated antibody and incubated between 2 and 22 hours depending on the kit. Thus, each molecule of antigen will be bound to an antibody in the base that retains it and a second antibody that label it. After that, wells are washed (between 3 and 6 times depending on the kit) to remove unbound sample and enzyme labelled antibody. Then, the bound conjugate is detected by reaction with 3,3'-5,5'-tetramethylbenzidine (TMB) (incubation between 15 and 30 minutes depending on the kit). The reaction is finally stopped by the addition of an acid stop solution, giving a colorimetric endpoint that is read spectrophotometrically at 450 nm (HEALES microplate reader, China). This process is summarized in **Figure 22**.

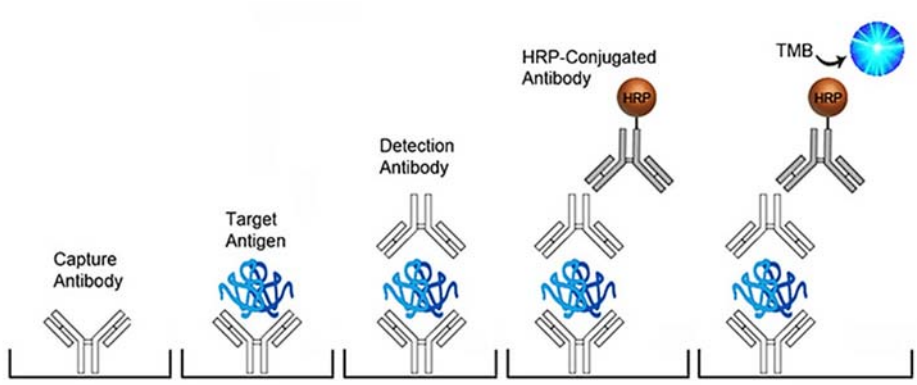

Figure 22. Illustration of an ELISA sandwich technique. Retrieved from LifeSpan Bioscience, Inc.

ELISA kits used in this study have been summarized in **Table 7**.

Protein	Source	ELISA
Insulin	Human islet supernatant/Intracellular	MERCODIA INSULIN ELISA #10-1113-01
	Mouse islet supernatant/Intracellular	MERCODIA MOUSE INSULIN ELISA #10-1247-01
	INS1-E / Rat islets supernatant/Intracellular	MERCODIA RAT INSULIN ELISA #10-1250-01
	Mouse plasma	MERCODIA ULTRASENSITIVE MOUSE INSULIN ELISA #10-1249-01
C-peptide	Mouse plasma	ALPCO MOUSE C-PEPTIDE ELISA #80-CPTMS-E01
Proinsulin	Human islet supernatant/Intracellular	MERCODIA PROINSULIN ELISA #10-1118-01
	Mouse islet supernatant/Intracellular	MERCODIA RAT/MOUSE PROINSULIN ELISA #10-1232-01

Table 7. List of hormones analyzed and type of ELISA that was used.

5.9 WESTERN-BLOTTING

Pancreatic islets and INS1-E cells were homogenized in lysis buffer (125 mM Tris-Cl pH 6.8, 2% SDS, 1 mM DTT) supplemented with protease and phospathase cocktail inhibitors (Sigma-Aldrich, USA). Samples were briefly sonicated and protein content was quantified by the Micro BCA Kit (Thermo Scientific, USA). Protein extracts were mixed with LSB (Laemmli Sample Buffer: 60 mM Tris-Cl pH 6.8, 2% SDS, 10% glycerol, 5% β-mercaptoethanol, 0.01% bromophenol blue) and heated at 100 °C for 5 minutes. 20 µg of protein samples were loaded per well. Proteins samples were separated by their molecular weight using 7.5 % polyacrylamide gels under denaturing conditions (SDS-PAGE). Gel electrophoresis was carried out at 150 V in electrophoresis buffer (Biorad Laboratories, USA) and then transferred to PDVF Immobilon-P membranes (Millipore, USA) at 30V overnight in transfer buffer (Biorad Laboratories, USA) at

4°C. Transferred membranes were blocked for 1 hour at room temperature with blocking solution (PBS-0.1% Tween 20 (Sigma-Aldrich, USA) and 5% not-fat dry milk). Blots were incubated subsequently for 1 hour at room temperature for the appropriate antibody in 1:10 diluted blocking solution. Primary antibodies used are summarized in **Table 8**.

Antibody	Supplier	Reference	Dilution	Species	Size
IDE	Millipore	#9210	1:15000	Rabbit	110 kDa
Actin Ab-5	Bioscience	#612656	1:8000	Mouse	42 kDa

Table 8. List of primary antibodies used for Western-Blot.

Afterwards, membranes were washed 3 times for 10 minutes with PBS-0.1% Tween and incubated with corresponding secondary antibodies conjugated with peroxidase in 1:10 diluted blocking solution for 30 minutes at room temperature. Secondary antibodies used are schematized in **Table 9.**

Antibody	Supplier	Reference	Dilution	Species
Anti-Rabbit Ig-G HRP	Jackson Inmuno	#711-035-152	1:12000	Rabbit
Anti-Mouse Ig-G HRP	GE Healthcare	#NA9310	1:2000	Mouse

Table 9. List of secondary antibodies used for Western-Blot.

Membranes were washed 3 times with PBS-0.1% Tween and bound peroxidase activity was visualized by the enhanced chemiluminescence kit Immun-Star WesternC (Bio-Rad, EEUU) and Super RX-N X-Ray films (Fujifilm, Japan) to capture de signal. ImageJ software (NIH, USA) was used for processing and analysis of band densitometry. Results were normalized to control values on each membrane.

5.10 RNA ISOLATION, cDNA SYNTHESIS AND RT-qPCR

Total RNA isolation from tissues of B-IDE-KO mice and INS1-E cells were obtained using Trizol reagent (Invitrogen Life Technologies, USA). Tissues and cells were homogenized in Trizol reagent and centrifuged 10 min at 2800 X *g* to remove undissolved samples. Next, chloroform (PanReac AppliChem, Germany) is added to the supernatant to extract RNA and centrifuged for 15 minutes at 2800 X *g*, which causes the formation of two phases by density difference: an organic phenolic phase containing DNA and denatured protein residues, and the upper aqueous phase containing RNA. Phase containing RNA is transferred to a new tube and added isopropanol (PanReac AppliChem, Germany) and centrifuged 10 min at 2800 X *g* to precipitate the RNA. After that, isopropanol is discarded and the pellet is washed in 75% ethanol and allowed to dry. Finally, the pellet containing RNA is resuspended in H_2O DNAse RNAse free and mRNA levels were measured with NanoDrop™ N-D1000.

Once RNA isolation was completed, DNA residues were removed by RapidOut DNA removal kit (Thermo-Fisher Scientific, USA) to avoid amplification out of genomic DNA. First strand cDNA was synthesized with iScript cDNA Synthesis Kit (Bio Rad, USA), which is a highly sensitive reagent optimized for reliable cDNA synthesis for gene expression analysis using real-time reverse transcription quantitative PCR (RT-qPCR).

The reverse transcription reaction was incubated in a thermal cycler Applied Biosystems™ 2720 Thermal Cycler. mRNA levels were determined by RT-qPCR with SYBR Green assays or TaqMan® Probes (Applied Biosystems, USA), two techniques that use different detection systems schematized in **Figure 23** to perform a quantitative measurement of the gene expression.

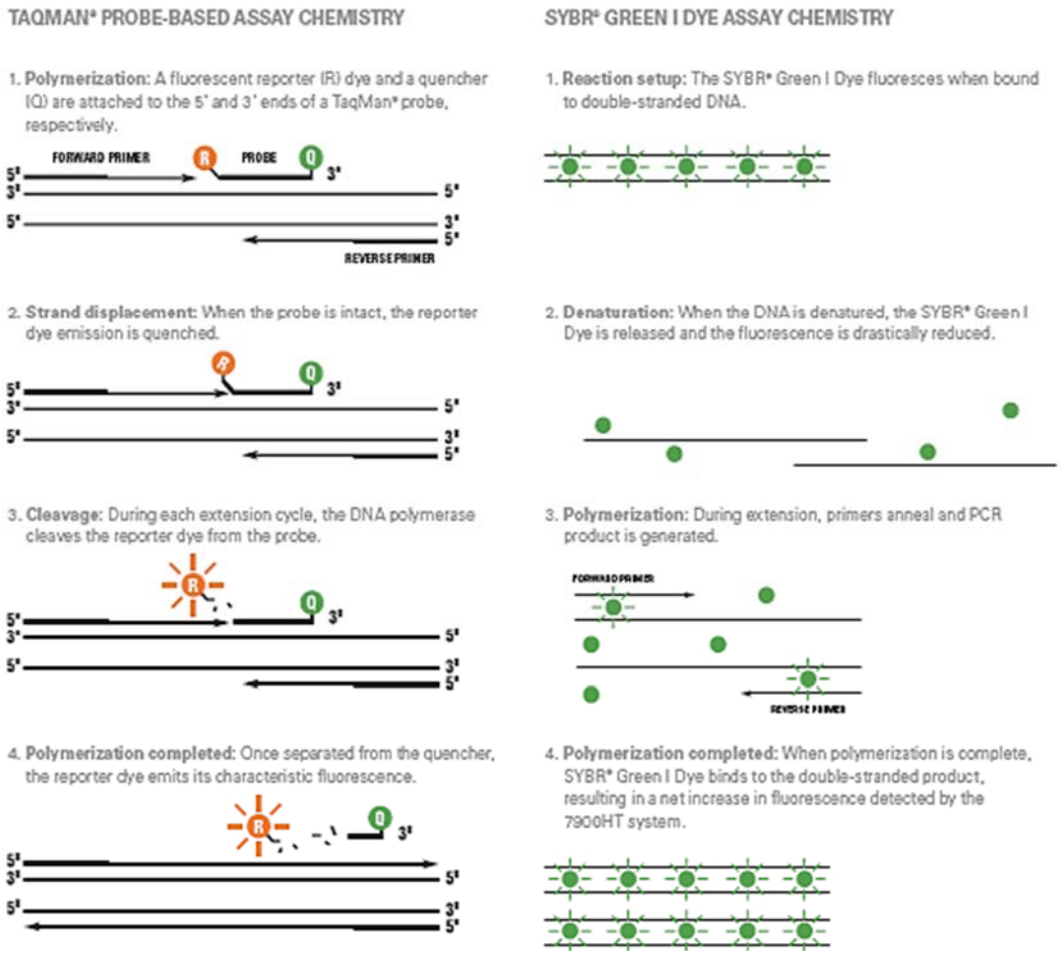

Figure 23. Comparison of detection workflows based on TaqMan and SYBR Green. Retrieved from Thermo Fisher Scientific.

A list SYBR Green assays or TaqMan® Probes used are shown in **Table 10 and Table 11.** These reactions were performed in a Rotor-Gene 3000 thermocycler (Corbett Life Science, USA). Data were normalized with the housekeeping gene RPL18 and relative expression was quantified using the comparative 2-ΔΔCT method.

Gene ID	Description	TaqMan® Probe
Ide	Insulin-degrading enzyme	Mm00473077_m1
Ins1	Insulin I	Mm01259683_g1
Ins2	Insulin II	Mm00731595_gH
Nkx2-2	NK2 homeobox 2	Mm00839794_m1
Nkx6-1	NK6 homeobox 1	Mm00454961_m1
Pax6	Paired box 6	Mm00443081_m1
Pdx1	Pancreatic and duodenal homeobox 1	Mm00435565_m1
Neurod1	Neurogenic differentiation 1	Mm01280117_m1
Mafb	v-maf musculoaponeurotic fibrosarcoma oncogene family, protein B	Mm00627481_s1
Ucn3	Urocortin 3	Mm00453206_s1
Syt4	Synaptotagmin IV	Mm01157571_m1
Slc2a1	Solute carrier family 2 (facilitated glucose transporter), member 1	Mm00441480_m1
Slc2a2	Solute carrier family 2 (facilitated glucose transporter), member 2	Mm00446229_m1
Slc2a3	Solute carrier family 2 (facilitated glucose transporter), member 3	Mm00441483_m1
Gck	Glucokinase	Mm00439129_m1
Kcnj11	Potassium voltage-gated channel subfamily J member 11	Mm00440050_s1
Abcc8	ATP binding cassette subfamily C member 8	Mm00803450_m1
Cacna1a	Calcium channel, voltage-dependent, P/Q type, alpha 1A subunit	Mm00432190_m1
G6pc	Glucose-6-phosphatase catalytic subunit	Mm00839363_m1
Pck1	Phosphoenolpyruvate carboxykinase 1	Mm01247058_m1

Table 10. List of TaqMan probes used.

Gene ID	Description	SYBR Green assay
Mafa	v-maf musculoaponeurotic fibrosarcoma oncogene family, protein A	F: 5´-GAGGAGGTCATCCGACTGAAA-3´ R: 5´-GCACTTCTCGCTCTCCAGAAT-3´
Pcsk1/3	Proprotein convertase subtilisin/kexin type 1	F: 5'-CTGGCCAATGGGTCGTACTC-3' R: 5'-TGGAGGCAAACCCAAATCTTAC- 3'
Pcsk2	Proprotein convertase subtilisin/kexin type 2	F: 5'-AGGCAGCTGGCGTGTTTG-3' R: 5'-GAAGCTGGTTCCGCTTGGA-3'

Table 11. List of SYBR Green assays used.

5.11 STATISTICAL ANALYSIS

Statistical analysis of data was performed using GraphPad Prism Software 6.0 (CA, USA). Data are represented as the mean +/- the standard error of the media. To check the normality of distributions, we used Kolmogorov-Smirnov test. To analyze statistical differences between two sets of data we use Student's t-test (parametric data) or Mann–Whitney U test (non-parametric data). Comparisons between more than two sets of data were done using one-way ANOVA or two-way ANOVA (two independent variables) for parametric data and Kruskal-Wallis test or Friedman´s test (two independent variables) for non-parametric data. Post-hoc analyses were done using Bonferroni test (parametric data) or Durnett (non-parametric data). Statistically differences were considered significant at $p<0.05$.

RESULTS

6. RESULTS

Part 1. IDE expression in pancreatic islet cells

1.1 IDE IS EXPRESSED IN RODENTS AND HUMANS PANCREATIC ALPHA- AND BETA-CELLS

To explore whether IDE is expressed in pancreatic alpha- and beta-cells, we performed IDE immunofluorescence (IF) on paraffin-embedded pancreas sections of humans and mice. We validated our antibody for IDE immunohistochemistry using Total-IDE-KO mice pancreata [193]; where no staining was observed. Pancreas staining revealed that IDE is expressed in both alpha- and beta-cells of wild type mice and human pancreata (**Figure 24**).

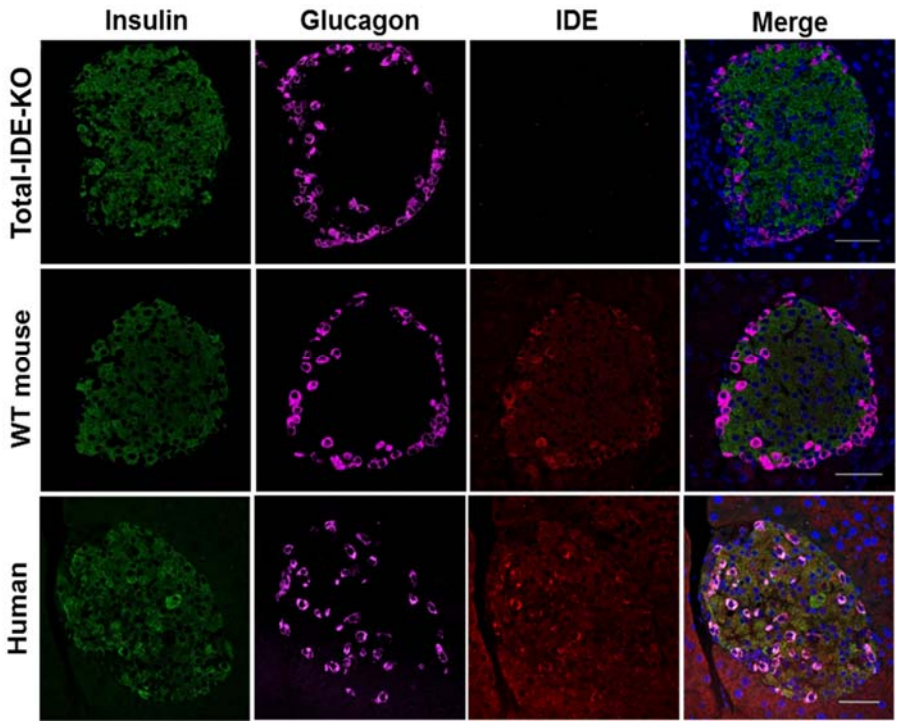

Figure 24 Localization of IDE in mouse and human pancreatic islet cells. Representative images acquired by confocal microscopy with 20X objective from Total-IDE-KO mice, wild-type (WT) mice and human pancreata**.** Insulin (green), glucagon (pink), IDE (red) and DAPI (blue). Scale bar: 50µm.

Interestingly, IDE staining in alpha-cells was more intense than in beta-cells or any other cell type in the pancreatic islet, indicating a higher expression of IDE in alpha-cells.

1.2 TYPE-2 DIABETIC HUMAN ISLETS SHOW IMPAIRED BETA-CELL TO ALPHA-CELL RATIO

In order to clarify if IDE expression varies in pathophysiological conditions, we examined IDE expression pattern in human pancreas samples. We obtained paraffin-embedded sections of human cadaveric donors pancreata from three different populations:

- Control patients
- T2DM patients treated with oral antidiabetic agents (OHAs)
- T2DM patients treated with exogenous insulin.

These human samples were obtained from the Biobank of San Carlos Clinical Hospital (Madrid, Spain). Detailed information about human donors are shown in **Table 12**.

	ID	Sex	Age	Treatment	Cause of death
Control	HC10	M	76		Respiratory insufficiency
	HC30	M	40		Septic shock
	HC23	M	54		Multiorgan failure
	HC 25	M	48		Multiorgan failure
	CM27	F	42		Unknown
	CM15	F	75		Status epilepticus
	CM22	F	52		Adult respiratory distress syndrome
	CM28	F	40		Cardiogenic shock
	CM21	F	63		Septic shock
T2DM+OHAs	HA11	M	63	OHA (Metformin)	Cardiogenic shock
	HA15	M	65	OHA (unknown)	Septic shock
	HA16	M	65	OHA (unknown)	Septic shock
	HA21	M	59	OHA (unknown)	Unknown
	HA7	M	78	OHA (Metformin)	Unknown
	MA9	F	76	OHA (Metformin)	Cerebral haemorrhage
	MA13	F	65	OHA (Metformin)	Massive pulmonary embolism
	MA19	F	58	OHA (Metformin)	Post surgery shock
	MA16	F	69	OHA (unknown)	Unknown
T2DM+Insulin	HI2	M	77	Insulin (unknown)	Septic shock
	HI16	M	60	Insulin (NPH)	Cardiogenic shock
	HI15	M	67	Insulin (Mixtard 30)	Acute Pulmonary Edema
	HI18	M	44	Insulin (unknown)	Septic shock
	MI12	F	63	Insulin (unknown)	Urological sepsis
	MI9	F	71	Insulin (Lantus)	Pulmonary aspergillosis
	MI6	F	75	Insulin (NPH)	Cardiogenic shock
	MI5	F	72	Insulin (unknown)	Respiratory insufficiency

Table 12: Demographic data of pancreas donors included in the study. Control = non-diabetic donor; T2DM+OHAs = type-2 diabetic donor treated with oral anti-diabetic agents; T2DM+Insulin = type-2 diabetic donor treated with insulin

Prior to the study of IDE protein levels in these samples, we characterized pancreatic alpha- and beta-cell populations of control and T2DM patients. To this end, a histomorphometric study was conducted using two different techniques: quantification of positive alpha- and beta-cells per islet; and quantification of alpha- and beta-cell area per islet area.

For detection of alpha- and beta-cell populations, an immunostaining was performed with antibodies against insulin and glucagon (**Figure 25**).

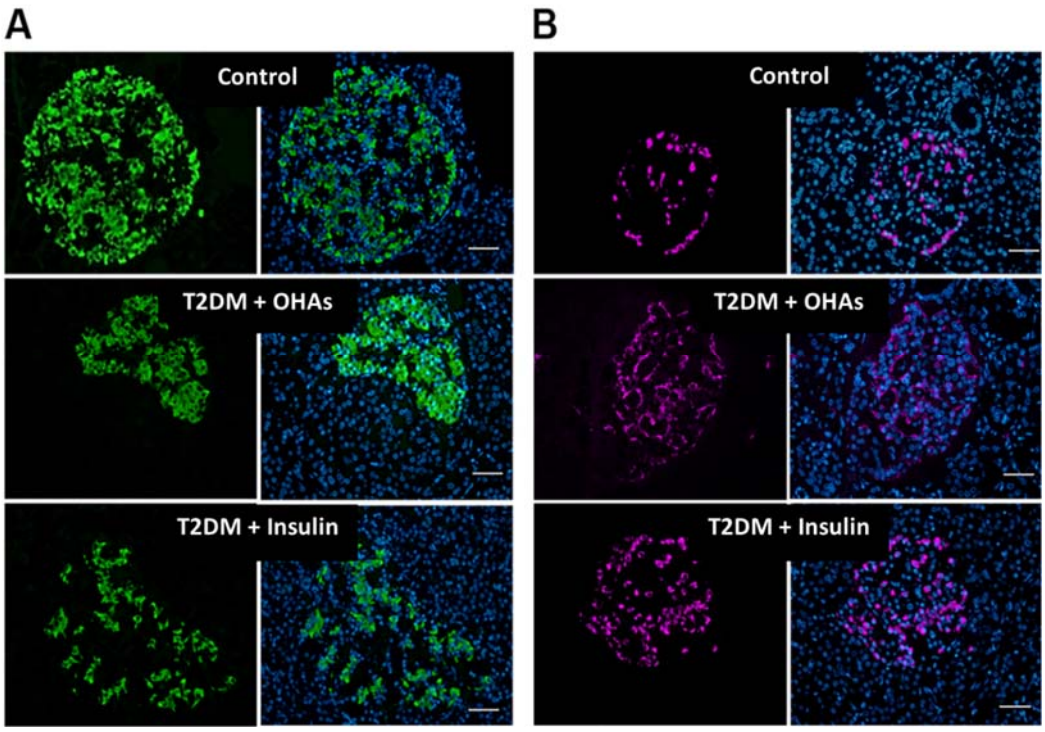

Figure 25: Beta- and alpha-cells distribution in human pancreata. Representative images acquired by fluorescence microscopy with 20X objective from control = non-diabetic donor; T2DM = type-2 diabetic donor; T2DM+OHAs = type-2 diabetic donor treated with oral anti-diabetic agents; T2DM+Insulin = type-2 diabetic donor treated with insulin. **A.** Insulin staining (green) and DAPI (blue). **B.** Glucagon staining (pink) and DAPI (blue). Scale bar: 50 µm

Quantification of percentage of beta-cell number of cells per islet cells did not show any differences when comparing T2DM population to controls. Neither when T2DM population was together (**Figure 26 A)** nor when it was separated in to T2DM+OHAs and T2DM+Insulin groups (**Figure 26 B**). Pancreas from T2DM population showed no difference in beta-cell area when compared to control population when considering T2DM patients all together (**Figure 26 C**). In contrast, a significant 40% decrease was observed in beta-cell area when T2DM+OHAs and T2DM+Insulin data were separated and insulin-treated T2DM patients were compared to control patients (**Figure 26 D**).

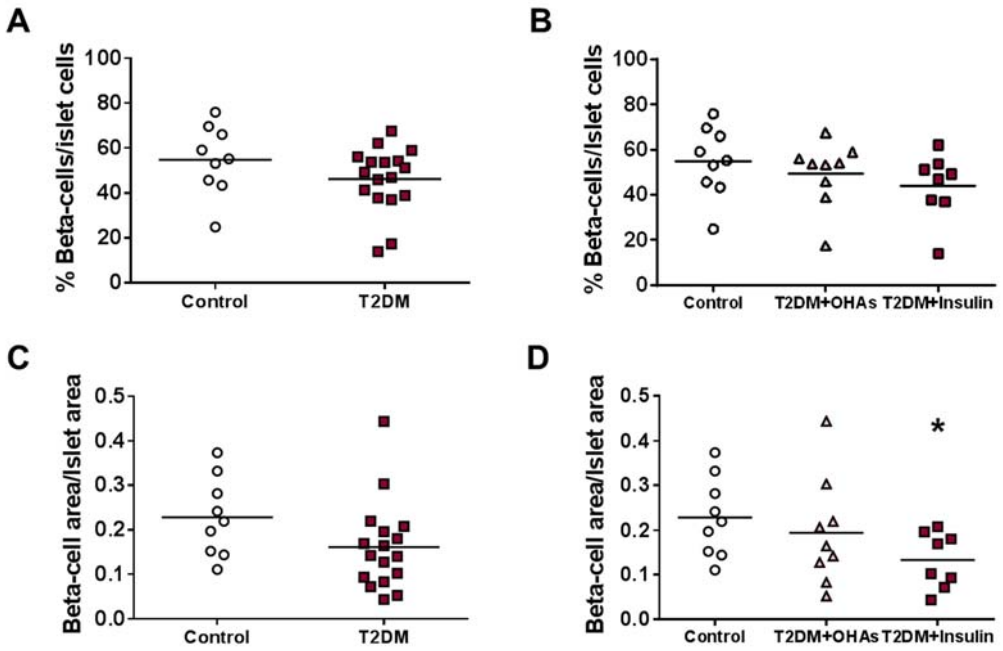

Figure 26: Beta-cells quantification in human pancreata. Percentage of insulin-positive cells per total islet cell number in controls compared to (**A**) all T2DM patients or (**B**) T2DM patients separated by treatment condition. Beta-cell area/islet area in control compared to (**C**) all T2DM patients or (**D**) T2DM patients separated by treatment condition. n=9 control; n=9 T2DM+OHA; n=8 T2DM+Insulin.Data are presented as mean ± SEM. *p< 0.05 versus control by one-way ANOVA.

On the other hand, regarding to alpha cell population, we observed that T2DM pancreata of both the T2DM+OHAs and the T2DM+Insulin groups exhibited a significant 30% increase in alpha-cell numbers, but they did not show differences in alpha-cell area (**Figure 27**). These results are pointing to an increased population of glucagon-positive cells in T2DM patients.

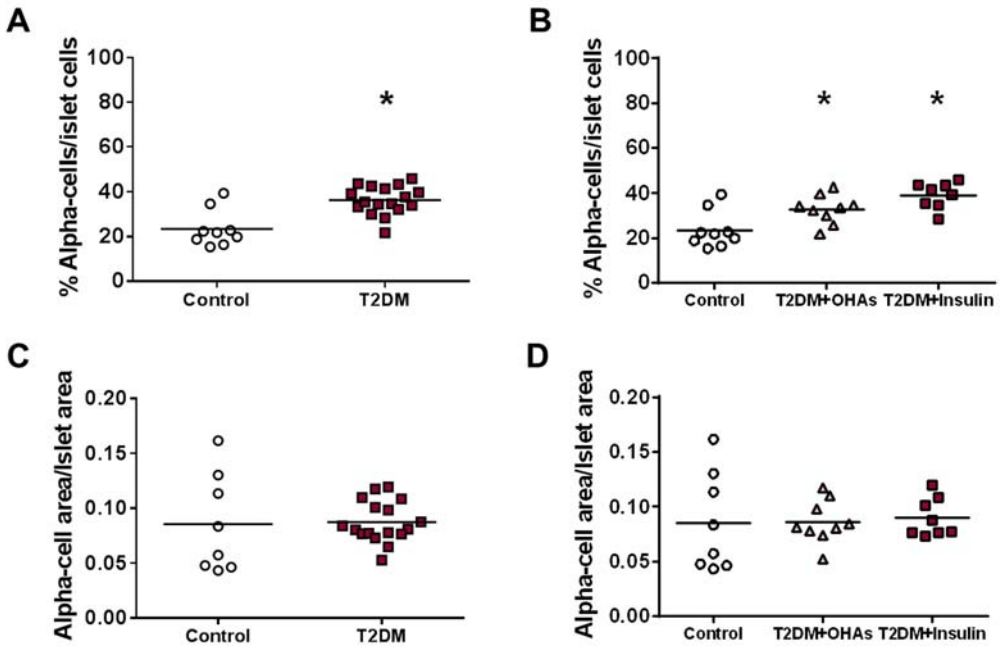

Figure 27: Alpha-cells quantification in human pancreata. Percentage of glucagon-positive cells per total islet cell number in controls compared to (**A**) all T2DM patients or (**B**) T2DM patients separated by treatment condition. Alpha-cell area/islet area in controls compared to (**C**) all T2DM patients or (**D**) T2DM patients separated by treatment condition. n=9 control; n=9 T2DM+OHA; n=8 T2DM+Insulin.Data are presented as mean ± SEM. *p< 0.05 versus control by Student´s t test or by one-way ANOVA.

Additionally, we calculated the ratio of beta- to alpha-cells using both types of quantification (cell number and area). Pancreas from T2DM patients showed a 50% reduction in beta-/alpha-cell ratio by both methods of quantification (**Figure 28**).

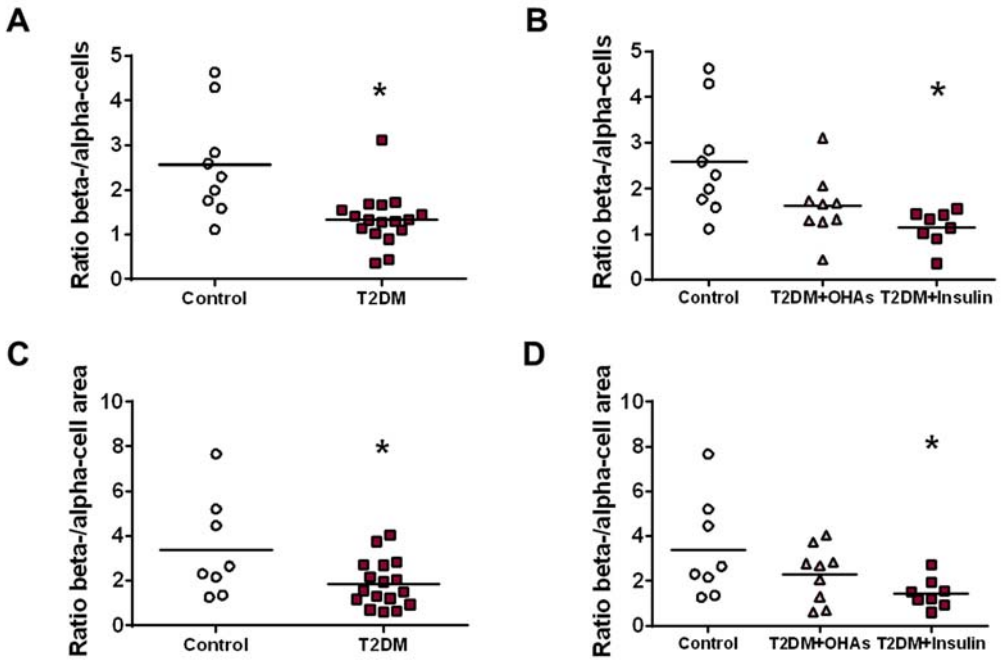

Figure 28: Ratio beta-/alpha-cells quantification in human pancreata. Ratio of beta- per alpha-cell number in controls compared to (**A**) all T2DM patients or (**B**) T2DM patients separated by treatment condition. Ratio beta- per alpha-cell area in controls compared to (**C**) all T2DM patients or (**D**) T2DM patients separated by treatment condition. n=9 control; n=9 T2DM+OHA; n=8 T2DM+Insulin. Data are presented as mean ± SEM. *p< 0.05 versus control by Student´s t test or by one-way ANOVA.

Taken together, these data indicate an impaired distribution of pancreatic alpha- and beta-cells during the course of T2DM, which has been previously described in the literature [27, 198]. These results emphasize the relevance of increased glucagon-producing cells in type 2 diabetes pathophysiology.

1.3 IDE PROTEIN LEVELS ARE DOWN-REGULATED IN ISLETS OF T2DM PATIENTS TREATED WITH OHAS AND UP-REGULATED IN T2DM PATIENTS TREATED WITH INSULIN

In order to measure IDE expression in pathophysiological stages, we analyzed IDE protein levels in pancreas samples from T2DM patients treated with OHAs or with insulin treatment, and compared them to control individuals.

For detection of IDE protein in alpha- and beta-cell populations, a double staining was performed using antibodies against IDE + insulin or IDE + glucagon as shown in **Figure 29**.

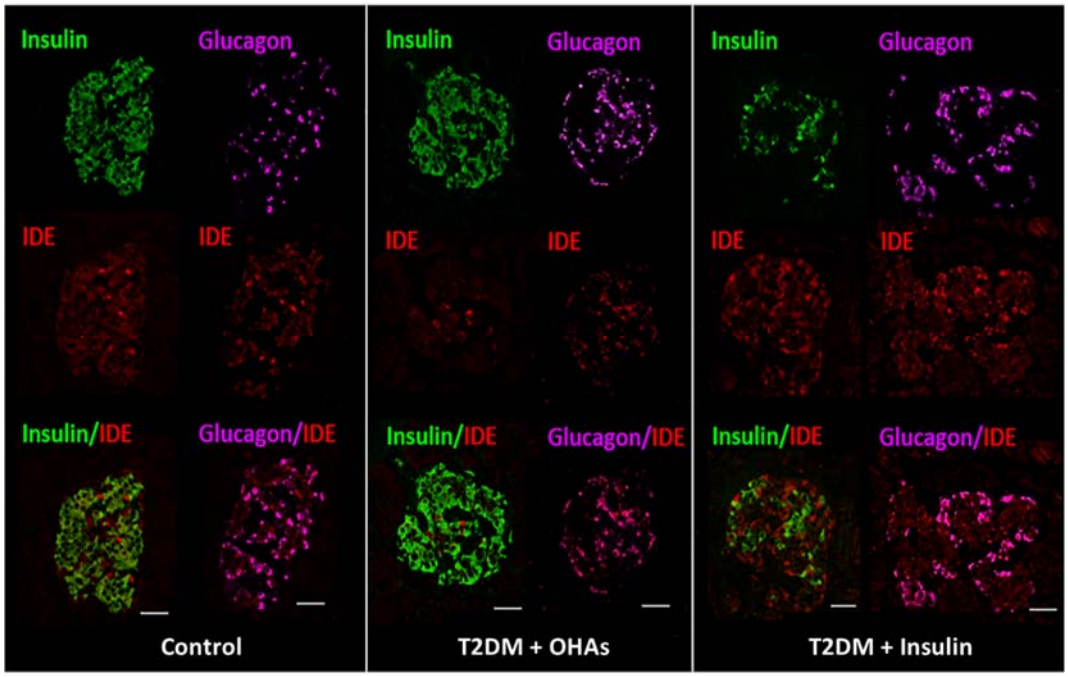

Figure 29: IDE staining in human endocrine pancreata. Representative images acquired by fluorescence microscopy with 20X objective of IDE/insulin (green/pink) and IDE/glucagon staining (red/pink).

IDE integrated intensity showed a marked increase in IDE protein levels in alpha-area versus beta-area (**Figure 30**). These results are in good agreement with results obtained from rodents in **Figure 24**, demonstrating that IDE expression is higher in alpha- than in beta-cells.

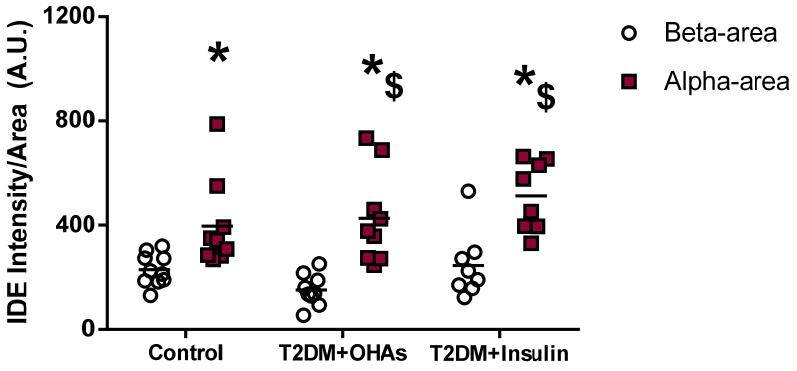

Figure 30: IDE expression in human endocrine pancreata. Comparison of IDE integrated density by beta-cell area and IDE integrated density by alpha-cell area. n=9 control; n=9 T2DM+OHA; n=8 T2DM+Insulin. Data are presented as mean ± SEM. *p< 0.05 versus beta-area; $p< 0.05 versus control by one-way ANOVA.

In regard to IDE expression in diabetic pancreas, when all T2DM patients were compared to controls, no differences were detected (**Figure 31 A**). Interestingly, two patterns of expression were observed depending upon the specific type of pharmacological treatment: beta-cells from T2DM+OHAs patients showed a significant 40% decrease in IDE protein level compared to control subjects. Unexpectedly, beta-cells from T2DM+insulin subjects exhibited 40% increased IDE level as compared to T2DM+OHAs, reaching similar levels to control subjects. (**Figure 31 B**).

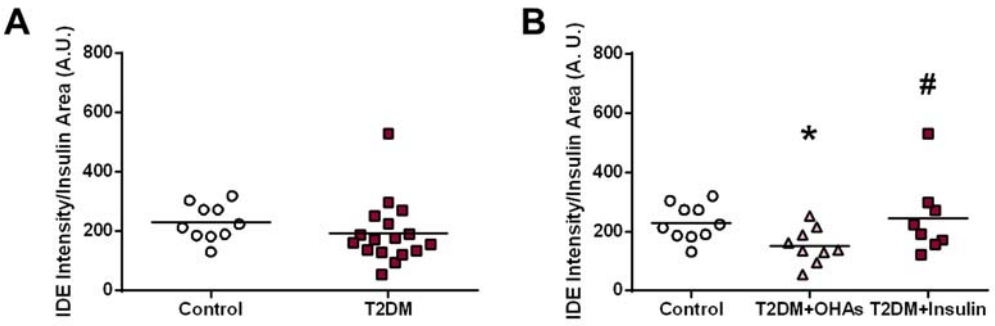

Figure 31: IDE expression in human beta-cell area. IDE integrated density per insulin area in controls compared to (**A**) all T2DM patients or (**B**) T2DM patients separated by treatment condition. n=9 control; n=9 T2DM+OHA; n=8 T2DM+Insulin. Data are presented as mean ± SEM. *p< 0.05 versus control; #p< 0.05 versus T2DM+OHA by one-way ANOVA.

In contrast, no significant changes were observed in IDE expression in alpha-cells of T2DM groups versus the control group neither when compared as a whole group (T2DM) (**Figure 32 A**) or when separated in two populations (T2DM+OHAs and T2DM+Insulin) (**Figure 32 B**).

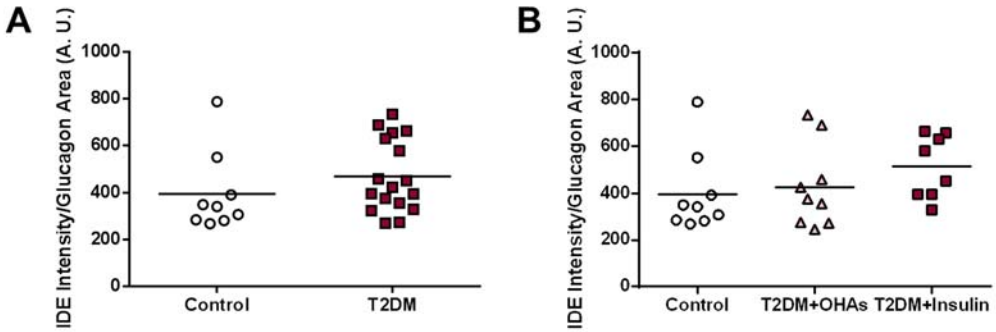

Figure 32: IDE expression in human alpha-cell area. IDE integrated density per glucagon area in controls compared to (**A**) all T2DM patients or (**B**) T2DM patients separated by treatment condition. n=9 control; n=9 T2DM+OHA; n=8 T2DM+Insulin. Data are presented as mean ± SEM.

These results suggest that diabetes mellitus can decrease IDE protein levels in beta-cells, but under insulin treatment IDE is upregulated returning to control levels.

1.4 IDE PROTEIN LEVELS ARE AUGMENTED IN ISLET-CELLS OF PRECLINICAL MODELS OF HYPERINSULINEMIA

To clarify whether IDE expression is altered in diabetes-related models with increased insulin levels, we analyzed the expression pattern of this protein in two preclinical models of hyperinsulinemia: *db/db* mice (*Insulin: 5.0 ng/mL vs. control 0.5 ng/mL, *p<0.05*) and HFD mice (*Insulin: 16.9 ng/mL vs. SD 1.0 ng/mL, *p<0.05*).

To this end, IDE protein was detected by immunofluorescence. Co-staining with insulin or glucagon was used to indicate IDE localization, on pancreas sections of db/db and HFD mice and their respective controls. To quantify IDE expression level per endocrine cell type area, IDE-integrated intensity was measured, and it was divided by glucagon or insulin area respectively.

No significant changes were detected in IDE protein level comparing *db/db* versus control mice. However, a 52% increase in IDE expression was observed in alpha-cells in respect to beta-cells of wild type mice (*p=0.05*) (**Figure 33**).

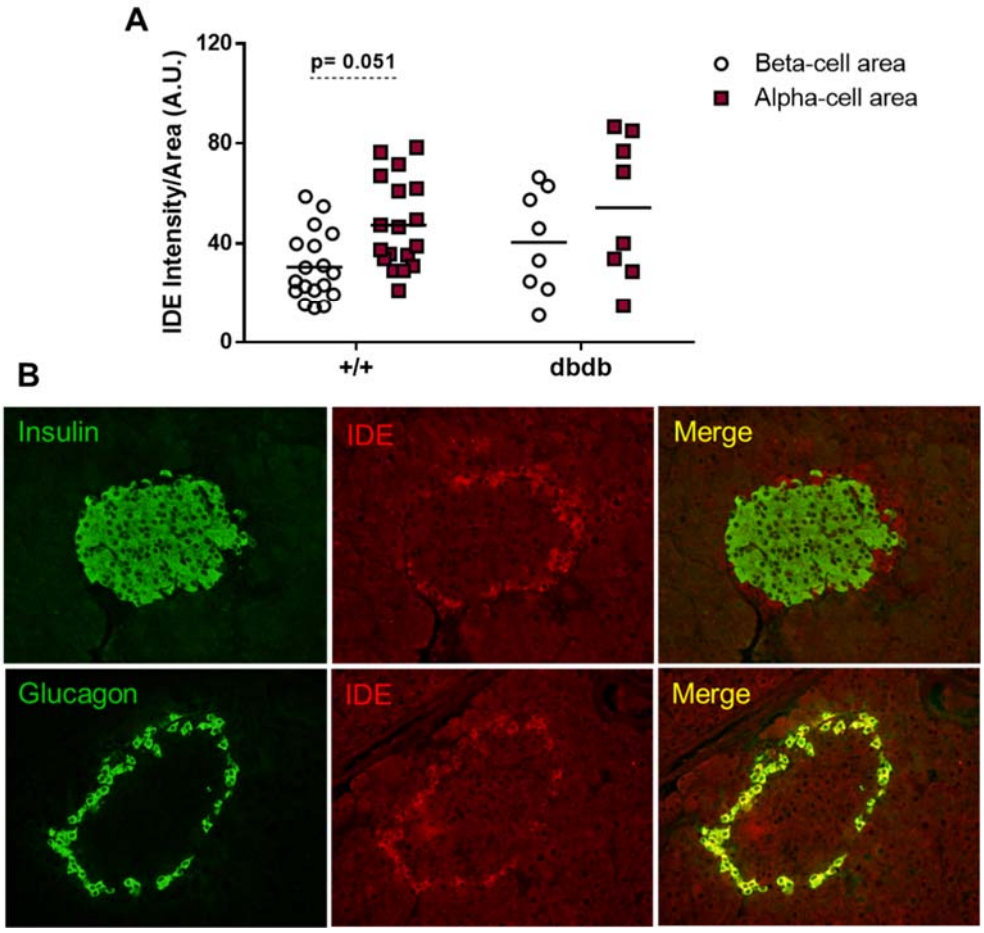

Figure 33: IDE expression in preclinical models of diabetes and obesity: *db/db* mice. **A.** IDE integrated density per insulin or glucagon area was measured in pancreas of wild-type (+/+) or db/db mice. **B.** Representative images acquired by fluorescence microscopy with 20X objective from +/+ mice. Insulin/Glucagon (green) and IDE (red). n=18 +/+; n=8 db/db. Data are presented as mean ± SEM.

Similarly, IDE integrated intensity of pancreas from HFD mice exhibited similar levels compared to control animals fed with standard diet (SD) (**Figure 34**). Of note, IDE level is clearly augmented in alpha- compared to beta-cell population. This result is clearly similar to what we previously reported in *db/db* mice (**Figure 33**).

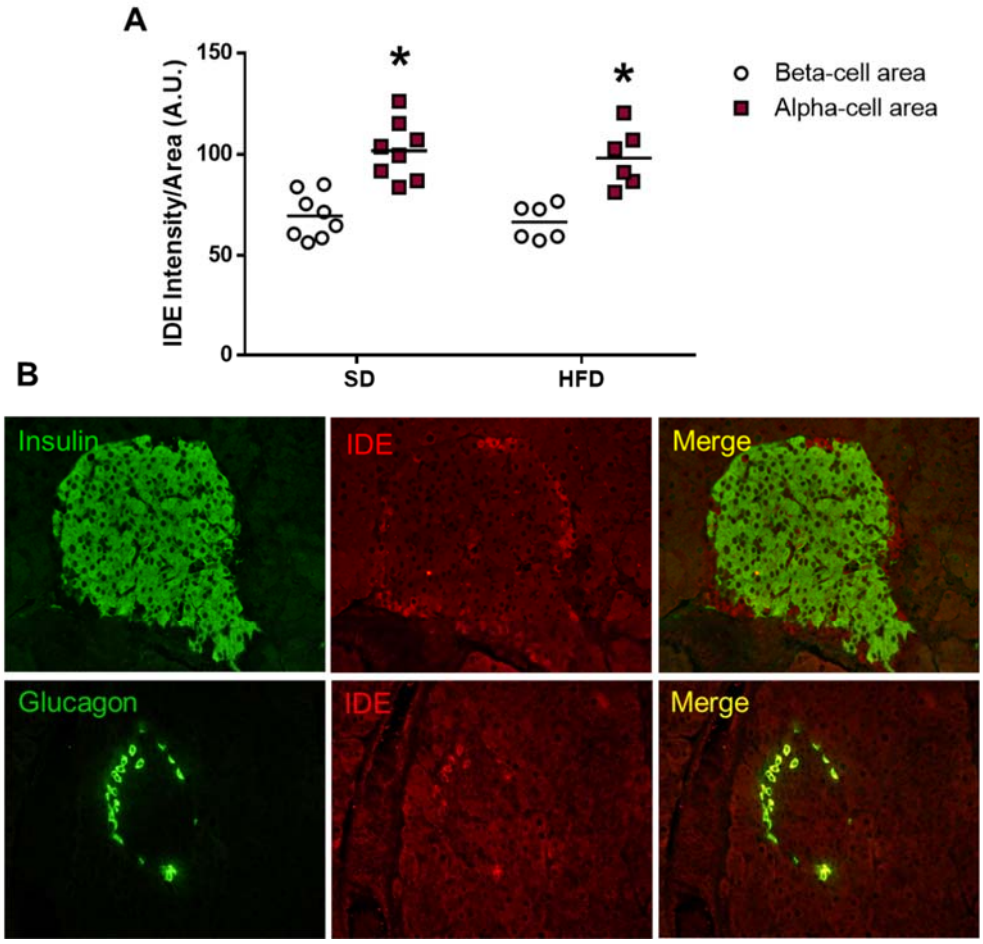

Figure 34: IDE expression in preclinical models of diabetes and obesity: HFD mice. A. IDE integrated density per insulin and glucagon area was measured in pancreas of mice fed with standard diet (SD) or high-fat diet (HFD). **B.** Representative images acquired by fluorescence microscopy with 20X objective from SD mice. Insulin/Glucagon (green) and IDE (red). n=8 SD; n=6 HFD. Data are presented as mean ± SEM. *p< 0.05 versus beta-area by two-way ANOVA.

Interestingly, when pancreatic islets were isolated of HFD and SD mice and IDE expression analyzed by Western-Blot, we detected a significant 30% increase in IDE protein level in HFD isolated islets compared to SD islets (**Figure 35**).

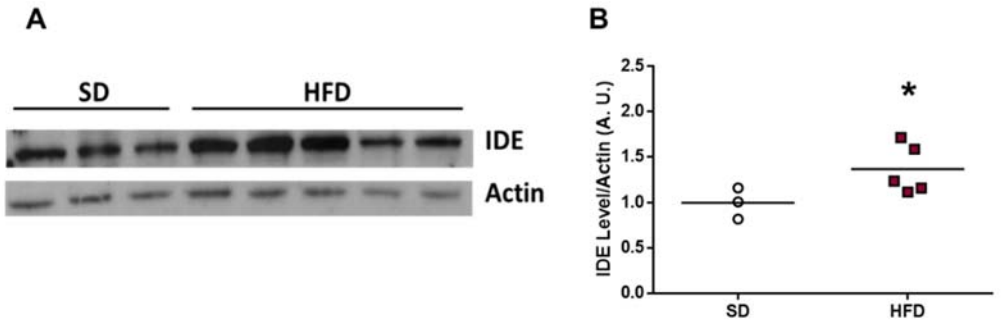

Figure 35: IDE expression in preclinical models of diabetes and obesity. A. Representative IDE western-blot of SD and HFD islets. **B.** Quantification of IDE western-blot. n=3 SD; n=5 HFD. Data are presented as mean ± SEM. *p< 0.05 versus SD by Student´s t test.

These findings nicely correlate with the potential effect of insulin on IDE expression that we observed in T2DM patients treated with insulin (**Figure 31 B**).

In summary, these data suggest that hyperinsulinemia stimulates IDE protein levels in pancreatic islet cells.

1.5 INSULIN TREATMENT AUGMENTS IDE PROTEIN LEVELS IN INS1-E AND ISLET CELLS *IN VITRO*

In view of our results, we decided to explore the potential influence of insulin treatment on IDE levels in pancreatic cells *in vitro* and *ex vivo*.

First, we cultured INS1-E cells and treated them with 500 nM insulin for 1, 2 or 4 hours. For detection of IDE and insulin, double-staining was performed on fixed cells (**Figure 36**).

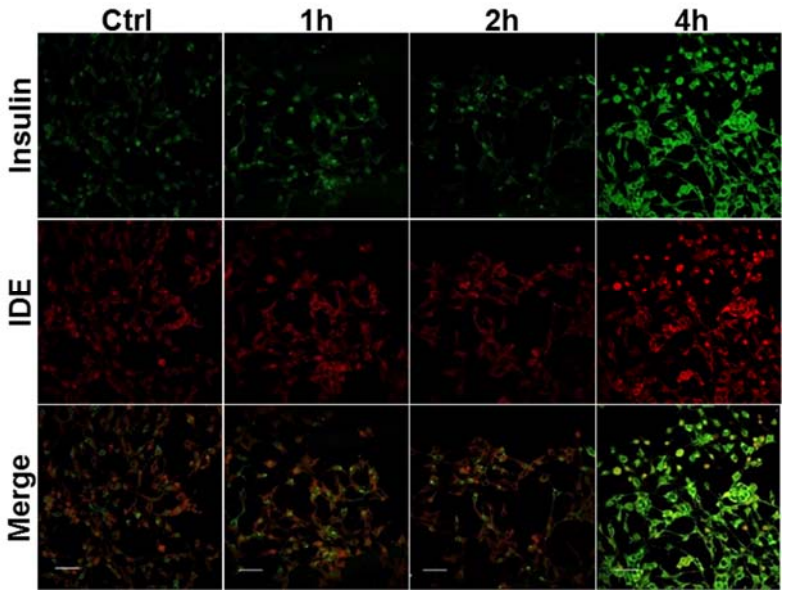

Figure 36: IDE staining in INS1-E cells after insulin treatment. Representative pictures acquired by fluorescence microscopy with 20X objective of insulin (green) and IDE staining (red) in INS1-E cells stimulated with insulin. Scale bar: 50µm.

Afterwards, IDE protein levels were measured by quantification of immunostaining intensity. IDE level in INS1-E cells was found to be significantly increased by 40% after 4 h of insulin treatment (**Figure 37**).

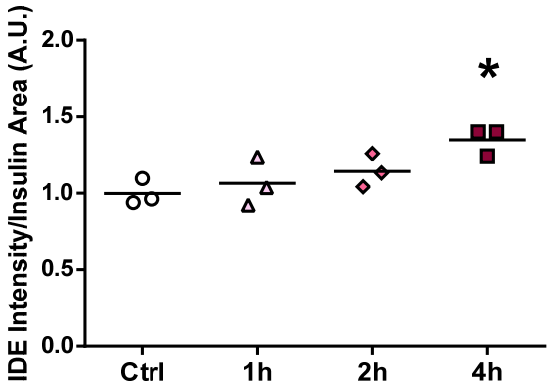

Figure 37: IDE expression in INS1-E cells after insulin treatment. IDE integrated density per insulin area in INS1-E cells stimulated with insulin. n=3 different experiments. Data are presented as mean ± SEM. *p< 0.05 versus control by one-way ANOVA.

Likewise, isolated rat islets in culture were treated for 4 hours with 500 nM insulin. Islets were fixed and paraffin embedded. Sections of these preparation were double stained with IDE + insulin or IDE + glucagon (**Figure 38**).

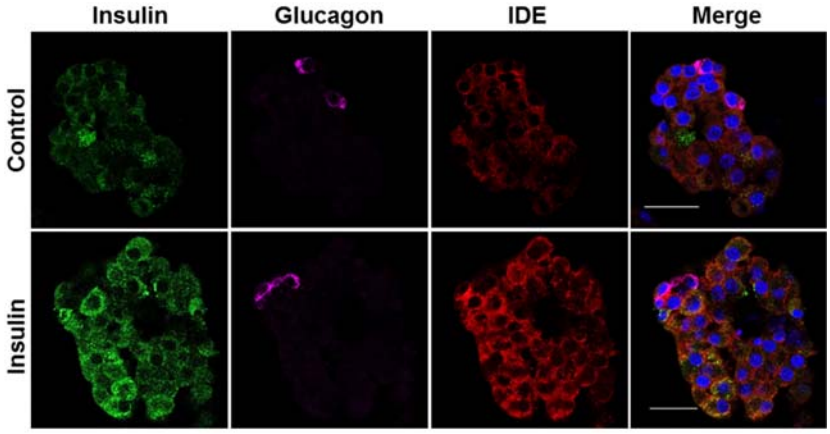

Figure 38: IDE staining in rat islets after insulin treatment. Representative pictures of insulin (green), glucagon (pink), IDE (red) and cell nuclei (blue) in rat islets treated with 500 nM insulin (Insulin) or not (Control). Scale bar: 25µm.

In the same way, quantification of IDE immunostaining intensity showed an increase of 60% of IDE expression in insulin-treated beta-cells compared to non-treated control (**Figure 39**).

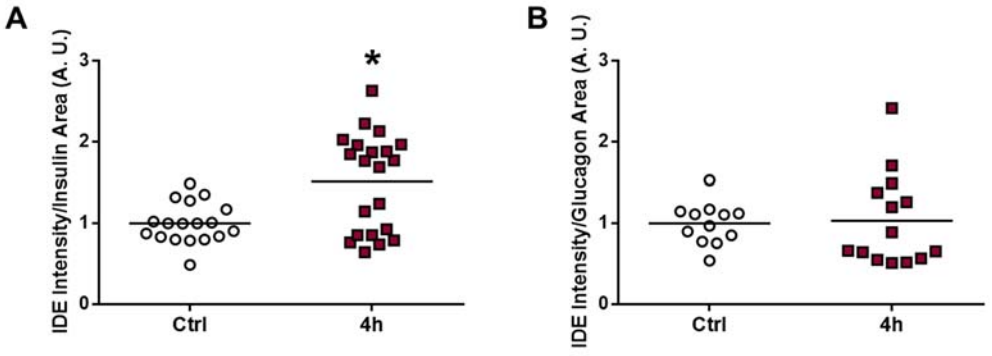

Figure 39: IDE expression in rat islets after insulin treatment. A. IDE integrated density per insulin area in rat islets stimulated with insulin. n= 18-21. **B.** IDE integrated density per glucagon area in rat islets stimulated with insulin. n= 12-14. Data are presented as mean ± SEM. *p< 0.05 versus control by Student's t test.

In addition, we had the opportunity to observe the influence of insulin treatment on IDE levels in two preparations of isolated human islets. Pancreatic islets from healthy human donors were treated with 500 nM insulin at different time points. In this case, the expression of IDE was analyzed by western-blot. As can be observed in **Figure 40**, insulin treatment triggers an increase of IDE expression at 4 hours.

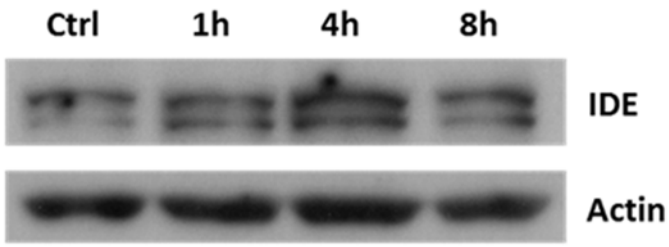

Figure 40: IDE expression in human islets after insulin treatment. Representative western-blot of IDE expression in human islets no stimulated (Ctrl) or stimulated with 500 nM insulin for 1 to 8 hours. n= 2 different human islet preparations.

These results are in accordance with findings observed in INS1-E cell line and rat islets after insulin treatment.

In summary, we have demonstrated that insulin increases IDE protein levels in pancreatic beta-cells. These results support that insulin is responsible for IDE upregulation observed in insulin-treated diabetic patients versus OHAs-treated patients (**Figure 31 B**).

Part 2. Role of IDE in pancreatic beta-cell function

2.1 TRANSIENT PHARMACOLOGICAL INHIBITION OF IDE LEADS TO IMPAIRED BETA-CELL FUNCTION

In view of our previous results, we hypothesized that IDE protein levels play a key role in the physiology of the beta-cell.

To deepen the knowledge of IDE function, we tested the impact of pharmacological inhibition of IDE activity in pancreatic beta-cells. For this purpose, the activity of IDE was decreased by pharmacological IDE inhibitors (1,10-Phenantroline and NTE-2) in different beta-cell study models. 1,10-Phenantroline is a non-specific metalloprotease inhibitor [167], meanwhile NTE-2 is an IDE-specific inhibitor designed by Lilly Research Laboratories. NTE-2 binds to an exosite of IDE to inhibit its proteolytic activity [191].

INS1-E cells were treated with 1,10-Phenantroline and its functionality was evaluated using GSIS. IDE inhibition showed impaired beta-cell function as measured by GSIS (**Figure 41)**.

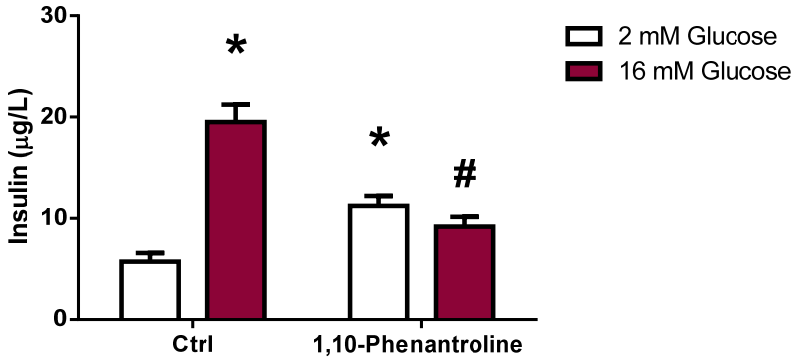

Figure 41: *In vitro* effects of transient IDE inhibition with 1,10-Phenantroline. Glucose-stimulated insulin secretion (GSIS) from INS1-E cells exposed to 2 mM glucose or 16 mM glucose after 30 min 1,10-Phenantroline treatment. n= 3 different experiments by duplicate. Data are presented as mean ± SEM.*p< 0.05 versus ctrl-2mM; #p< 0.05 versus ctrl-16mM by two-way ANOVA.

In view of these surprising results, we tried to verify these results in pancreatic islets. For this purpose, we used NTE-2. Rat islets and human islets were NTE-2 treated and later exposed to a glucose overload to verify the functionality of pancreatic beta-cells. In agreement with our previous results, islets showed a significant decrease in insulin secretion in response to high glucose levels, both in rat (**Figure 42**) and human islets (**Figure 43 A).**

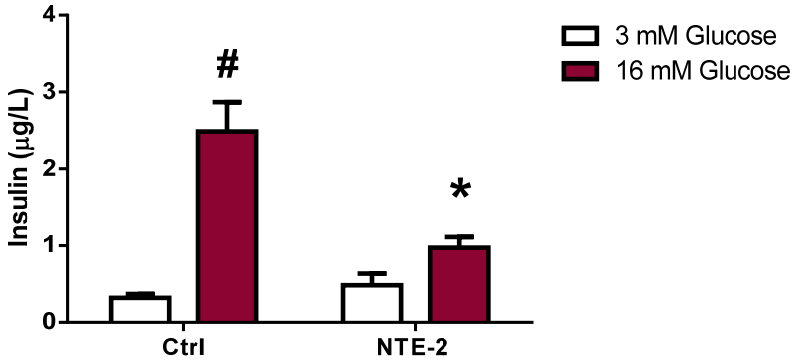

Figure 42. *Ex vivo* effects of transient IDE inhibition with NTE-2 in rat pancreatic islets. Glucose-stimulated insulin secretion (GSIS) from rat islets exposed to 2.2 mM glucose or 22mM glucose after 1h treatment with NTE-2. n= 3 different experiments by quintupled. Data are presented as mean ± SEM. #p< 0.05 versus 2.2 mM condition; *p< 0.05 versus control condition by two-way ANOVA.

Furthermore, in human islets we did not observe changes in intracellular insulin content (**Figure 43 B**). In parallel, we also measured proinsulin secretion, in order to verify the correct maturation of insulin. 1-2% proinsulin is not maturated after normal GSIS [90, 91], thus, a low percentage of insulin granules contain proinsulin. Results observed are according to normal insulin secretion, thus, discarding the presence of immature granules (**Figure 43 C-D**).

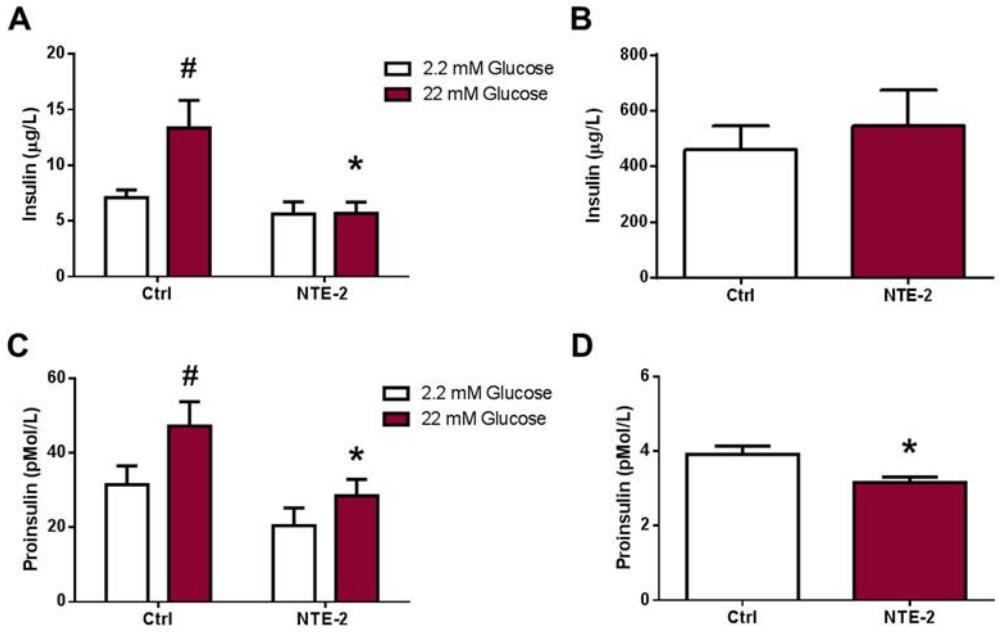

Figure 43. ***Ex vivo*** **effects of transient IDE inhibition with NTE-2 in human pancreatic islets. A.** Glucose-stimulated insulin secretion (GSIS) from human islets exposed to 2.2 mM glucose or 22mM glucose after 1h treatment with NTE-2. **B.** Intracellular levels of insulin measured from ethanol islet extracts. **C.** Proinsulin secretion (GSIS) from human islets after 1h treatment with NTE-2. **B.** Intracellular levels of proinsulin measured from ethanol islet extracts n= 2 different human islet preparations by triplicate. Data are presented as mean ± SEM. #p< 0.05 versus 2.2 mM condition; *p< 0.05 versus control condition by two-way ANOVA or by Student's t test.

In summary, these results indicate that acute pharmacological inhibition of IDE in pancreatic beta-cells causes an impairment of the secretion of insulin in response to glucose. This suggests that IDE plays a fundamental role in beta-cell function and it is probably involved in the mechanism of insulin secretion.

This fact also demonstrates the importance of our previous results in human pancreas, indicating that reduced IDE levels observed in T2DM+OHAs patients versus healthy humans is probably a signal of beta-cell dysfunction.

2.2 GENERATION AND ANALYSIS OF IDE-KO BETA-CELL LINE: INS1-E SHRNA-IDE

To further investigating the role of IDE in pancreatic beta-cell insulin secretory machinery we generated INS1-E cells lacking IDE expression, using shRNA delivered by lentiviral particles as described in Material and Methods section. In this way, we can observe how chronic ablation of IDE affects to beta-cell function. We obtained 3 different cell lines named: shRNA-C (control cell line with empty vector), shRNA-IDE p18 and shRNA-IDE p25 (each containing different target sequences against IDE).

We performed quantitative RT-QPCR to verify IDE expression in these cell lines. mRNA levels were significantly ~70% decreased in shRNA-IDE p18 cell line and ~85% decreased in shRNA-IDE p25 cell line (**Figure 44**).

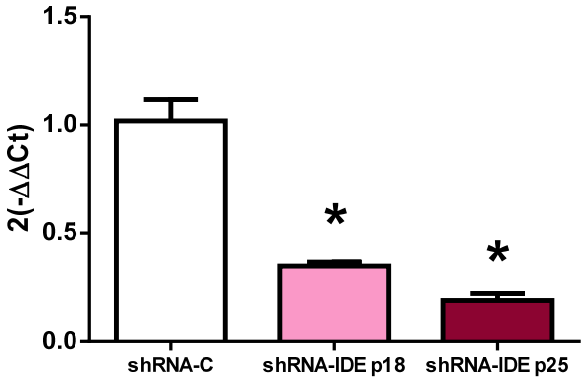

Figure 44. mRNA levels of IDE in INS1-E shRNA-IDE cells. Results of quantitative PCR measurements of IDE expression in shRNA-C, shRNA-IDE p18 and shRNA-IDE p25 cell lines. n= 3 different experiments by duplicate. Data are presented as mean ± SEM. *p < 0.05 versus shRNA-C was by one-way ANOVA.

In the same way, we also verified IDE protein levels by western-blot in order to verify IDE ablation in these cells. Approximately ~10% less protein was observed in shRNA-IDE p18 and ~30% less IDE protein in shRNA-IDE p25, indicating a higher level of ablation in shRNA-IDE p25 cell type (**Figure 45**).

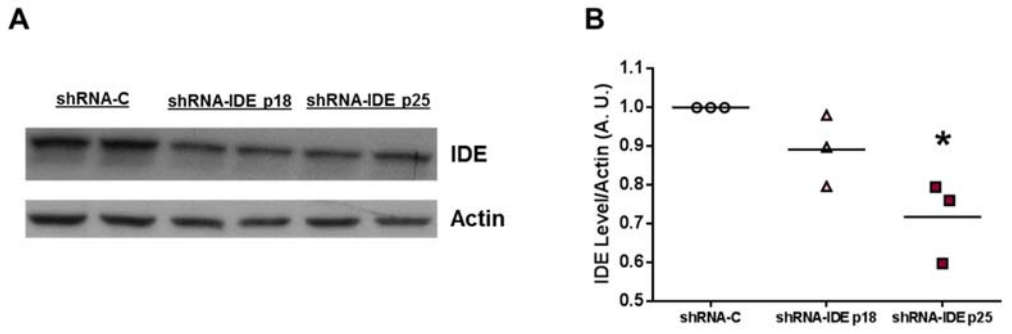

Figure 45. IDE protein levels in INS1-E shRNA-IDE cells. A. Representative IDE/Actin western-blot of shRNA-C, shRNA-IDE p18 and shRNA-IDE p25 cell lines. **B.** Quantification of IDE/Actin western-blot. n= 3 different experiments. Data are presented as mean ± SEM. *p < 0.05 versus shRNA-C by one-way ANOVA.

In summary, these results clearly show that IDE knockdown worked efficiently in these newly generated beta-cell lines.

2.2.1 INSULIN SECRETION IS IMPAIRED IN SHRNA-IDE INS1-E CELL LINE

To characterize theses cell lines, we first tested beta-cell function. To this end, we analyzed glucose-stimulated insulin secretion (GSIS). Consistent with our previous findings, IDE suppression in beta-cells resulted in a marked decreased insulin secretion in response to glucose overload (**Figure 46**).

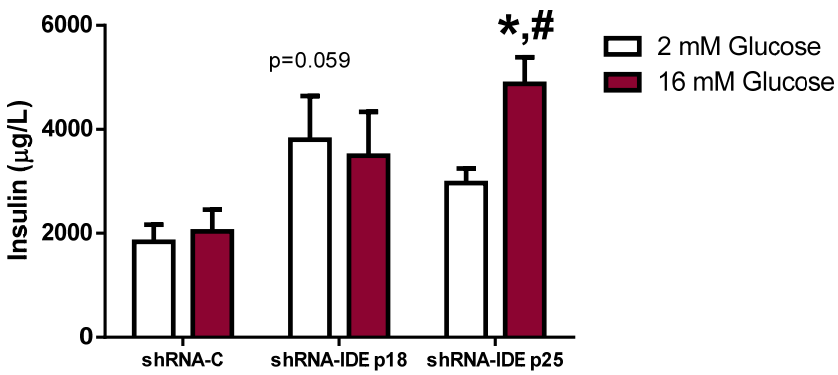

Figure 46. ***In vitro*** **effects of IDE inhibition on insulin secretion in INS1-E shRNA-IDE cells.** Glucose-stimulated insulin secretion (GSIS) in INS1-E cell lines exposed to 2 mM glucose or 16mM glucose. n= 3 different experiments by duplicates. Data are presented as mean ± SEM. $^{*}p< 0.05$ versus 2mM condition. $^{\#}p< 0.05$ versus shRNA-C by two-way ANOVA.

2.2.2 IDE ABLATION INCREASES INTRACELLULAR INSULIN CONTENT IN INS1-E CELLS

With regard to intracellular content of insulin after performing GSIS, cell lines lacking IDE shRNA-IDE p18 and shRNA-IDE p25 showed higher levels of intracellular insulin content than control cells probably due to the chronic defect on insulin secretion (**Figure 47**).

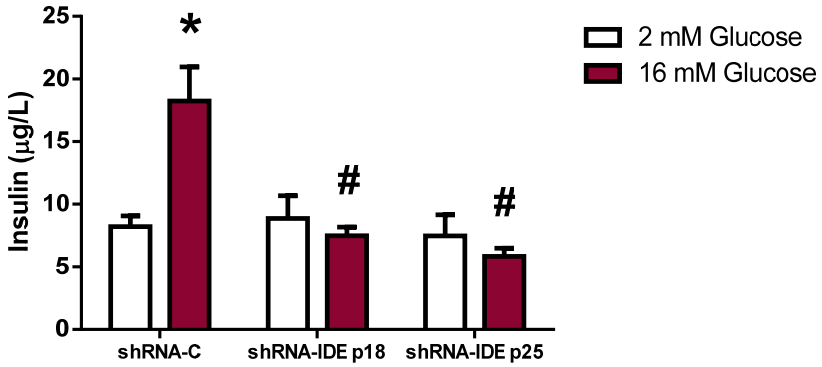

Figure 47. Intracellular insulin content in INS1-E shRNA-IDE cells. Insulin was measured on ethanol cell extracts after glucose-stimulated insulin secretion (GSIS) from shRNA-C, shRNA-IDE p18 and shRNA-IDE p25 cell lines exposed to 2 mM glucose or 16mM glucose. n= 3 different experiments by duplicate. Data are presented as mean ± SEM. *p< 0.05 versus 2mM condition. #p< 0.05 versus shRNA-C by two-way ANOVA

To understand the causes of insulin secretion impairment we studied INS1-E shRNA-IDE p25 ultrastructure by electronic microscopy, showing that there was 2-fold density of insulin granules in shRNA-IDE p25 cells after glucose overload when compared to control cells, which points to a defect on insulin vesicles mobility across the cytoplasm (**Figure 48**).

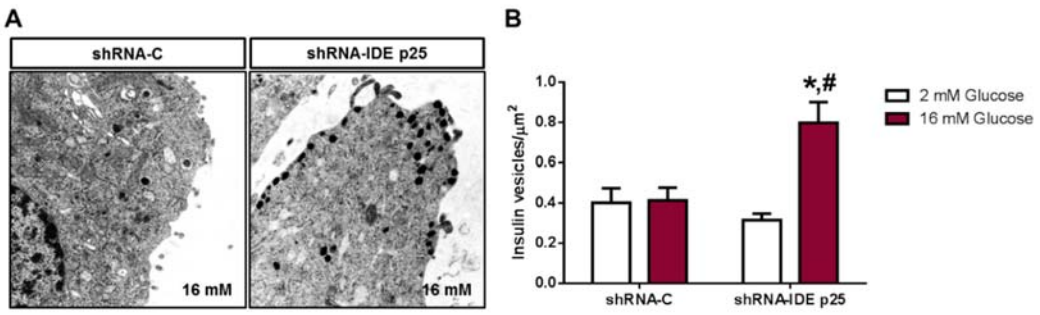

Figure 48. Intracellular insulin vesicle density in INS1-E shRNA-IDE cells. A. Representative images acquired by electron microscopy from shRNA INS1-E cells. **B.** Quantification of insulin vesicle density in shRNA INS1-E cells after GSIS. n=16-21 cells per condition. Data are presented as mean ± SEM. *p< 0.05 versus 2mM condition. #p< 0.05 versus shRNA-C by two-way ANOVA.

2.3 GENERATION AND ANALYSIS OF BETA-CELL SPECIFIC IDE KNOCK-OUT MICE

Analyzing all these previous *in vitro* results, we can clearly confirm that IDE plays a key role in the correct function of the beta-cell. Taken together, these results indicate that acute deletion/inhibition of IDE *in vitro* (INS1-E) and *ex vivo* (isolated islets) leads to impaired GSIS. However, these studies do not address the effect of chronic deficiency of IDE specifically in the beta-cell nor they reveal any insight on the role of IDE in the beta-cell *in vivo*. For that purpose, we generated an *in vivo* model to study the long-term effect of the ablation of this protein: beta-cell specific IDE knock-out mice.

Pancreatic beta-cell specific IDE knock-out mice were generated by breeding mice homozygous for a floxed *Ide* allele $Ide^{flox/flox}$ [193] with transgenic mice that express Cre recombinase cDNA under the control of the insulin promoter Ins-Cre [195], which is active in pancreatic beta-cells. Thus, we obtained our experimental litter $Ide^{flox/flox}$*; Ins-Cre/*+, named hereafter B-IDE-KO, and their controls $Ide^{flox/flox}$*;* +/+ or $Ide^{flox/+}$*;* +/+.

In order to verify IDE loss of expression in beta-cells, pancreatic islets were obtained from WT ($Ide^{flox/flox}$*;* +/+), HT ($Ide^{flox/+}$*;* Ins-Cre/+), B-IDE-KO ($Ide^{flox/flox}$*; Ins-Cre/*+) and from Total-IDE-KO mice ($Ide^{flox/flox}$*; Cre/*+). Islets extracts were prepared and IDE protein was detected by western-blot. IDE appears drastically decreased in B-IDE-KO islets compared to WT islets both by western-blot. There is a slight IDE band at 110 kDa in B-IDE-KO due to 20% non-beta-cells present in pancreatic islets (**Figure 49**).

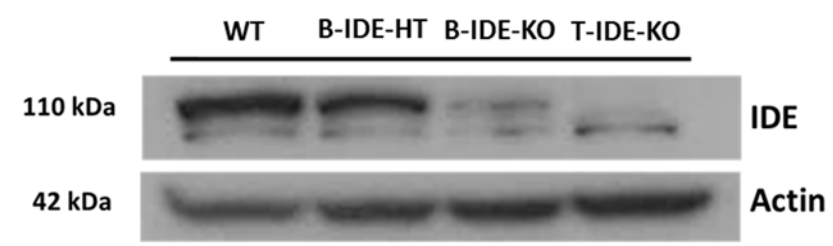

Figure 49. IDE expression in B-IDE-KO mice islets. Representative IDE western blot of isolated islets lysates from WT, HT, B-IDE-KO and Total IDE-KO mice using anti-IDE and anti-actin antibodies.

We also checked IDE loss of expression in beta-cells by immunofluorescence, where we verified that IDE was ablated in beta-cells, but it was still present in the rest of the cell types of the islet (**Figure 50**).

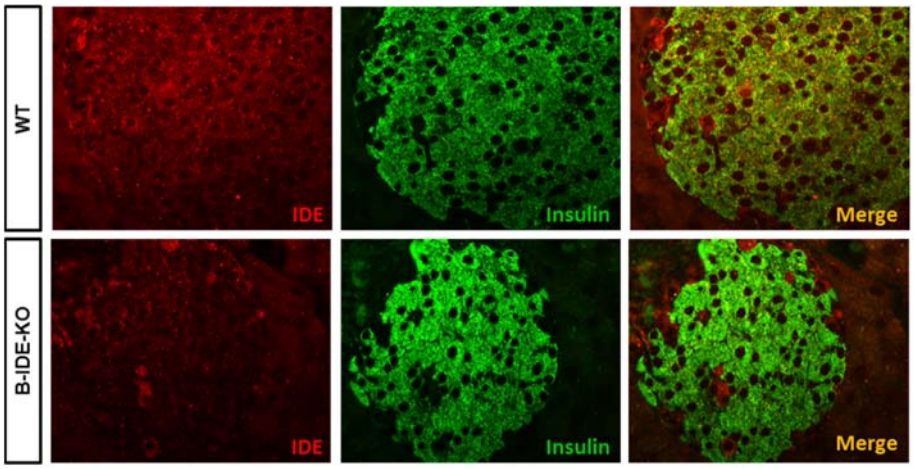

Figure 50. IDE expression in B-IDE-KO mice pancreas. Representative images acquired by fluorescence microscopy with 40X objective from WT and B-IDE-KO mice. IDE (red) and Insulin (green).

To determine whether IDE genetic ablation was tissue specific we performed IDE quantitative PCR of pancreatic islets, skeletal muscle, kidney, liver and hypothalamus (**Figure 51)**. IDE mRNA levels were reduced by 70% in pancreatic islets. No differences were observed in the rest of tissues between B-IDE-KO and WT mice.

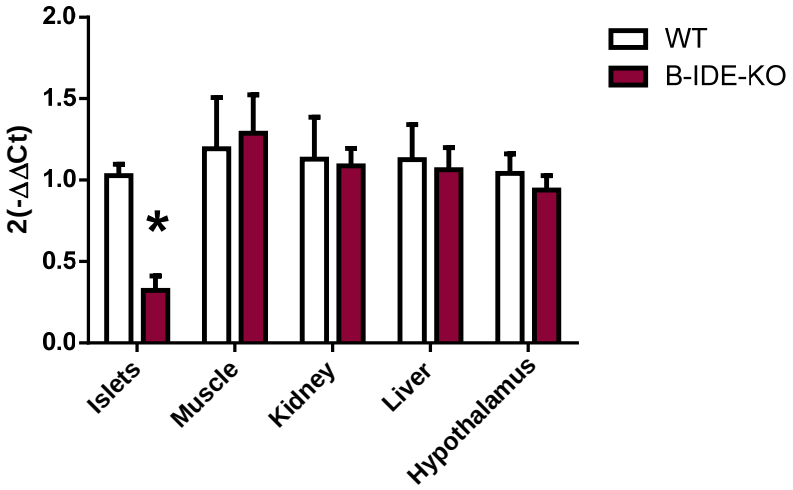

Figure 51. IDE expression in B-IDE-KO mice body. Quantitative PCR measurements of IDE expression in isolated mRNA from different tissues of B-IDE-KO and WT mice. n=3 WT; n=2 B-IDE-KO. All samples were normalized by L18 mRNA. Data are presented as mean ± SEM. *p < 0.05 versus WT by two-way ANOVA.

2.4 METABOLIC CHARACTERIZATION OF B-IDE-KO MICE

In order to clarify the role of IDE on pancreatic beta-cells and insulin secretion, we performed metabolic characterization of B-IDE-KO mice at 2 and 6 months of age.

2.4.1 BODY WEIGHT IS UNCHANGED IN B-IDE-KO MICE

First, we checked if body weight of B-IDE-KO mice was altered compared to WT mice. We observed that body weight remains unchanged in B-IDE-KO mice (**Figure 52**).

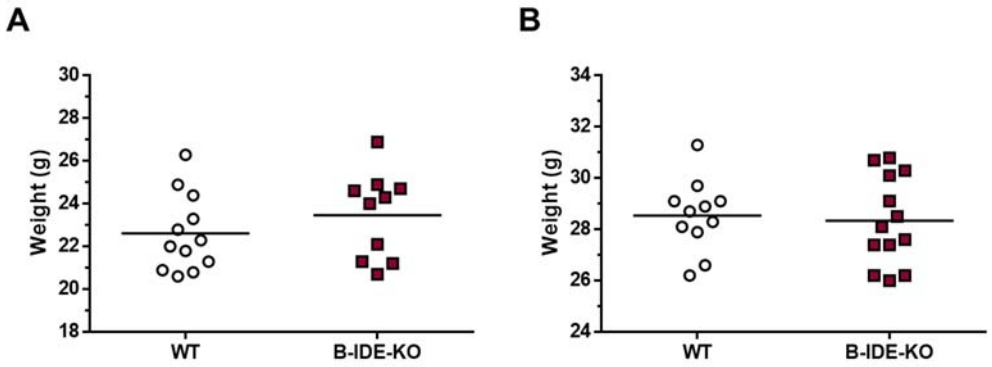

Figure 52. Body weight of B-IDE-KO mice at 2 and 6 months. A. Body weight of mice at 2 months. **B.** Weight of mice at 6 months. n=10–13 mice per genotype. Data are presented as mean ± SEM.

2.4.2 B-IDE-KO MICE EXHIBIT MILD NON-FASTING HYPERGLYCEMIA

We measured blood glucose and plasma insulin levels in fasting and non-fasting conditions. These measurements were done at 2 and 6 months of age (**Figure 53 and 54**).

Fasting glucose at 6 and 16 h were normal (**Figures 53 A-B and 54 A-B**), as well as non-fasting insulin levels (**Figures 53 C and 54 C**). However, B-IDE-KO mice showed increased non-fasting glucose levels at 6 months of age (**Figure 54 C**).

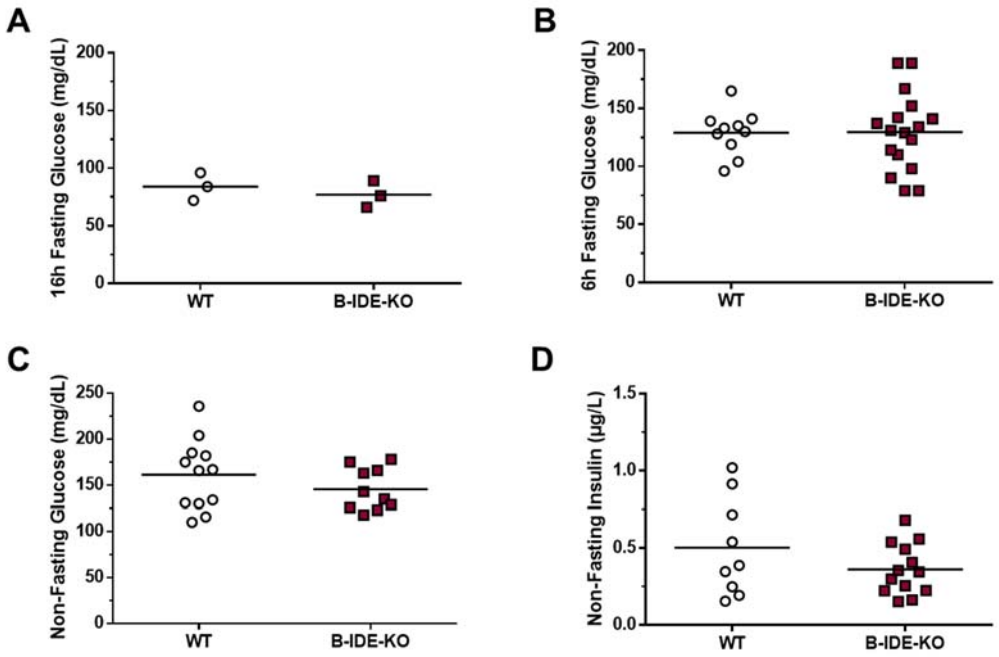

Figure 53. Circulating levels of glucose and insulin of B-IDE-KO mice at 2 months. **A.** Blood glucose levels under 16h fasting conditions **B.** Blood glucose levels under 6h fasting conditions **C.** Blood glucose levels under non-fasting conditions **D.** Plasma insulin levels under non-fasting conditions. n=3–20 mice per genotype.

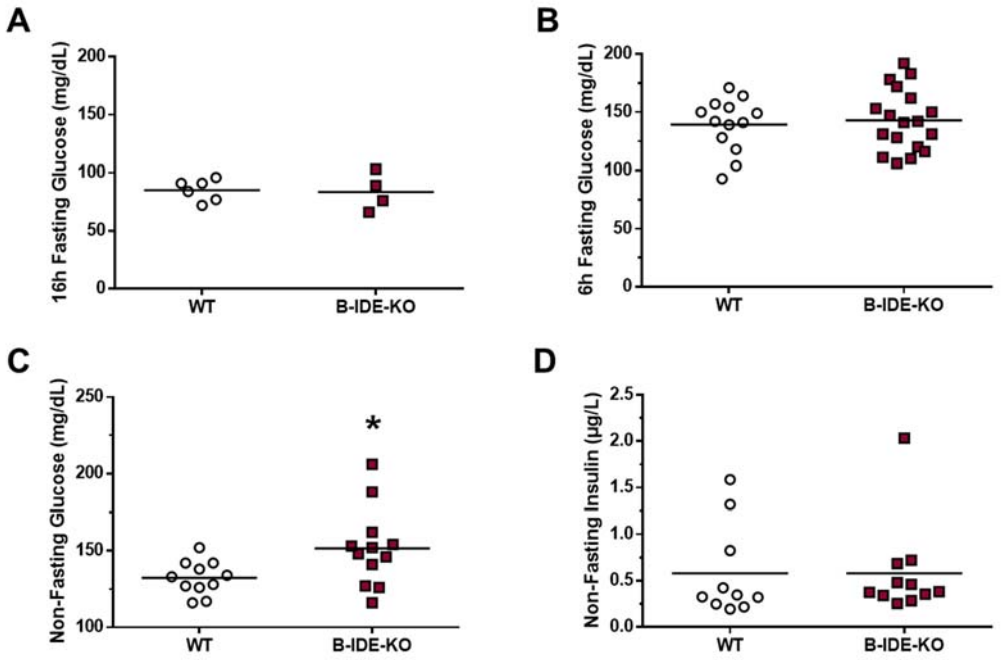

Figure 54. Circulating levels of glucose and insulin of B-IDE-KO mice at 6 months. **A**. Blood glucose levels under 16h fasting conditions **B.** Blood glucose levels under 6h fasting conditions **C.** Blood glucose levels under non-fasting conditions **D.** Plasma insulin levels under non-fasting conditions. n=6–18 mice per genotype. Data are presented as mean ± SEM. *p<0.05 versus WT by Student's t test.

2.4.3 PLASMA C-PEPTIDE LEVELS ARE INCREASED IN B-IDE-KO MICE

To understand the role of IDE in insulin metabolism, we checked circulating C-peptide levels both in fasting and not fasting conditions, as after intraperitoneal glucose overload (IP-GTT). B-IDE-KO exhibited a slight tendency toward higher levels at 2 months (**Figure 55**) and increased plasma C-peptide levels when compared to WT mice at 6 months of age (**Figure 56**).

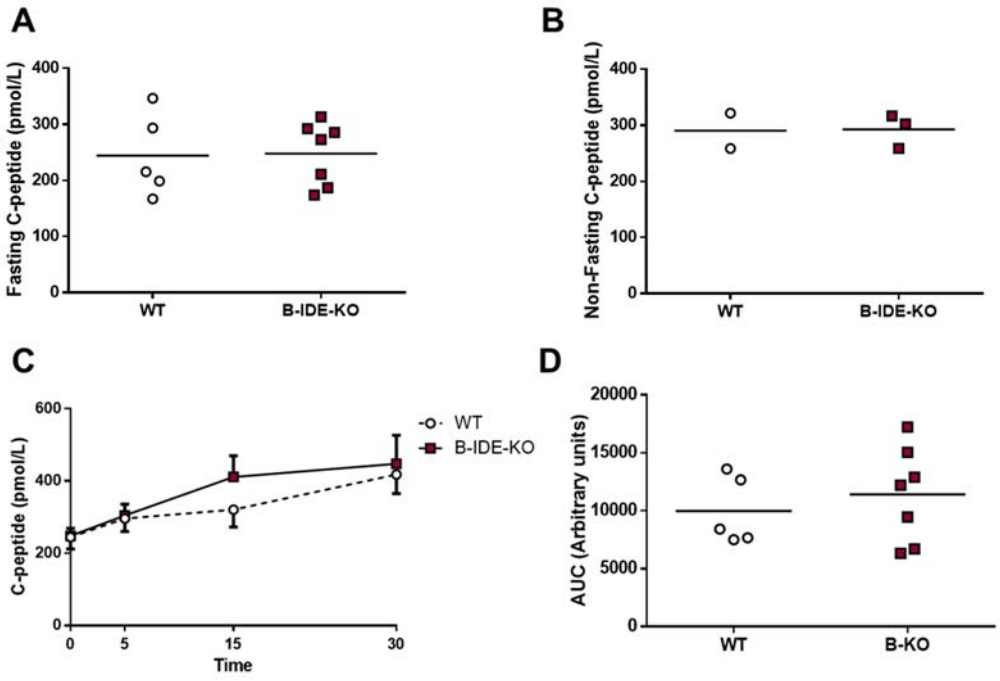

Figure 55. Circulating C-peptide levels after a glucose challenge at 2 months in B-IDE-KO mice. A. Plasma C-peptide levels under fasting conditions. **B.** Plasma C-peptide levels under non-fasting conditions. **C.** Plasma C-peptide levels at 0, 5, 15 and 30 min after intraperitoneal injection of glucose (2g/kg) n=2-5 WT; n=3-7 B-IDE-KO. **D.** Area under the curve of figure A. Data are presented as mean ± SEM. *p<0.05 by Student's t test.

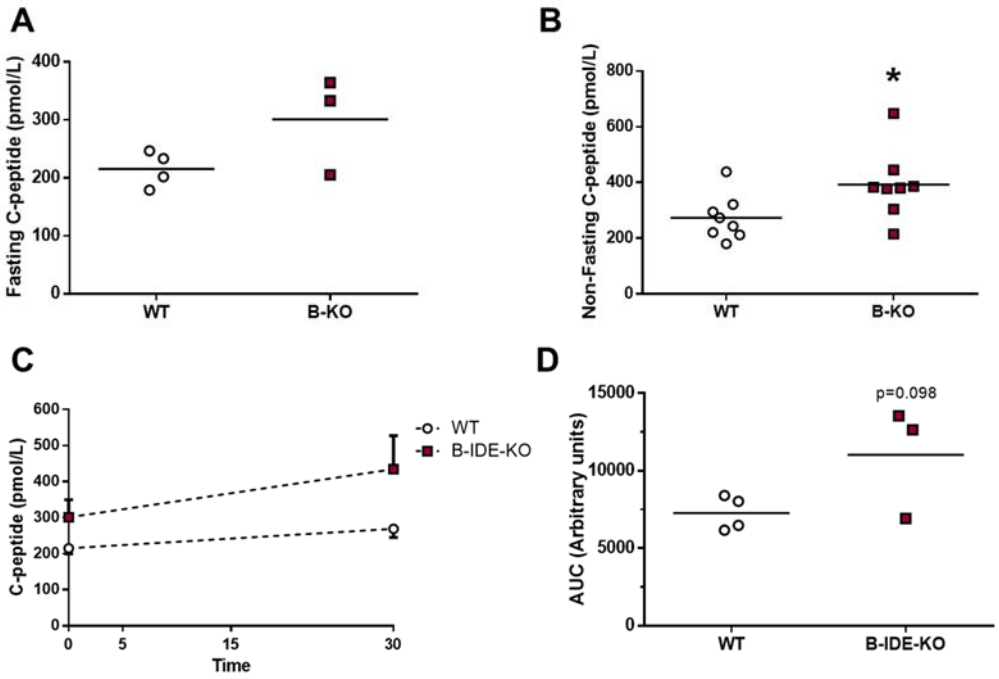

Figure 56. Circulating C-peptide levels after glucose challenge at 6 months in B-IDE-KO mice. A. Plasma C-peptide levels under fasting conditions. **B.** Plasma C-peptide levels under non-fasting conditions. **C.** Plasma C-peptide levels at 0, 5, 15 and 30'min after intraperitoneal injection of glucose (2g/kg) n=4-8 WT; n=3-8 B-IDE-KO. **D.** Area under the curve of figure C. Data are presented as mean ± SEM. *p<0.05 versus WT by Student's t test.

This data is pointing that beta-cells in our B-IDE-KO mice could be secreting higher insulin levels than WT mice

2.4.4 MILD GLUCOSE INTOLERANCE AND INSULIN RESISTANCE IN B-IDE-KO

Glucose homeostasis was analyzed in B-IDE-KO mice by IP-GTT at 2 and 6 months of age. Intraperitoneal glucose tolerance test revealed normal glucose tolerance in B-IDE-KO mice at 2 months (**Figure 57**), and significant hyperglycemic levels at 15 minutes after glucose overload at 6 months of age (**Figure 58 A**).

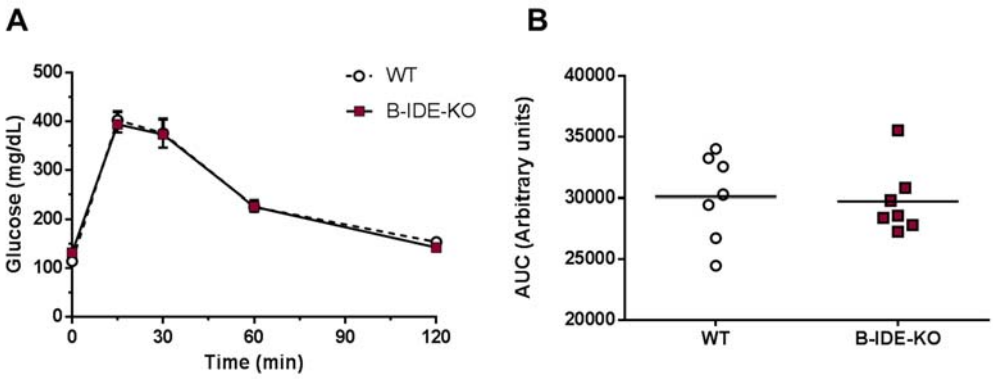

Figure 57. Intraperitoneal Glucose Tolerance Test at 2 months in B-IDE-KO mice. A. IP-GTT: Blood glucose levels after glucose challenge (2g/kg). **B.** Area under the curve of figure A. n=7 WT; n=7 B-IDE-KO. Data are presented as mean ± SEM.

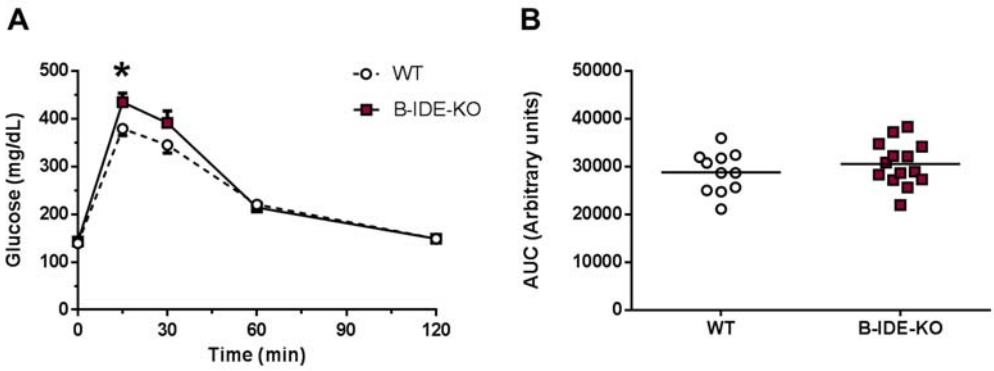

Figure 58. Intraperitoneal Glucose Tolerance Test at 6 months in B-IDE-KO mice. A. IP-GTT: Blood glucose levels after glucose challenge (2g/kg). **B.** Area under the curve of figure A. n=11 WT; n=14 B-IDE-KO. Data are presented as mean ± SEM. *p<0.05 versus WT by Student's t test.

Taking into account that C-peptide levels were increased in circulation, these results point out to a possible insulin resistance state.

To demonstrate this end, we obtained livers from WT and B-IDE-KO mice. mRNA and cDNA were obtained and levels of *Pck1* (phosphoenolpyruvate carboxykinase 1) and *G6pc* (glucose-6-phosphatase) were quantified to study the expression of the main enzymes implicated in hepatic gluconeogenesis. As shown in **Figure 59**, mRNA levels of both enzymes are significantly elevated, confirming an increase in hepatic gluconeogenesis in B-IDE-KO mice.

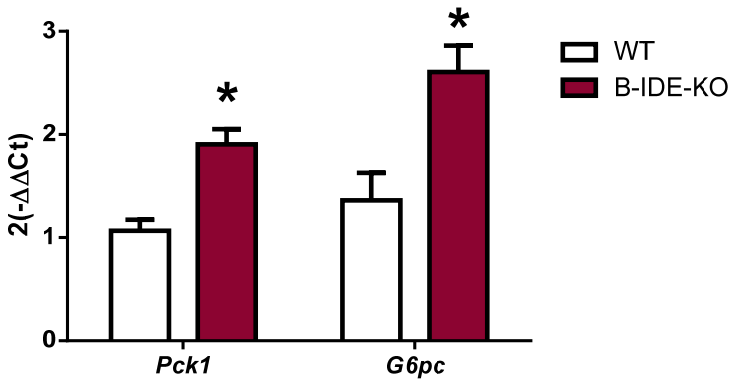

Figure 59. Analysis of B-IDE-KO mouse liver genes involved in hepatic gluconeogenesis by qPCR. Results of quantitative PCR experiments showing expression of *Pck1* and *G6pc* genes normalized to *L18* expression as housekeeping gene in B-IDE-KO and WT mouse livers at 6 months of age. Each bar is the mean of liver extracts from 4-5 different mice per group in triplicate for each condition. Data are expressed using the (2−ΔΔCt) formula ± SEM. *p < 0.05 *vs.* WT by Student's t test.

Furthermore, we investigated insulin sensitivity in B-IDE-KO and WT mice using intraperitoneal insulin tolerance test (IP-ITT).

At 2 months of age, B-IDE-KO mice showed the same insulin sensitivity as WT mice (**Figure 60**).

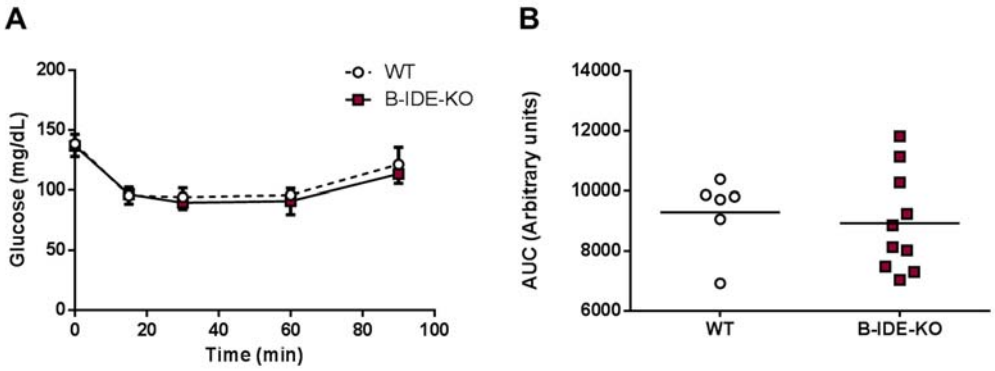

Figure 60. Insulin Tolerance Test at 2 months in B-IDE-KO mice. A. ITT: Blood glucose levels after insulin injection (0.75 U/kg). **B.** Area under the curve of figure A. n=6 WT; n=10 B-IDE-KO. Data are presented as mean ± SEM.

Likewise, insulin sensitivity of 6-month old B-IDE-KO mice remained unchanged compared to WT mice (**Figure 61**).

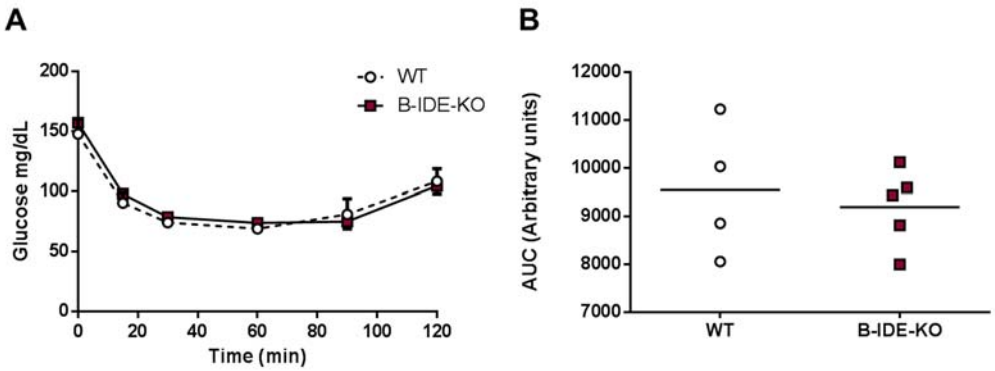

Figure 61. Insulin Tolerance Test at 6 months in B-IDE-KO mice. A. ITT: Blood glucose levels after insulin injection (1.5 U/kg). **B.** Area under the curve of figure A. n=4 WT; n=5 B-IDE-KO. Data are presented as mean ± SEM.

Although IP-ITT shows normal curves for B-IDE-KO mice, increased gluconeogenesis enzymes points to dysregulated hepatic metabolism that is compatible with hepatic insulin resistance.

2.5 FUNCTIONAL CHARACTERIZATION OF B-IDE-KO MOUSE ISLETS

After the metabolic characterization, both whole pancreas and pancreatic islets were extracted. Morphometric, functional and genetic studies were carried out to clarify the effect of IDE ablation on beta-cells *ex vivo*.

2.5.1 *IDE* ABLATION IN PANCREATIC BETA-CELLS ALTERS NEITHER PANCREATIC ALPHA- NOR BETA-CELL AREA

Beta- and alpha-cell area were analyzed trying to understand if a defect in beta- and/or alpha-cell area may be responsible for altered C-peptide levels. Beta- and alpha-cell area were unchanged in B-IDE-KO mice compared with WT mice (**Figure 62** and **Figure 63**).

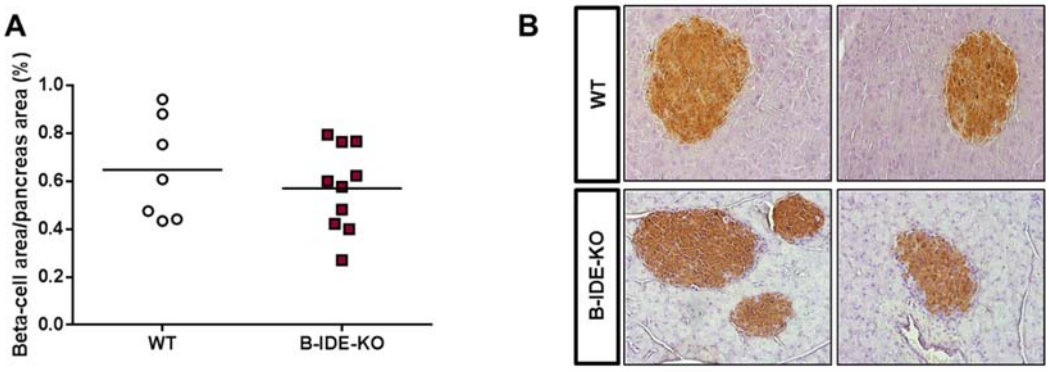

Figure 62. Quantification of beta-cell area in B-IDE-KO mice. A. Beta-cell area of 6 months old B-IDE-KO mice. n=7 WT; n=10 B-IDE-KO. **B.** Representative images of insulin staining. Data are presented as mean ± SEM.

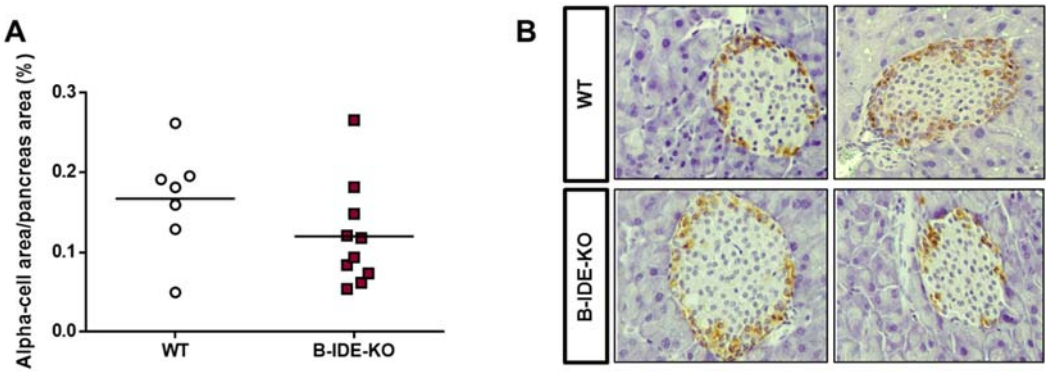

Figure 63. Quantification of alpha-cell area in B-IDE-KO mice. A. Alpha-cell area of 6 months old B-IDE-KO mice. n=7 WT; n=10 B-IDE-KO. **B.** Representative images of glucagon staining. Data are presented as mean ± SEM.

Therefore, changes in endocrine cell mass were not responsible of altered C-peptide levels observed in these mice.

2.5.2 *IDE* ABLATION IN PANCREATIC BETA-CELLS LEADS TO CONSTITUTIVE AND DYSREGULATED INSULIN SECRETION

After observing the dysregulated plasma C-peptide levels of the B-IDE-KO mouse, pancreatic islets were extracted to analyze insulin secretion of these cells ex-vivo. In this way, we would not have any interference from the rest of tissues and we could observe directly how IDE ablation affects to the insulin release from beta-cells in response to glucose.

Therefore, we analyzed glucose-stimulated insulin secretion (GSIS) from B-IDE-KO islets. As expected, B-IDE-KO islets showed a ~70-50% decreased insulin release in response to a glucose challenge compared to WT mice. Surprisingly, B-IDE-KO islets showed constitutive insulin secretion independently of glucose concentrations, which is a typical characteristic of immature beta-cells [72, 79,

199]. These phenotypes are maintained over time, as we can see in islets of mice at 2 and 6 months of age (**Figures 64 and 65**).

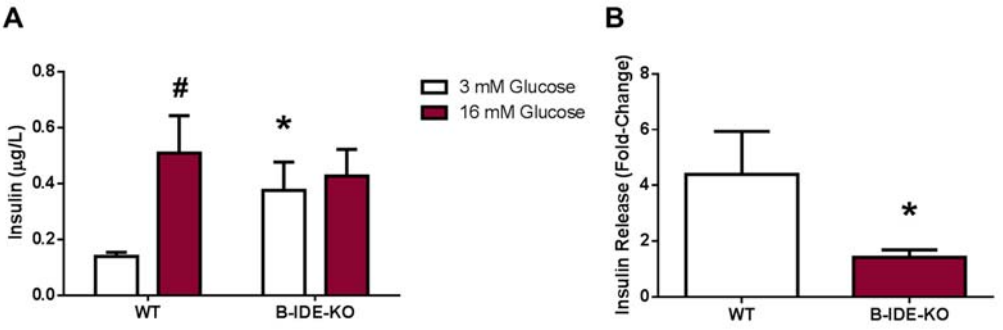

Figure 64. ***In vivo*** **effects of genetic ablation of IDE in pancreatic beta-cells on GSIS at 2 months. A.** Glucose-stimulated insulin secretion (GSIS) from B-IDE-KO mice islets exposed to 3 mM glucose or 16 mM glucose. **B.** Fold change of insulin release. n=3 WT; n=3 B-IDE-KO islets preparations by triplicate. Data are presented as mean ± SEM. #p<0.05 versus 3mM condition; *p<0.05 versus WT condition by two-way ANOVA or by Student's t test.

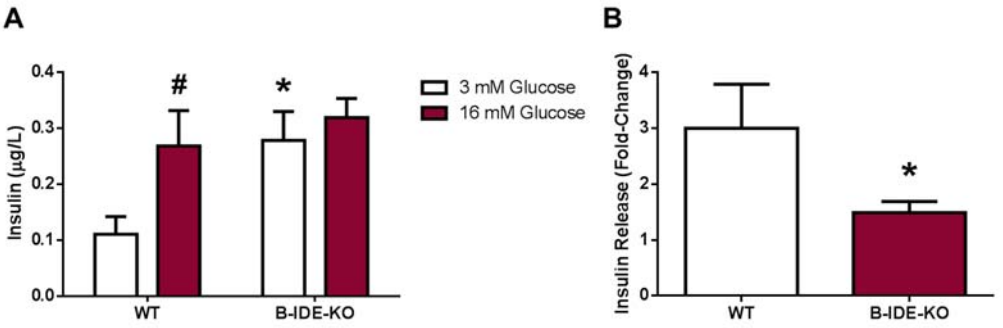

Figure 65. ***In vivo*** **effects of genetic ablation of IDE in pancreatic beta-cells on GSIS at 6 months. A.** Glucose-stimulated insulin secretion (GSIS) from B-IDE-KO mice islets exposed to 3 mM glucose or 16 mM glucose. **B.** Fold change of insulin release. n=3 WT; n=4 B-IDE-KO islets preparations by triplicate. Data are presented as mean ± SEM. #p<0.05 versus 3mM condition; *p<0.05 versus WT condition by two-way ANOVA or by Student's t test.

Intracellular insulin content of islets was analyzed, without observing any significant change (**Figure 66**). These results points out to normal insulin production but a failure in insulin secretion.

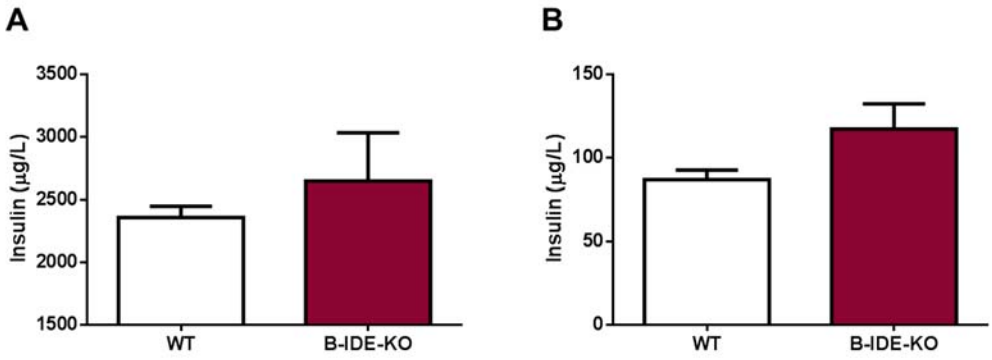

Figure 66. Intracellular insulin content of B-IDE-KO mice islets. A. Intracellular insulin content of B-IDE-KO mice islets at 2 months. n=3 WT; n=3 B-IDE-KO islets preparations by triplicate. **B.** Intracellular insulin content of B-IDE-KO mice islets at 6 months. n=3 WT; n=4 B-IDE-KO islets preparations in triplicate.

2.5.3 *IDE* ABLATION IN PANCREATIC BETA-CELLS LEADS TO INCREASED PROINSULIN SECRETION

In the same way, we analyzed proinsulin secretion in response to GSIS. We observed that islets from B-IDE-KO mice, there is a higher secretion of proinsulin than in those from WT mice, mostly at 2 months old (**Figure 67**).

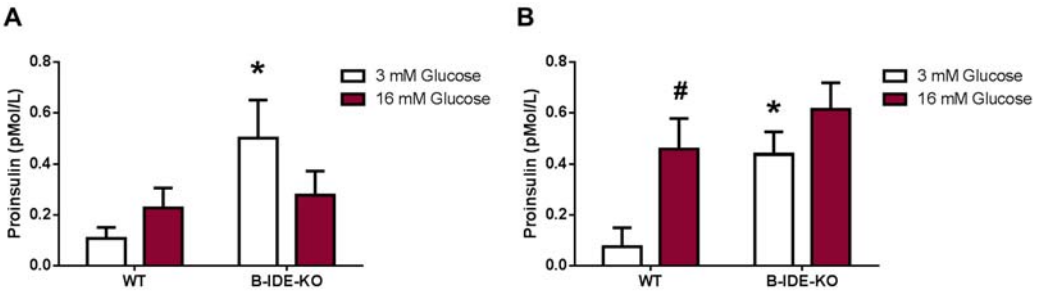

Figure 67. Proinsulin release of B-IDE-KO mice islets. A. Proinsulin release after GSIS from B-IDE-KO mice islets at 2 months. n=3 WT; n=3 B-IDE-KO islets preparations by triplicate. **B.** Proinsulin release GSIS from B-IDE-KO mice islets at 6 months. n=3 WT; n=4 B-IDE-KO islets preparations by triplicate. #p<0.05 versus 3mM condition; *p<0.05 versus WT condition by two-way ANOVA.

This over-secretion of proinsulin indicates poor insulin processing. This is another characteristic process that is related to the immaturity of the pancreatic beta-cell [79].

These results are supported by lower levels in B-IDE-KO mouse islets of *Pcsk1/3* and *Pcsk2,* genes encoding enzymes in charge of proinsulin processing to generate mature insulin (**Figure 68**).

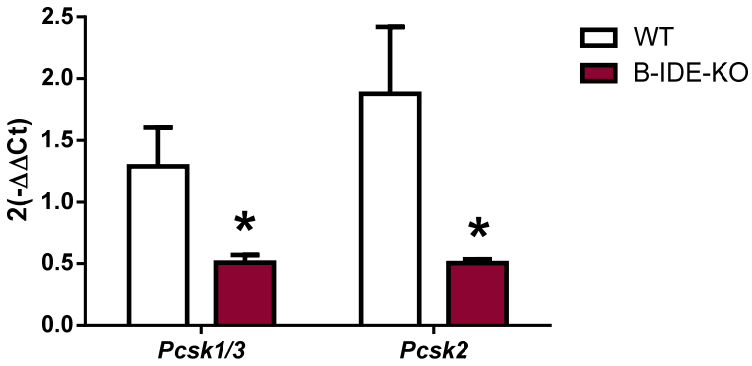

Figure 68. Analysis of B-IDE-KO mice islets genes involved in insulin processing by qPCR. Results of quantitative PCR experiments showing expression of *Pcsk1/3* and *Pcsk2* genes normalized to *L18* expression as housekeeping gene in B-IDE-KO and WT mice islets. Each bar is the mean of islets from 3-5 different mice per group in duplicate for each condition. Data are expressed using the (2−ΔΔCt) formula ± SEM. *p < 0.05 *vs.* WT by Student's t test.

In summary, the phenotype of B-IDE-KO beta-cells has similarities to that observed in previous *in vitro* studies. In both cases, the secretion of insulin is dysregulated. However, in the *in vivo* situation, we also observed disturbances, such as constitutive insulin release in parallel with augmented proinsulin secretion. These results support a potential phenotype of beta-cell immaturity [71, 72, 78, 79].

2.5.4 *IDE* ABLATION IN PANCREATIC BETA-CELL ALTERS THE EXPRESSION OF GENES INVOLVED IN THE INSULIN SECRETORY PATHWAY AND BETA-CELL DEVELOPMENT

In an attempt to elucidate the molecular mechanisms underlying this loss-of-mature beta-cell phenotype, we analyzed islets mRNA levels by RT-qPCR of several transcription factors that are thought to be required for beta-cell maturity: *Ins1*, *Ins2*, *NKx2-2*, *NKx6-1*, *Pax6*, *Pdx1*, *Neurod1*, *Mafa*, *Mafb*, *UCN3* and *Syt4* (**Figure 69**) These genes are described in **Table 10 and 11** of the Material and Methods section, above.

Among genes checked for beta-cell maturity, *Ins2* gene was decreased ~60% in B-IDE-KO mice; as well as *Ucn3* gene, with a ~40% decrease observed (**Figure 69**).

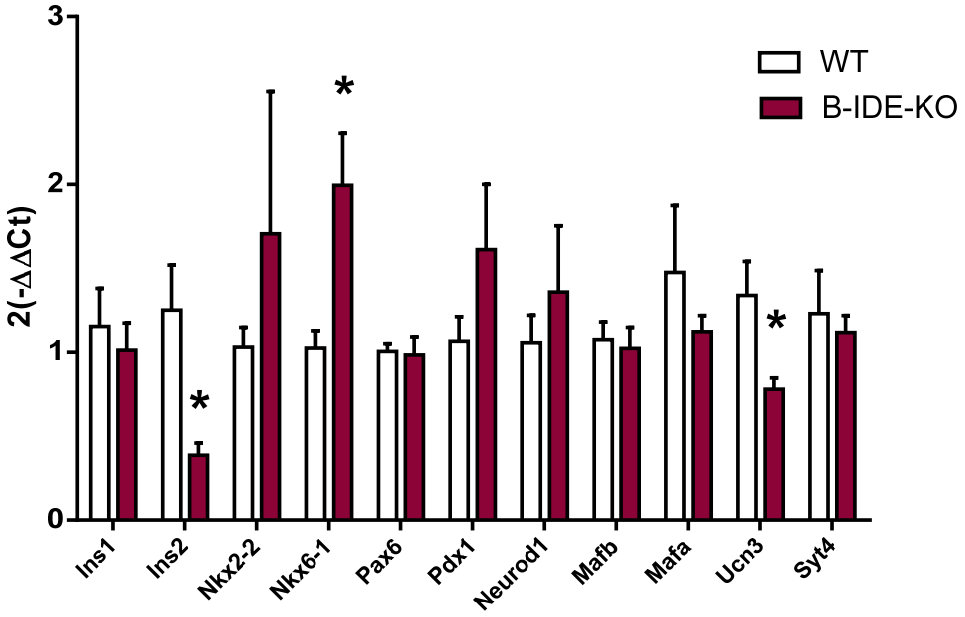

Figure 69. Analysis of B-IDE-KO mice islets genes involved in beta-cell maturity by qPCR. Results of quantitative PCR experiments showing expression of different genes normalized to *L18* expression as housekeeping gene in B-IDE-KO and WT mice islets at 6 months old. Each bar is the mean of islets from 3-6 different mice per group in duplicate for each condition. Data are expressed using the (2−ΔΔCt) formula ± SEM. *p < 0.05 versus WT by Student's t test.

We also used RT-qPCR to quantify the expression of key proteins for insulin secretory machinery: GLUT2 (*Slc2a2*), GLUT1 (*Slc2a1*), GLUT3 (*Slc2a3*), glucokinase (*Gck*), ATP-sensitive potassium channel subunits Kir6.2 (*Kcnj11*) and Sur1 (*Abcc8*), and calcium voltage-gated channel Cav2.1 (*Cacna1a*) (**Figure 70**). These genes are described in **Table 10 and 11** of the Material and Methods section, above.

Interestingly, we found that most of the genes involved in the secretory machinery of the beta-cell were upregulated significantly with respect to WT mice (GLUT1, glucokinase, Sur1 and calcium channel), which nicely correlates with activation of cell metabolism and constitutive insulin secretion observed in B-IDE-KO islets (**Figure 70**). The increase in *Scl2a1* levels is particularly notable, as it points to an increase in GLUT1 transporter; meanwhile, GLUT2, which is the main glucose transporter in mouse beta-cells, remains unchanged.

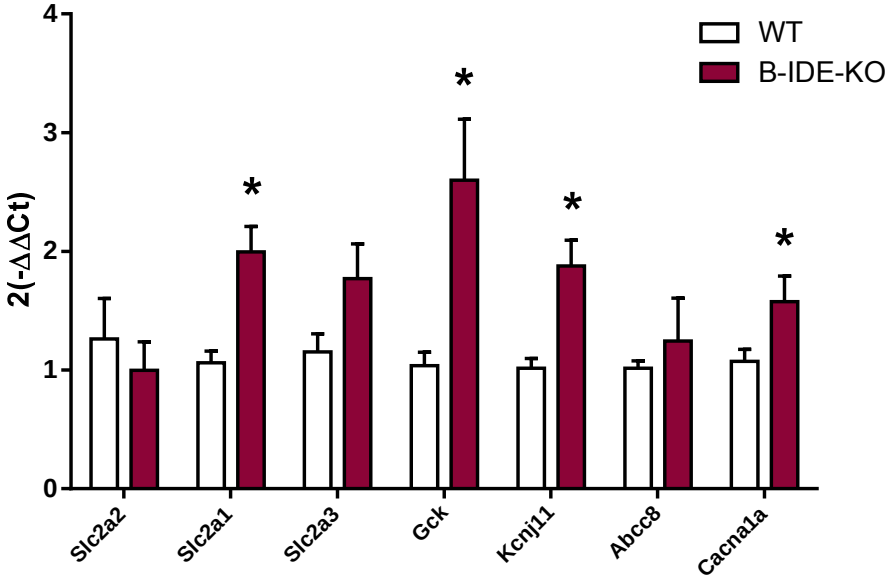

Figure 70. Analysis of B-IDE-KO mice islets beta-cell secretory machinery by qPCR. Results of quantitative PCR experiments showing expression of different genes normalized to *L18* expression as housekeeping gene in B-IDE-KO mice islets. Each bar is the mean of islets from 3-6 different mice per group in duplicate for each condition. Data are expressed using the (2−ΔΔCt) formula ± SEM. *p < 0.05 versus WT was by Student's t test.

The Km values of GLUT1 for glucose is 1-3 mM [200, 201] which indicates high affinity for glucose and can perfectly explain glucose transport at 3 mM and constitutive insulin release. GLUT1 is normally the minority glucose transporter in mouse beta-cells, with GLUT2 being the main glucose transporter in rodents [95].

2.5.5 B-IDE-KO ISLETS SHOW INCREASED LEVELS OF GLUT1 AND DECREASED LEVELS OF GLUT2 IN THE PLASMA MEMBRANE

After observing increased GLUT1 mRNA, we decided further explore this by checking the protein levels of this transporter. For this purpose, we performed GLUT1 immunofluorescence in pancreata of WT and B-IDE-KO mice.

As predicted by qPCR, GLUT1 expression was highly increased in B-IDE-KO beta-cells, as shown by quantification of the fluorescence intensity in this cell type (**Figure 71**). This 50% increase in GLUT1 expression in B-IDE-KO might be responsible of the increase in insulin secretion at low glucose concentrations.

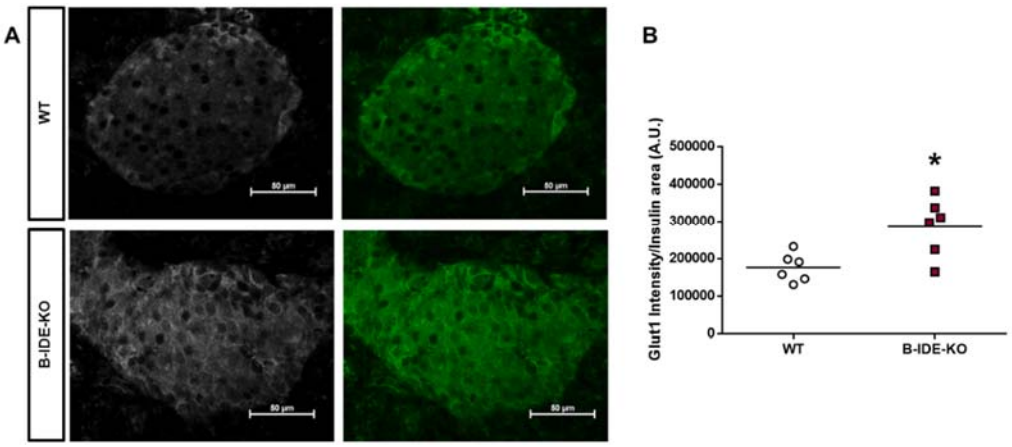

Figure 71: GLUT1 expression in B-IDE-KO mice islets. A. Representative images of GLUT1 immunofluorescence acquired by fluorescence microscopy with 40X objective in pancreas of WT and B-IDE-KO mice. **B.** Quantification of fluorescence intensity of GLUT1 measured in pancreatic beta-cells. n=6 WT; n=6 B-IDE-KO. Data are presented as mean ± SEM. *p< 0.05 versus WT by Student´s t test.

Impaired GSIS can be explained by an impairment in GLUT2 [29, 202-204], thus, we have detected GLUT2 in pancreas of WT and B-IDE-KO mice. These results show decreased GLUT2 levels in the plasma membrane of B-IDE-KO mice as can be observed in **Figure 72**.

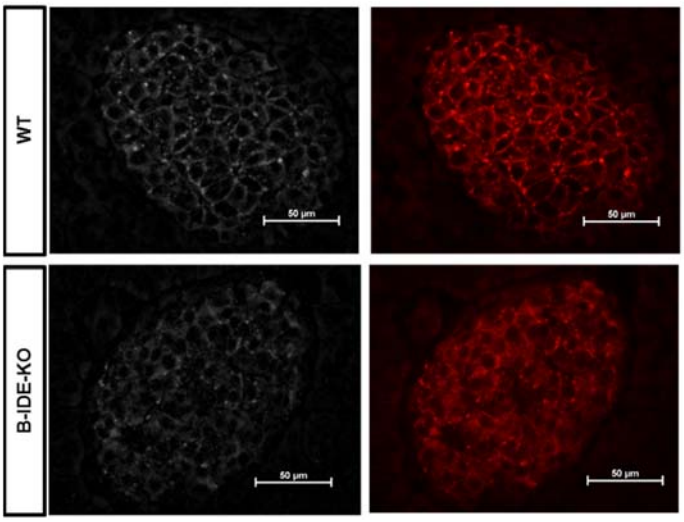

Figure 72: GLUT2 expression in B-IDE-KO mice islets. A. Representative images of GLUT2 immunofluorescence acquired by fluorescence microscopy with 40X objective in pancreas of WT and B-IDE-KO mice. n=6 WT; n=6 B-IDE-KO.

These results reinforce the idea that IDE may have a key role in the maturity of the beta-cell, since B-IDE-KO beta-cells showing several characteristics of beta-cell immaturity, such as the increase of GLUT1 [205] and decreased GLUT2 levels [72, 79-81]. This fact is of great relevance since it would suggest a new function never described for IDE in the regulation of glucose transport on beta-cells.

DISCUSSION

7. DISCUSSION

Diabetes mellitus is one of the most impactful pandemics of the 21st century. The global prevalence of diabetes among adults has risen from 4.7% in 1980 to 8.5% in 2014 [18]. Alarmingly, in 2016 it was estimated that diabetes was 7th leading cause of death in the world [19]. These disturbing statistics highlight the need to halt the spread of this pandemic, which is only possible by improving our knowledge of the disease at cellular and molecular levels.

Despite the great advances achieved in the last decades, there is still much to know about the complex mechanisms that underlie the development of diabetes mellitus. Moreover, much remains to be investigated about the molecular mechanisms that occur during the development of diabetes in the leading cells involved in this pathology: pancreatic beta-cells. In spite of being a cell type whose physiology has been extensively studied, there are still many unknowns about certain behaviors that it acquires in pathophysiological situations. One of the great current challenges is to modify beta-cell dysfunction developed in pathophysiological situations, such as T2DM.

Recent hypotheses have been proposed to explain beta-cell dysfunction in T2DM, like cell death [206, 207], de-differentiation [208, 209], trans-differentiation [210, 211] and loss of identity [73, 212]. Understanding molecular mechanisms underlying each of these processes will help to develop new strategies to recover beta-cell function.

According to the World Health Organization, there are three fundamental pillars for reducing the burden of T2DM: prevention, diagnosis and treatment. In this regard, insulin-degrading enzyme (IDE) has awakened a great level of interest as a potential therapeutic target in the treatment of T2DM patients. However, the

expression and role of IDE in beta-cells remains largely unknown. In this work, we have analyzed, for the first time, the expression of IDE in pancreatic islets, as well as the specific function of IDE in beta-cells, conducting studies in a wide range of rodent and human models and conditions. We have shed light on the importance of IDE in this cell type, raising the basic knowledge on beta-cell biology and highlighting its potential as a therapeutic target.

Differential IDE expression in pancreatic islet cells

As mentioned before, from many decades IDE was considered to be an attractive therapeutic target for the treatment of diabetes. This interest lies largely in the genetic associations observed between the IDE locus and the susceptibility to suffer T2DM and hyperglycemia [175-179] and in other hand because of the proteolytic activity of IDE on circulating insulin. Thus, many researchers have tried to inhibit IDE looking to prolong the levels of insulin after its secretion from the pancreas. Despite widespread interest in this topic, almost nothing was known about IDE expression levels in the cells most centrally involved in the pathogenesis of DM: endocrine pancreatic cells. Thanks to imaging techniques, we observed how IDE was expressed in all cells types of the pancreatic islet, both human and murine models, corroborating its ubiquitous distribution that has been previously described [154]. Nevertheless, we observe an unexpected fact: IDE is expressed in higher levels in alpha- than in beta-cells or in any other islet cell type. This could indicate that IDE plays a major role in alpha cells, since it is also described that IDE is able to degrade glucagon [151] although with less affinity than for insulin [150]. Glucagon release is decompensated in T2DM, where patients frequently present hyperglucagonemia [213, 214], so it is reasonable to think that IDE can play an important role in this cell type function. This discovery opens new avenues to the investigation of IDE in other pancreatic cell types, which also play fundamental roles in the regulation of glucose homeostasis.

Once the presence of IDE in the pancreatic beta-cell was established, we decided to observe if this expression was modulated in pathological conditions. Despite the knowledge and controversy generated by the role of IDE in T2DM, there is no publication that quantified IDE expression by immunostaining in any study model (animal or human tissue), neither under physiological nor pathophysiological conditions. In this work, we conducted the first comparative study of IDE protein levels in human pancreas from T2DM patients and control subjects, and even more relevant, comparing the type of antidiabetic treatment used, on OHAs treatment versus insulin-treated T2DM patients.

Initially, we corroborated several observations about the pancreata of diabetic patients: first, a decrease in the beta-cell area, which indicates that beta-cells have already passed the compensatory phase that occurs in early T2DM [206, 215], pointing to an advanced stage of the disease. Second, a significant increase in the number of alpha cells in the diabetic population. Some studies show that in advanced stages of T2DM in which there is a clear dysfunction of the beta-cell, both the mass and the function of the alpha-cells are increased [216]. And third, we observed a decrease in the beta- / alpha-cell ratio, characteristic of patients with T2DM [216, 217].

Once the morphology of the pancreas was characterized, we asked if IDE protein levels were differentially expressed in diabetic versus healthy humans. Surprisingly, we observed that IDE was decreased in patients treated with oral antidiabetics, and that this decrease was recovered at control levels in patients treated with insulin. There are many other papers that show contradictory IDE patterns in different tissues of diabetic patients. Some of these authors report increased IDE levels in plasma and human erythrocytes of T2DM patients, both in insulin- and non-insulin dependent patients [180] and [181]. In contrast, other

studies reported low IDE expression in other tissues from diabetic patients, such as adipocytes [182] and liver [184]. There is a single study in the literature that reports IDE levels in pancreatic islets of diabetic patients. Steneberg et al. showed decreased IDE levels in islets of T2DM patients [183]. However, it is difficult to compare these results with the data obtained in our research, since they do not provide information about the pharmacological therapy of these patients, which makes it difficult to interpret them. These controversial results are due to the differences between the tissues studied and the multifactorial role of IDE in each one, thus reflecting the need to deepen into cell-specific studies

It is important to highlight the fact that this study has been carried out in human pancreas which is a high valued tissue since it can only be obtained out of cadaveric donors. Steneberg et al. had previously shown data on IDE expression in T2DM islets. They showed by western-blot that IDE protein levels are decreased by 40% in whole islets of T2DM patients compared to controls [183]. These data would agree with our data in T2DM+OHAs population, but this study did not report the age, sex or treatment of these patients. Furthermore, their study was done in complete islet and not in beta-cells, which makes their results difficult to interpret. The most commonly used drug in this T2DM+OHAs population is metformin. Although main metformin target is liver insulin resistance [218], there is evidence that treatment with metformin positively affects the beta-cells, increasing their insulin content [219] and improving GSIS [220]. At this point we were wondering if it was metformin´s effect the one causing IDE expression reduction and then, impairing beta-cell function. This hypothesis was clarified with a different set of experiments in the second part of the thesis.

Regarding the data of patients treated with insulin, IDE levels are increased in respect to diabetic treated with OHAs, suggesting that insulin treatment could increase IDE expression. This finding is in agreement with the work of Pivorarova et al., showing in hepatocytes that insulin increases IDE activity [185].

Pursuing the hypothesis that hyperinsulinemia in patients treated with insulin is promoting upregulation of IDE levels in beta-cells, we confirmed this issue with two preclinical murine models of hyperinsulinemia, such as *db/db* mice and mice fed with high fat diet. Our studies support our previous hypothesis, since they showed that in both models IDE protein is significantly increased compared to controls. The results observed both in humans and in murine models suggested that insulin treatment stimulates elevated IDE protein levels.

In order to clearly attribute the effect of increasing IDE levels to insulin and not to other environmental factors, insulin was administered to immortalized beta-cells and pancreatic islets isolated from both rats and humans. In all these models it was confirmed that insulin exposure significantly increased the levels of IDE in pancreatic beta-cells, without affecting IDE levels in alpha-cells. These results are in agreement with those previously shown by Zhao and colleagues, where they reported that treatment of primary hippocampal neurons with insulin increased IDE protein levels by approximately 25% [221].

These facts reveal that IDE upregulation by high insulin may be part of a counter-regulatory islet adaptation to clear insulin in order to avoid this hyperinsulinemic microenvironment. This could be possible because insulin that is not cleared by liver and kidney is ultimately removed by other insulin-sensitive cells [152].

In conclusion, these findings confirm the modulation of IDE expression in pancreatic beta-cells in response to different stimuli, potentially in order to modify their function in a way that best preserves glycemic control. Our results suggest that the use of regulators of the expression or activity of IDE in the beta-cell are possible mechanisms to control insulin secretion.

Modulation of IDE activity in the beta-pancreatic cell: a new therapeutic target?

There are numerous published studies about the effect of IDE inhibition in animal models [149, 153, 165, 183, 186-193]. However, the ubiquity of this protein and its multifactorial role makes the analysis of these results a complicated task. Although the published literature about IDE and the associations described by several studies between IDE and the pathogenesis of T2DM [175-177, 179], its role in glucose homeostasis remains unresolved.

Some authors have proposed the transient inhibition of IDE as a possible treatment for T2DM, based on the assumption that these inhibitors would lengthen the half-life of insulin in circulation, enhancing their hypoglycemic action. This assumption, however, focuses only on the ability of IDE to degrade insulin, neglecting other potential functions for IDE in different tissues of the body.

More than six decades ago, the first IDE pharmacological inhibitor was reported [186]. Since then, new, more specific inhibitors of IDE activity with well-characterized molecular binding sites have been developed [149, 165, 187-191]. To the extent that we can generalize about experimental compounds with very different mechanisms of inhibition and varying or undetermined pharmacokinetic properties, most of these IDE inhibitors elicit changes in insulinemia, which over time leads to a deterioration in glucose tolerance. Another common feature is the assumption that changes in plasma insulin levels are only due to changes in clearance, and not in insulin production or secretion. None of the manuscripts describing these inhibitors investigated how IDE inhibition affects beta-cell function. That is why it was critical for us to assess how pharmacological inhibition of IDE affect the function of pancreatic beta-cells, including insulin production and secretion.

The primary function and key identity of pancreatic beta-cells is characterized by the secretion of insulin in response to glucose stimulus. Our investigations showed that IDE plays a key role on the function of beta-pancreatic cells, since we observed a common pattern in all our models both *in vitro* and *in vivo*: IDE inhibition leads to an abolishment of the glucose-stimulated insulin secretion.

We tested two different inhibitors for the action of IDE: 1,10-phenanthroline, a general inhibitor of metalloproteases [187]; and NTE-2, one of the most recent published IDE specific inhibitors [191]. The use of both in the INS1-E beta-cell line, and in rodent and human islets showed the same result: pharmacological inhibition of IDE resulted in GSIS impairment. It should be noted that this effect was reproducible both within an immortalized cell line and within freshly prepared pancreatic islets. Moreover, we showed for the first time, how IDE modulation affects human islets cell functions.

In these models, we are dealing with transient IDE inhibition, which led us to become interested in the question of what consequences would follow from stable reduction in IDE in beta-cells. Thus, we generated shRNA-IDE INS1-E cells. Interestingly, these cells also did not secrete insulin in response to glucose, notably, even though IDE protein levels were only partially decreased. This fact confirms our hypothesis that IDE plays a fundamental role in the pancreatic beta-cell, regulating insulin secretion. This finding is consistent with the decrease in insulin secretion associated with gene variations of the HHEX/IDE loci in humans [175, 222] and with the study of Steneberg et al., which described deficient GSIS in mice lacking globally IDE gene [183]. Of note, in the shRNA-IDE INS1-E cells we observed an increase in the intracellular insulin content after GSIS. Electron microscopy images showed that there was an increase in the amount of insulin granules in the cytoplasm, pointing to a delayed movement of the granules through the cytoplasm. This fact is consistent with previous data showing that impaired

GSIS caused by IDE ablation is associated with the polymerization of alpha-synuclein, a protein involved in the reorganization of cellular microtubules [183]. Depolymerization of microtubules is a limiting step for the GSIS, since its correct organization allows the transport of the insulin granules through the cytoplasm to reach the plasma membrane and be secreted [111] (**Figure 73**).

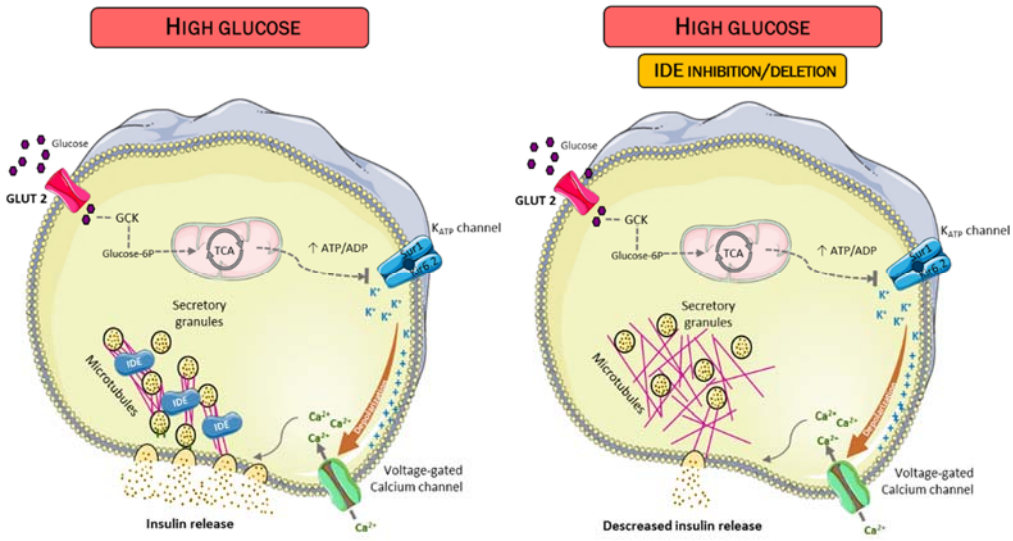

Figure 73: Proposed effect of IDE inhibition/deletion on an adult beta-cell.

Another plausible theory of this increased intracellular insulin in beta-cells due to IDE ablation is its possible proteolytic action in the degradation of intracellular insulin. To maintain a constant number of insulin-containing granules in β-cells, it has been reported that beta-cells are capable of degrading insulin granules that did not undergo exocytosis from intracellular space through processes of autophagy and/or crinophagy [223-225], introducing the secretory granules into the lysosomal compartment. It has been described that IDE has little proteolytic activity in the acidic environment [226], as is the case with the lysosomal compartment,

but its role in this process is unclear. More studies are needed in this regard to clarify the role of IDE in intracellular insulin degradation.

All these data support the idea that IDE is a key piece in the regulation of insulin secretion. Moreover, these results would seem to argue against the use of IDE inhibitors as a potential treatment for diabetes. However, to confirm these results, there is a need to check them in an intact animal, where beta-cells are in physiological conditions and interconnected with the rest of the tissues and organs.

The controversy of genetic ablation of insulin-degrading enzyme

Some authors have pursued, as we do, the hypothesis that a decrease in IDE levels or activity could represent a plausible treatment for T2DM. To investigate that hypothesis, some authors have previously published the metabolic phenotype resulting from whole-body *Ide* genetic ablation. Analyzing the literature on Total-IDE-KO model, the results are highly contradictory, even reaching opposite conclusions. Some authors showed that the total IDE ablation induces glucose intolerance, hyperinsulinemia and insulin resistance, attributed mainly to the role of IDE in the hepatic insulin clearance [192, 193]. On the other hand, other authors reported an opposite phenotype: Total-IDE-KO mice showed glucose intolerance but decreased plasma insulin levels [183]. These contradictory results observed in germ-line Total-IDE-KO mice make difficult to understand the precise role of IDE *in vivo*. In addition, since IDE is a ubiquitous protein, total knock-out models can only reveal overall metabolic results, potentially obscuring complex interactions and limiting the understanding of IDE's tissue-specific roles in glucose homeostasis.

Recently, Villa-Perez et al. reported the first tissue-specific IDE knockout mouse, the liver specific IDE-KO mice (L-IDE-KO) [153]. These mice showed

glucose intolerance and insulin resistance. Surprisingly, mice showed unchanged plasma insulin levels and intact hepatic insulin clearance as control mice, pointing out that IDE is not the main protein involved in hepatic insulin clearance, challenging the claims of previous studies. This study also reveals a new role for IDE in the etiology of hepatic insulin resistance, demonstrating the pleiotropic nature of IDE, beyond its degradative role, and revealing the importance of performing tissue-specific studies on IDE. For this reason, the generation of mice with beta-cell specific *Ide* deletion (B-IDE-KO mice) was necessary to accurately investigate its role *in vivo* in this cell type. By utilizing Cre-LoxP System, we have developed an ideal model to elucidate the role of IDE in beta-cell function.

Since IDE was discovered in 1949 [150], the function of IDE has been widely suggested to be limited to its proteolytic activity. The first reports on total genetic ablation of IDE confirmed this view [192, 193], since the animals showed hyperinsulinemia, hypothetically associated with the reduction of hepatic insulin clearance. Interestingly, beta-cell function was not examined. However, in recent years, subsequent studies have repealed this simplistic idea about the action of IDE. The pioneering study by Villa-Pérez et al. questioned the previous assumptions about hepatic function of IDE. Using a liver-specific model of IDE ablation (L-IDE-KO mouse), they concluded that IDE is not the main enzyme involved in hepatic insulin clearance, but it may be involved in the regulation of intracellular insulin receptor trafficking. [4]. Similarly, Steneberg et al. uncovered evidence that impaired insulin secretion observed from Total-IDE-KO was not caused by a proteolytic mechanism, if not by the relationship of IDE with scaffold proteins of the cytoplasm, which worsened vesicular trafficking [183]. These *in vivo* data unravel how IDE may be involved in many other cellular processes, independent of their proteolytic action.

Despite the controversy, all these previous models of *Ide* genetic ablation have in common that all mice exhibit impaired glucose homeostasis at some point. In contrast, B-IDE-KO mice do not fully recapitulate a deregulation in glucose homeostasis. This finding clearly demonstrates that the effects of IDE deletion on glucose homeostasis are not explained by its role in beta-cells on insulin secretion exclusively. Thus, our study reinforces the idea that IDE role in glucose homeostasis may be highly multifactorial in nature, hardly attributable to a single tissue, which deserve to be explored further.

In agreement with Steneberg and colleagues, and with all our previous *in vitro* results, B-IDE-KO mice show that IDE ablation in beta-cells causes a failure in the regulation of GSIS in pancreatic islets. Surprisingly, isolated islets of our model showed an effect never observed before in IDE ablation models: beta-cells present constitutive insulin secretion independently of glucose concentrations. This significant finding made us to reconsider the role of IDE in the beta-cells. These observations suggest a plausible explanation for the hyperinsulinemia reported in some studies of Total IDE-KO mice [192, 193]. These studies hypothesized that hyperinsulinemia is due to decreased hepatic catabolism of insulin, however, subsequently L-IDE-KO mice showed normal insulin levels [153], leaving unexplained the hyperinsulinemia of these models.

In our model, increased plasma C-peptide levels and sustained constitutive insulin secretion in B-IDE-KO islets led to hepatic insulin resistance, as we see reflected in the increased expression of gluconeogenic genes *Pck1* and *G6pc*. This increased hepatic gluconeogenesis may be the origin of mild glucose intolerance observed in B-IDE-KO.

After investigating potential mechanisms involved in this constitutive insulin secretion, we uncovered the novel finding that beta-cells from B-IDE-KO mice have decreased levels of the glucose transporter GLUT2 in the plasma membrane and

increased levels of GLUT1, a fact observed both by RT-qPCR and by IF. This unexpected result perfectly explains the secretion pattern observed in the islets of B-IDE-KO: GLUT1 is a high-affinity transporter that is operative at low glucose concentrations (between 1 and 3 mM glucose) [97]. This means that in the beta-cells of the B-IDE-KO mouse, GLUT1 transporter would be transporting glucose into the cell at low glucose concentrations and then stimulating insulin secretion (**Figure 74**). In addition, an impairment is observed in GSIS at high glucose levels. This fact is supported by the observation of decreased levels of the GLUT2 in the plasma membrane [29, 202-204], which is operative at high concentrations of glucose (15-20 mM glucose) [97].

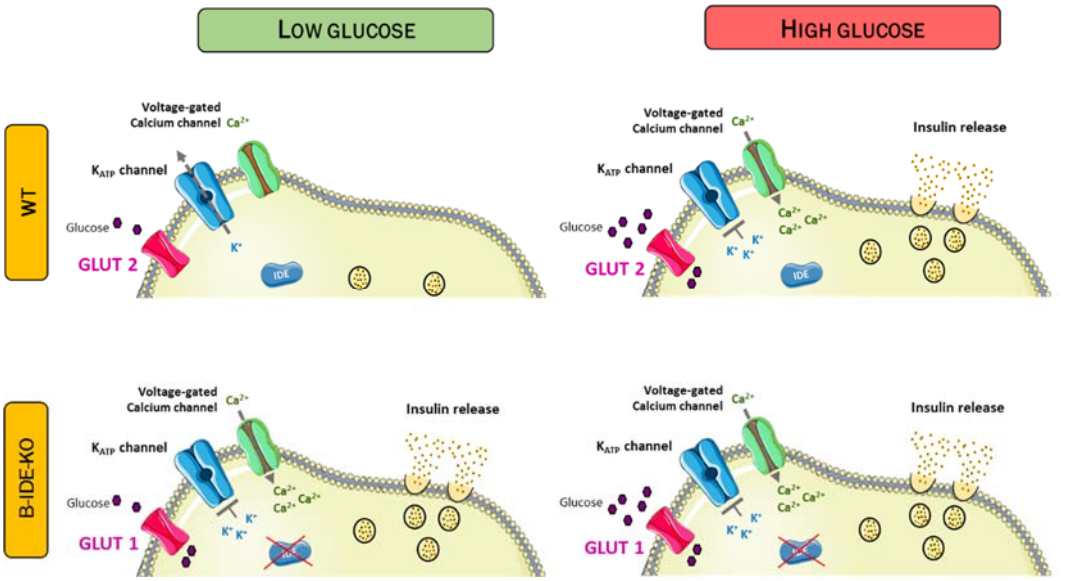

Figure 74: Proposed effect of IDE ablation since embryonic life on a beta-cell.

To this, we must add that many elements of the insulin secretory machinery are upregulated. There is an increased expression of glucokinase, potassium channel and calcium channel. This hyperactive secretory machinery could be an adaptive

mechanism of the beta-cell in order to increase insulin secretion in response to glucose stimulus.

Constitutive insulin secretion has been reported as a hallmark of beta-cell dysfunction and immaturity [71, 72, 79, 199]. It is well established that beta-cells in embryonic and neonatal stages secrete insulin constitutively [71, 72, 78, 79]. Curiously, it has been described that embryonic tissues have more GLUT1 than any other glucose transporter in their membrane. This is attributed to the fact that fetal cells present rapid growth, which requires high supply of energy, with glucose being one of the most important nutrients required to obtain ATP [205]. These results would also support the abnormal pattern of GLUT2 observed in the plasma membrane of our mice, which is described to be altered in immature and dysfunctional beta-cells [72, 79-81].

In the islets of B-IDE-KO mice, not only is the secretion of insulin affected, but there is also an increase in the secretion of proinsulin, as well as decreases in the *Pcsk1/3* and *Pcsk2* genes encoding proteases responsible for processing insulin from proinsulin. This situation results in the secretion of immature insulin granules into the intracellular space, another characteristic of immature beta-cells [79]. In addition, genetic analysis performed in the pancreatic islets of the B-IDE-KO mouse showed other markers that support beta-cell immaturity, such as decreased levels of *Ins2* and *Ucn3*, which are required to achieve mature beta-cells [71].

Looking at these results together, they seem to point to the conclusion that IDE could have a relevant role in the maturation process of the beta-cell. This would also explain the differences we observed between *in vitro* and *in vivo* studies. It is not the first time that IDE has been suggested to have a role in cell maturation. Kayalar and colleagues already showed how IDE inhibition prevented the correct differentiation of myoblasts [171]. In addition, Kuo et al. described how the IDE levels were developmentally regulated in various rat tissues [172]. Therefore, our

study reinforces the idea that IDE has multiple functions in addition to its proteolytic activity, which deserve to be further explored, especially in those tissues closely related to the pathogenesis of T2DM, such as pancreatic islet cells.

In summary, this study has helped to shed light on a largely unexplored topic: the relationship between IDE and the pancreatic beta-cell. We have confirmed that IDE is present in beta-cells and that its expression can be modulated by the effect of external pathophysiological stimuli. This work has clarified the importance of the role of IDE in pancreatic beta-cells: its inhibition both acute and chronic at a mature stage of adult beta-cells leads to impaired glucose-stimulated insulin secretion. However, its chronic ablation of beta-cells since embryonic life leads to immaturity, pointing to a new role of IDE in beta-cell development. These discoveries should encourage the broader scientific community to study proteins linked to T2DM in tissue-specific models. In light of this, we can also conclude that the inhibition of IDE in pancreatic beta-cells is not a good therapeutic approach for the treatment of T2DM, since acute and chronic deletion has several detrimental effects on their function.

CONCLUSIONS

8. CONCLUSIONS

1. IDE is expressed in beta- and alpha-cells of the pancreatic islet, both in humans and rodents, with increased expression in alpha- than in beta-cells. This result suggests a major role of IDE in alpha-cell function.

2. Pathophysiological conditions that are accompanied by hyperinsulinemia show increased IDE expression in pancreatic beta-cells, pointing out that IDE is involved in adaptive cellular mechanisms of beta-cells to the hyperinsulinemic environment.

3. Both acute and chronic inhibition of IDE in mature beta-cells leads to impaired glucose-stimulated insulin secretion, revealing that IDE plays a key role in beta-cell function.

4. Genetic ablation of *Ide* in pancreatic beta-cells in embryonic life leads to constitutive insulin secretion and beta-cell immaturity, pointing to a new role of IDE in beta-cell development.

5. IDE inhibition in pancreatic beta-cells is not a good therapeutic approach for the treatment of T2DM.

REFERENCES

9. REFERENCES

1. Röder, P.V., et al., *Pancreatic regulation of glucose homeostasis.* Experimental &Amp; Molecular Medicine, 2016. **48**: p. e219.
2. Lecavalier, L., et al., *Contributions of gluconeogenesis and glycogenolysis during glucose counterregulation in normal humans.* Am J Physiol, 1989. **256**(6 Pt 1): p. E844-51.
3. Freychet, L., et al., *Effect of intranasal glucagon on blood glucose levels in healthy subjects and hypoglycaemic patients with insulin-dependent diabetes.* Lancet, 1988. **1**(8599): p. 1364-6.
4. Khan, A.H. and J.E. Pessin, *Insulin regulation of glucose uptake: a complex interplay of intracellular signalling pathways.* Diabetologia, 2002. **45**(11): p. 1475-83.
5. Kohn, A.D., et al., *Expression of a constitutively active Akt Ser/Thr kinase in 3T3-L1 adipocytes stimulates glucose uptake and glucose transporter 4 translocation.* J Biol Chem, 1996. **271**(49): p. 31372-8.
6. Zisman, A., et al., *Targeted disruption of the glucose transporter 4 selectively in muscle causes insulin resistance and glucose intolerance.* Nat Med, 2000. **6**(8): p. 924-8.
7. Miller, T.B., Jr. and J. Larner, *Mechanism of control of hepatic glycogenesis by insulin.* J Biol Chem, 1973. **248**(10): p. 3483-8.
8. Akpan, J.O., R. Gardner, and S.R. Wagle, *Studies on the effects of insulin and acetylcholine on activation of glycogen synthase and on glycogenesis in hepatocytes isolated from normal fed rats.* Biochemical and Biophysical Research Communications, 1974. **61**(1): p. 222-229.
9. Walton, P.E. and T.D. Etherton, *Stimulation of lipogenesis by insulin in swine adipose tissue: antagonism by porcine growth hormone.* J Anim Sci, 1986. **62**(6): p. 1584-95.
10. Biolo, G., R.Y. Declan Fleming, and R.R. Wolfe, *Physiologic hyperinsulinemia stimulates protein synthesis and enhances transport of selected amino acids in human skeletal muscle.* J Clin Invest, 1995. **95**(2): p. 811-9.
11. Zimmet, P., K.G. Alberti, and J. Shaw, *Global and societal implications of the diabetes epidemic.* Nature, 2001. **414**(6865): p. 782-7.
12. *World Health Organization. (1999). Definition, diagnosis and classification of diabetes mellitus and its complications : report of a WHO consultation. Part 1, Diagnosis and classification of diabetes mellitus. Geneva : World Health Organization. .*
13. Amos, A.F., D.J. McCarty, and P. Zimmet, *The rising global burden of diabetes and its complications: estimates and projections to the year 2010.* Diabet Med, 1997. **14 Suppl 5**: p. S1-85.
14. *International Diabetes Federation Diabetes Atlas, 8th Edition*, IDF, Editor. 2017.

15. *World Health Organization Global Report On Diabetes 2016.* WHO, 2016.
16. Genuth, S., et al., *Follow-up report on the diagnosis of diabetes mellitus.* Diabetes Care, 2003. **26**(11): p. 3160-7.
17. Arnlov, J., et al., *Impact of BMI and the metabolic syndrome on the risk of diabetes in middle-aged men.* Diabetes Care, 2011. **34**(1): p. 61-5.
18. Sarwar, N., et al., *Diabetes mellitus, fasting blood glucose concentration, and risk of vascular disease: a collaborative meta-analysis of 102 prospective studies.* Lancet, 2010. **375**(9733): p. 2215-22.
19. *World Hearth Organization Mortality Database.* WHO, 2016.
20. *Economic Costs of Diabetes in the U.S. in 2017.* Diabetes Care, 2018. **41**(5): p. 917-928.
21. Eisenbarth, G.S., *Type I diabetes mellitus. A chronic autoimmune disease.* N Engl J Med, 1986. **314**(21): p. 1360-8.
22. Bach, J.F., *Insulin-dependent diabetes mellitus as an autoimmune disease.* Endocr Rev, 1994. **15**(4): p. 516-42.
23. Colledge, N.R., Walker, B. R., Ralston, S., & Davidson, S. (2010). Davidson's principles and practice of medicine. Edinburgh: Churchill Livingstone/Elsevier.
24. *Melmed S, Polonsky SK et al. Williams textbook of endocrinology. 12th edn Philadelphia: Elsevier/Saunders, 2011.*
25. Pociot, F. and M.F. McDermott, *Genetics of type 1 diabetes mellitus.* Genes Immun, 2002. **3**(5): p. 235-49.
26. You, W.P. and M. Henneberg, *Type 1 diabetes prevalence increasing globally and regionally: the role of natural selection and life expectancy at birth.* BMJ Open Diabetes Res Care, 2016. **4**(1): p. e000161.
27. Kahn, S.E., M.E. Cooper, and S. Del Prato, *Pathophysiology and treatment of type 2 diabetes: perspectives on the past, present, and future.* Lancet, 2014. **383**(9922): p. 1068-83.
28. Donath, M.Y. and P.A. Halban, *Decreased beta-cell mass in diabetes: significance, mechanisms and therapeutic implications.* Diabetologia, 2004. **47**(3): p. 581-589.
29. Unger, R.H., *Diabetic hyperglycemia: link to impaired glucose transport in pancreatic beta cells.* Science, 1991. **251**(4998): p. 1200-5.
30. Unger, R.H. and S. Grundy, *Hyperglycaemia as an inducer as well as a consequence of impaired islet cell function and insulin resistance: implications for the management of diabetes.* Diabetologia, 1985. **28**(3): p. 119-21.
31. Unger, R.H. and Y.T. Zhou, *Lipotoxicity of beta-cells in obesity and in other causes of fatty acid spillover.* Diabetes, 2001. **50 Suppl 1**: p. S118-21.
32. Robertson, R.P., et al., *Beta-cell glucose toxicity, lipotoxicity, and chronic oxidative stress in type 2 diabetes.* Diabetes, 2004. **53 Suppl 1**: p. S119-24.

33. Evans, J.L., et al., *Oxidative stress and stress-activated signaling pathways: a unifying hypothesis of type 2 diabetes.* Endocr Rev, 2002. **23**(5): p. 599-622.
34. Nordmann, T.M., et al., *The Role of Inflammation in β-cell Dedifferentiation.* Scientific Reports, 2017. **7**(1): p. 6285.
35. Boni-Schnetzler, M., et al., *Increased interleukin (IL)-1beta messenger ribonucleic acid expression in beta -cells of individuals with type 2 diabetes and regulation of IL-1beta in human islets by glucose and autostimulation.* J Clin Endocrinol Metab, 2008. **93**(10): p. 4065-74.
36. Jurgens, C.A., et al., *beta-cell loss and beta-cell apoptosis in human type 2 diabetes are related to islet amyloid deposition.* Am J Pathol, 2011. **178**(6): p. 2632-40.
37. Clark, A., et al., *Non-uniform distribution of islet amyloid in the pancreas of 'maturity-onset' diabetic patients.* Diabetologia, 1984. **27**(5): p. 527-8.
38. Marchetti, P., et al., *The endoplasmic reticulum in pancreatic beta cells of type 2 diabetes patients.* Diabetologia, 2007. **50**(12): p. 2486-94.
39. Oyadomari, S., E. Araki, and M. Mori, *Endoplasmic reticulum stress-mediated apoptosis in pancreatic beta-cells.* Apoptosis, 2002. **7**(4): p. 335-45.
40. Forouhi, N.G. and N.J. Wareham, *The EPIC-InterAct Study: A Study of the Interplay between Genetic and Lifestyle Behavioral Factors on the Risk of Type 2 Diabetes in European Populations.* Curr Nutr Rep, 2014. **3**(4): p. 355-363.
41. Pernicova, I. and M. Korbonits, *Metformin--mode of action and clinical implications for diabetes and cancer.* Nat Rev Endocrinol, 2014. **10**(3): p. 143-56.
42. Shaw, R.J., et al., *The kinase LKB1 mediates glucose homeostasis in liver and therapeutic effects of metformin.* Science, 2005. **310**(5754): p. 1642-6.
43. Czyzyk, A., et al., *Effect of biguanides on intestinal absorption of glucose.* Diabetes, 1968. **17**(8): p. 492-8.
44. McIntyre, H.D., et al., *Metformin increases insulin sensitivity and basal glucose clearance in type 2 (non-insulin dependent) diabetes mellitus.* Aust N Z J Med, 1991. **21**(5): p. 714-9.
45. *8. Pharmacologic Approaches to Glycemic Treatment: Standards of Medical Care in Diabetes-2018.* Diabetes Care, 2018. **41**(Suppl 1): p. S73-S85.
46. *Report of the Expert Committee on the Diagnosis and Classification of Diabetes Mellitus.* Diabetes Care, 1997. **20**(7): p. 1183-97.
47. Leslie, R.D., et al., *Diabetes at the crossroads: relevance of disease classification to pathophysiology and treatment.* Diabetologia, 2016. **59**(1): p. 13-20.
48. *2. Classification and Diagnosis of Diabetes: Standards of Medical Care in Diabetes-2018.* Diabetes Care, 2018. **41**(Suppl 1): p. S13-S27.

49. De Franco, E., et al., *The effect of early, comprehensive genomic testing on clinical care in neonatal diabetes: an international cohort study.* Lancet, 2015. **386**(9997): p. 957-63.
50. Husain, S. and E. Thrower, *Molecular and cellular regulation of pancreatic acinar cell function.* Curr Opin Gastroenterol, 2009. **25**(5): p. 466-71.
51. Dolensek, J., M.S. Rupnik, and A. Stozer, *Structural similarities and differences between the human and the mouse pancreas.* Islets, 2015. **7**(1): p. e1024405.
52. *OpenStax College. Anatomy & Physiology, Chapter 17.9 The Endocrine Pancreas.*
53. Saito, K., N. Iwama, and T. Takahashi, *Morphometrical analysis on topographical difference in size distribution, number and volume of islets in the human pancreas.* Tohoku J Exp Med, 1978. **124**(2): p. 177-86.
54. Goke, B., *Islet cell function: alpha and beta cells--partners towards normoglycaemia.* Int J Clin Pract Suppl, 2008(159): p. 2-7.
55. Cryer, P.E., *Minireview: Glucagon in the pathogenesis of hypoglycemia and hyperglycemia in diabetes.* Endocrinology, 2012. **153**(3): p. 1039-48.
56. Luft, R., S. Efendic, and T. Hokfelt, *Somatostatin--both hormone and neurotransmitter?* Diabetologia, 1978. **14**(1): p. 1-13.
57. Hauge-Evans, A.C., et al., *Somatostatin secreted by islet delta-cells fulfills multiple roles as a paracrine regulator of islet function.* Diabetes, 2009. **58**(2): p. 403-11.
58. Aragón, F., et al., *Pancreatic polypeptide regulates glucagon release through PPYR1 receptors expressed in mouse and human alpha-cells.* Biochimica et biophysica acta, 2015. **1850**(2): p. 343-351.
59. Katsuura, G., A. Asakawa, and A. Inui, *Roles of pancreatic polypeptide in regulation of food intake.* Peptides, 2002. **23**(2): p. 323-9.
60. Muller, T.D., et al., *Ghrelin.* Mol Metab, 2015. **4**(6): p. 437-60.
61. Cabrera, O., et al., *The unique cytoarchitecture of human pancreatic islets has implications for islet cell function.* Proc Natl Acad Sci U S A, 2006. **103**(7): p. 2334-9.
62. Steiner, D.J., et al., *Pancreatic islet plasticity: interspecies comparison of islet architecture and composition.* Islets, 2010. **2**(3): p. 135-45.
63. Jansson, L. and C. Hellerstrom, *Glucose-induced changes in pancreatic islet blood flow mediated by central nervous system.* Am J Physiol, 1986. **251**(6 Pt 1): p. E644-7.
64. Zorn, A.M. and J.M. Wells, *Vertebrate endoderm development and organ formation.* Annu Rev Cell Dev Biol, 2009. **25**: p. 221-51.
65. Gu, G., J. Dubauskaite, and D.A. Melton, *Direct evidence for the pancreatic lineage: NGN3+ cells are islet progenitors and are distinct from duct progenitors.* Development, 2002. **129**(10): p. 2447-57.
66. Gradwohl, G., et al., *neurogenin3 is required for the development of the four endocrine cell lineages of the pancreas.* Proc Natl Acad Sci U S A, 2000. **97**(4): p. 1607-11.

67. Desgraz, R. and P.L. Herrera, *Pancreatic neurogenin 3-expressing cells are unipotent islet precursors.* Development, 2009. **136**(21): p. 3567-74.
68. Pan, F.C. and M. Brissova, *Pancreas development in humans.* Curr Opin Endocrinol Diabetes Obes, 2014. **21**(2): p. 77-82.
69. Benitez, C.M., W.R. Goodyer, and S.K. Kim, *Deconstructing pancreas developmental biology.* Cold Spring Harb Perspect Biol, 2012. **4**(6).
70. Servitja, J.M. and J. Ferrer, *Transcriptional networks controlling pancreatic development and beta cell function.* Diabetologia, 2004. **47**(4): p. 597-613.
71. Blum, B., et al., *Functional beta-cell maturation is marked by an increased glucose threshold and by expression of urocortin 3.* Nat Biotechnol, 2012. **30**(3): p. 261-4.
72. Huang, C., et al., *Synaptotagmin 4 Regulates Pancreatic beta Cell Maturation by Modulating the Ca(2+) Sensitivity of Insulin Secretion Vesicles.* Dev Cell, 2018. **45**(3): p. 347-361 e5.
73. Brereton, M.F., M. Rohm, and F.M. Ashcroft, *beta-Cell dysfunction in diabetes: a crisis of identity?* Diabetes Obes Metab, 2016. **18 Suppl 1**: p. 102-9.
74. Pagliuca, F.W. and D.A. Melton, *How to make a functional β-cell.* Development, 2013. **140**(12): p. 2472-2483.
75. *Henquin J. C. (2005). Cell biology of insulin secretion, in Joslin's Diabetes Mellitus, eds Kahn C. R., Weir G. C., King G. L., Jacobson A. M., Moses A. C., Smith R. J., editors. (New York, NY: Lippincott Williams and Wilkins Ltd.), 83–10.*
76. Andrali, Sreenath S., et al., *Glucose regulation of insulin gene expression in pancreatic β-cells.* Biochemical Journal, 2008. **415**(1): p. 1-10.
77. Remedi, M.S. and C. Emfinger, *Pancreatic β-cell identity in diabetes.* Diabetes Obes Metab, 2016. **18 Suppl 1**(Suppl 1): p. 110-6.
78. Henquin, J.C. and M. Nenquin, *Immaturity of insulin secretion by pancreatic islets isolated from one human neonate.* J Diabetes Investig, 2018. **9**(2): p. 270-273.
79. Puri, S., et al., *Replication confers β cell immaturity.* Nature Communications, 2018. **9**(1): p. 485.
80. Kropp, P.A., et al., *Cooperative function of Pdx1 and Oc1 in multipotent pancreatic progenitors impacts postnatal islet maturation and adaptability.* Am J Physiol Endocrinol Metab, 2018. **314**(4): p. E308-E321.
81. Talchai, C., et al., *Pancreatic beta cell dedifferentiation as a mechanism of diabetic beta cell failure.* Cell, 2012. **150**(6): p. 1223-34.
82. Dhawan, S., et al., *DNA methylation directs functional maturation of pancreatic β cells.* The Journal of Clinical Investigation, 2015. **125**(7): p. 2851-2860.
83. Pullen, T.J., et al., *Identification of genes selectively disallowed in the pancreatic islet.* Islets, 2010. **2**(2): p. 89-95.
84. Poitout, V., et al., *Regulation of the insulin gene by glucose and fatty acids.* J Nutr, 2006. **136**(4): p. 873-6.

85. *Artner, I., and R. Stein. 2008. Transcriptional regulation of insulin gene expression. In Pancreatic Beta Cell in Health and Disease. Springer, Tokyo. 13–30.*
86. Vecchio, I., et al., *The Discovery of Insulin: An Important Milestone in the History of Medicine.* Frontiers in endocrinology, 2018. **9**: p. 613-613.
87. Banting, F.G., et al., *Pancreatic Extracts in the Treatment of Diabetes Mellitus.* Canadian Medical Association journal, 1922. **12**(3): p. 141-146.
88. Hutton, J.C., *Insulin secretory granule biogenesis and the proinsulin-processing endopeptidases.* Diabetologia, 1994. **37 Suppl 2**: p. S48-56.
89. *Lodish HF (1988) Transport of secretory and membrane glycoproteins from the rough endoplasmic reticulum to the Golgi. J Biol Chem 263:2107–2110.*
90. Tokarz, V.L., P.E. MacDonald, and A. Klip, *The cell biology of systemic insulin function.* J Cell Biol, 2018. **217**(7): p. 2273-2289.
91. Sando, H., J. Borg, and D.F. Steiner, *Studies on the secretion of newly synthesized proinsulin and insulin from isolated rat islets of Langerhans.* J Clin Invest, 1972. **51**(6): p. 1476-85.
92. Fu, Z., E.R. Gilbert, and D. Liu, *Regulation of insulin synthesis and secretion and pancreatic Beta-cell dysfunction in diabetes.* Curr Diabetes Rev, 2013. **9**(1): p. 25-53.
93. Kuhtreiber, W.M., et al., *Low levels of C-peptide have clinical significance for established Type 1 diabetes.* Diabet Med, 2015. **32**(10): p. 1346-53.
94. Ashcroft, F.M., et al., *Stimulus-secretion coupling in pancreatic beta cells.* J Cell Biochem, 1994. **55 Suppl**: p. 54-65.
95. McCulloch, L.J., et al., *GLUT2 (SLC2A2) is not the principal glucose transporter in human pancreatic beta cells: implications for understanding genetic association signals at this locus.* Mol Genet Metab, 2011. **104**(4): p. 648-53.
96. Heimberg, H., et al., *Differences in glucose transporter gene expression between rat pancreatic alpha- and beta-cells are correlated to differences in glucose transport but not in glucose utilization.* J Biol Chem, 1995. **270**(15): p. 8971-5.
97. Lachaal, M., R.A. Spangler, and C.Y. Jung, *High Km of GLUT-2 glucose transporter does not explain its role in insulin secretion.* Am J Physiol, 1993. **265**(6 Pt 1): p. E914-9.
98. De Vos, A., et al., *Human and rat beta cells differ in glucose transporter but not in glucokinase gene expression.* The Journal of Clinical Investigation, 1995. **96**(5): p. 2489-2495.
99. Ashcroft, F.M., D.E. Harrison, and S.J. Ashcroft, *Glucose induces closure of single potassium channels in isolated rat pancreatic beta-cells.* Nature, 1984. **312**(5993): p. 446-8.
100. Rorsman, P., M. Braun, and Q. Zhang, *Regulation of calcium in pancreatic alpha- and beta-cells in health and disease.* Cell Calcium, 2012. **51**(3-4): p. 300-8.

101. Rorsman, P. and F.M. Ashcroft, *Pancreatic beta-Cell Electrical Activity and Insulin Secretion: Of Mice and Men.* Physiol Rev, 2018. **98**(1): p. 117-214.
102. Rorsman, P. and E. Renstrom, *Insulin granule dynamics in pancreatic beta cells.* Diabetologia, 2003. **46**(8): p. 1029-45.
103. Dean, P.M., *Ultrastructural morphometry of the pancreatic -cell.* Diabetologia, 1973. **9**(2): p. 115-9.
104. Heaslip, A.T., et al., *Cytoskeletal dependence of insulin granule movement dynamics in INS-1 beta-cells in response to glucose.* PLoS One, 2014. **9**(10): p. e109082.
105. Vitale, M.L., E.P. Seward, and J.M. Trifaro, *Chromaffin cell cortical actin network dynamics control the size of the release-ready vesicle pool and the initial rate of exocytosis.* Neuron, 1995. **14**(2): p. 353-63.
106. Trifaro, J.M., et al., *Pathways that control cortical F-actin dynamics during secretion.* Neurochem Res, 2002. **27**(11): p. 1371-85.
107. van Obberghen, E., et al., *Dynamics of insulin release and microtubular-microfilamentous system. I. Effect of cytochalasin B.* J Clin Invest, 1973. **52**(5): p. 1041-51.
108. Orci, L., K.H. Gabbay, and W.J. Malaisse, *Pancreatic beta-cell web: its possible role in insulin secretion.* Science, 1972. **175**(4026): p. 1128-30.
109. Kanazawa, Y., et al., *The relationship of intracytoplasmic movement of beta granules to insulin release in monolayer-cultured pancreatic beta-cells.* Diabetes, 1980. **29**(12): p. 953-9.
110. Wang, Z. and D.C. Thurmond, *Mechanisms of biphasic insulin-granule exocytosis - roles of the cytoskeleton, small GTPases and SNARE proteins.* J Cell Sci, 2009. **122**(Pt 7): p. 893-903.
111. Zhu, X., et al., *Microtubules Negatively Regulate Insulin Secretion in Pancreatic beta Cells.* Dev Cell, 2015. **34**(6): p. 656-68.
112. Lacy, P.E., et al., *New hypothesis of insulin secretion.* Nature, 1968. **219**(5159): p. 1177-9.
113. Howell, S.L. and M. Tyhurst, *Interaction between insulin-storage granules and F-actin in vitro.* Biochem J, 1979. **178**(2): p. 367-71.
114. Kunii, M., et al., *Opposing roles for SNAP23 in secretion in exocrine and endocrine pancreatic cells.* J Cell Biol, 2016. **215**(1): p. 121-138.
115. Wheeler, M.B., et al., *Characterization of SNARE protein expression in beta cell lines and pancreatic islets.* Endocrinology, 1996. **137**(4): p. 1340-8.
116. Nagamatsu, S., et al., *Decreased expression of t-SNARE, syntaxin 1, and SNAP-25 in pancreatic beta-cells is involved in impaired insulin secretion from diabetic GK rat islets: restoration of decreased t-SNARE proteins improves impaired insulin secretion.* Diabetes, 1999. **48**(12): p. 2367-73.
117. Sollner, T., et al., *A protein assembly-disassembly pathway in vitro that may correspond to sequential steps of synaptic vesicle docking, activation, and fusion.* Cell, 1993. **75**(3): p. 409-18.
118. Susumu Seino, G.I.B., *Pancreatic Beta Cell in Health and Disease.* Springer, 2008.

119. Curry, D.L., L.L. Bennett, and G.M. Grodsky, *Dynamics of insulin secretion by the perfused rat pancreas.* Endocrinology, 1968. **83**(3): p. 572-84.
120. O'Connor, M.D., H. Landahl, and G.M. Grodsky, *Comparison of storage- and signal-limited models of pancreatic insulin secretion.* Am J Physiol, 1980. **238**(5): p. R378-89.
121. Grodsky, G.M., *A threshold distribution hypothesis for packet storage of insulin and its mathematical modeling.* J Clin Invest, 1972. **51**(8): p. 2047-59.
122. Ohara-Imaizumi, M., et al., *TIRF imaging of docking and fusion of single insulin granule motion in primary rat pancreatic beta-cells: different behaviour of granule motion between normal and Goto-Kakizaki diabetic rat beta-cells.* Biochem J, 2004. **381**(Pt 1): p. 13-8.
123. Petersen, M.C. and G.I. Shulman, *Mechanisms of Insulin Action and Insulin Resistance.* Physiol Rev, 2018. **98**(4): p. 2133-2223.
124. Haeusler, R.A., T.E. McGraw, and D. Accili, *Biochemical and cellular properties of insulin receptor signalling.* Nature Reviews Molecular Cell Biology, 2017. **19**: p. 31.
125. Leto, D. and A.R. Saltiel, *Regulation of glucose transport by insulin: traffic control of GLUT4.* Nature Reviews Molecular Cell Biology, 2012. **13**: p. 383.
126. Shepherd, P.R. and B.B. Kahn, *Glucose transporters and insulin action--implications for insulin resistance and diabetes mellitus.* N Engl J Med, 1999. **341**(4): p. 248-57.
127. Dimitriadis, G., et al., *Insulin effects in muscle and adipose tissue.* Diabetes Research and Clinical Practice, 2011. **93**: p. S52-S59.
128. Dimitriadis, G., et al., *The effects of insulin on transport and metabolism of glucose in skeletal muscle from hyperthyroid and hypothyroid rats.* Eur J Clin Invest, 1997. **27**(6): p. 475-83.
129. Liu, Z. and E.J. Barrett, *Human protein metabolism: its measurement and regulation.* Am J Physiol Endocrinol Metab, 2002. **283**(6): p. E1105-12.
130. Cherrington, A.D., D. Edgerton, and D.K. Sindelar, *The direct and indirect effects of insulin on hepatic glucose production in vivo.* Diabetologia, 1998. **41**(9): p. 987-996.
131. Rossetti, L. and A. Giaccari, *Relative contribution of glycogen synthesis and glycolysis to insulin-mediated glucose uptake. A dose-response euglycemic clamp study in normal and diabetic rats.* The Journal of clinical investigation, 1990. **85**(6): p. 1785-1792.
132. Roden, M., et al., *The roles of insulin and glucagon in the regulation of hepatic glycogen synthesis and turnover in humans.* The Journal of Clinical Investigation, 1996. **97**(3): p. 642-648.
133. Edgerton, D.S., et al., *Insulin's direct effects on the liver dominate the control of hepatic glucose production.* The Journal of Clinical Investigation, 2006. **116**(2): p. 521-527.
134. Claus, T.H. and S.J. Pilkis, *Regulation by insulin of gluconeogenesis in isolated rat hepatocytes.* Biochim Biophys Acta, 1976. **421**(2): p. 246-62.

135. Czech, M.P., et al., *Insulin signalling mechanisms for triacylglycerol storage.* Diabetologia, 2013. **56**(5): p. 949-64.
136. Leavens, K.F. and M.J. Birnbaum, *Insulin signaling to hepatic lipid metabolism in health and disease.* Critical Reviews in Biochemistry and Molecular Biology, 2011. **46**(3): p. 200-215.
137. Kraegen, E.W., et al., *Dose-response curves for in vivo insulin sensitivity in individual tissues in rats.* American Journal of Physiology-Endocrinology and Metabolism, 1985. **248**(3): p. E353-E362.
138. Coppack, S.W., J.N. Patel, and V.J. Lawrence, *Nutritional regulation of lipid metabolism in human adipose tissue.* Exp Clin Endocrinol Diabetes, 2001. **109 Suppl 2**: p. S202-14.
139. Dimitriadis, G., et al., *Glucose and lipid fluxes in the adipose tissue after meal ingestion in hyperthyroidism.* J Clin Endocrinol Metab, 2006. **91**(3): p. 1112-8.
140. Goodner, C.J., et al., *Insulin, glucagon, and glucose exhibit synchronous, sustained oscillations in fasting monkeys.* Science, 1977. **195**(4274): p. 177-9.
141. Porksen, N., et al., *Pulsatile insulin secretion accounts for 70% of total insulin secretion during fasting.* Am J Physiol, 1995. **269**(3 Pt 1): p. E478-88.
142. Meier, J.J., J.D. Veldhuis, and P.C. Butler, *Pulsatile Insulin Secretion Dictates Systemic Insulin Delivery by Regulating Hepatic Insulin Extraction In Humans.* Diabetes, 2005. **54**(6): p. 1649-1656.
143. Stevenson, R.W., A.D. Cherrington, and K.E. Steiner, *The relationship between plasma concentration and disappearance rate of immunoreactive insulin in the conscious dog.* Horm Metab Res, 1985. **17**(11): p. 551-3.
144. Zavaroni, I., et al., *Renal metabolism of C-peptide in man.* J Clin Endocrinol Metab, 1987. **65**(3): p. 494-8.
145. Van Cauter, E., et al., *Estimation of insulin secretion rates from C-peptide levels. Comparison of individual and standard kinetic parameters for C-peptide clearance.* Diabetes, 1992. **41**(3): p. 368-77.
146. Ader, M., et al., *Hepatic insulin clearance is the primary determinant of insulin sensitivity in the normal dog.* Obesity (Silver Spring), 2014. **22**(5): p. 1238-45.
147. Jung, S.H., et al., *Adapting to insulin resistance in obesity: role of insulin secretion and clearance.* Diabetologia, 2018. **61**(3): p. 681-687.
148. Rubenstein, A.H., et al., *The metabolism of proinsulin and insulin by the liver.* J Clin Invest, 1972. **51**(4): p. 912-21.
149. Duckworth, W.C., R.G. Bennett, and F.G. Hamel, *Insulin degradation: progress and potential.* Endocr Rev, 1998. **19**(5): p. 608-24.
150. Mirsky, I.A. and R.H. Broh-Kahn, *The inactivation of insulin by tissue extracts; the distribution and properties of insulin inactivating extracts.* Arch Biochem, 1949. **20**(1): p. 1-9.

151. Authier, F., B.I. Posner, and J.J. Bergeron, *Insulin-degrading enzyme.* Clin Invest Med, 1996. **19**(3): p. 149-60.
152. Duckworth, W.C., *Insulin degradation: mechanisms, products, and significance.* Endocr Rev, 1988. **9**(3): p. 319-45.
153. Villa-Perez, P., et al., *Liver-specific ablation of insulin-degrading enzyme causes hepatic insulin resistance and glucose intolerance, without affecting insulin clearance in mice.* Metabolism, 2018. **88**: p. 1-11.
154. Tang, W.J., *Targeting Insulin-Degrading Enzyme to Treat Type 2 Diabetes Mellitus.* Trends Endocrinol Metab, 2016. **27**(1): p. 24-34.
155. Shen, Y., et al., *Structures of human insulin-degrading enzyme reveal a new substrate recognition mechanism.* Nature, 2006. **443**(7113): p. 870-4.
156. McCord, L.A., et al., *Conformational states and recognition of amyloidogenic peptides of human insulin-degrading enzyme.* Proc Natl Acad Sci U S A, 2013. **110**(34): p. 13827-32.
157. Zhang, Z., et al., *Ensemble cryoEM elucidates the mechanism of insulin capture and degradation by human insulin degrading enzyme.* Elife, 2018. **7**.
158. Cronin, M.F., et al., *A Dynamical Model for Insulin Degrading Enzyme Conformational Transition between Closed and Open States.* Biophysical Journal, 2018. **114**(3, Supplement 1): p. 524a.
159. Farris, W., et al., *Alternative splicing of human insulin-degrading enzyme yields a novel isoform with a decreased ability to degrade insulin and amyloid beta-protein.* Biochemistry, 2005. **44**(17): p. 6513-25.
160. Hulse, R.E., L.A. Ralat, and T. Wei-Jen, *Structure, function, and regulation of insulin-degrading enzyme.* Vitamins and hormones, 2009. **80**: p. 635-648.
161. Shroyer, L.A. and P.T. Varandani, *Purification and characterization of a rat liver cytosol neutral thiol peptidase that degrades glucagon, insulin, and isolated insulin A and B chains.* Archives of Biochemistry and Biophysics, 1985. **236**(1): p. 205-219.
162. Suire, C.N., S. Lane, and M.A. Leissring, *Development and Characterization of Quantitative, High-Throughput-Compatible Assays for Proteolytic Degradation of Glucagon.* SLAS Discov, 2018. **23**(10): p. 1060-1069.
163. Pivovarova, O., et al., *Insulin-degrading enzyme: new therapeutic target for diabetes and Alzheimer's disease?* Ann Med, 2016. **48**(8): p. 614-624.
164. Malito, E., R.E. Hulse, and W.J. Tang, *Amyloid beta-degrading cryptidases: insulin degrading enzyme, presequence peptidase, and neprilysin.* Cell Mol Life Sci, 2008. **65**(16): p. 2574-85.
165. Maianti, J.P., et al., *Anti-diabetic activity of insulin-degrading enzyme inhibitors mediated by multiple hormones.* Nature, 2014. **511**(7507): p. 94-8.

166. Kupfer, S.R., E.M. Wilson, and F.S. French, *Androgen and glucocorticoid receptors interact with insulin degrading enzyme.* J Biol Chem, 1994. **269**(32): p. 20622-8.
167. Bennett, R.G., et al., *Insulin inhibition of the proteasome is dependent on degradation of insulin by insulin-degrading enzyme.* J Endocrinol, 2003. **177**(3): p. 399-405.
168. Udrisar, D.P., et al., *Androgen- and estrogen-dependent regulation of insulin-degrading enzyme in subcellular fractions of rat prostate and uterus.* Exp Biol Med (Maywood), 2005. **230**(7): p. 479-86.
169. Li, Q., M.A. Ali, and J.I. Cohen, *Insulin degrading enzyme is a cellular receptor mediating varicella-zoster virus infection and cell-to-cell spread.* Cell, 2006. **127**(2): p. 305-16.
170. Fernandez-Gamba, A., et al., *Insulin-degrading enzyme: structure-function relationship and its possible roles in health and disease.* Curr Pharm Des, 2009. **15**(31): p. 3644-55.
171. Kayalar, C. and W.T. Wong, *Metalloendoprotease inhibitors which block the differentiation of L6 myoblasts inhibit insulin degradation by the endogenous insulin-degrading enzyme.* J Biol Chem, 1989. **264**(15): p. 8928-34.
172. Kuo, W.L., A.G. Montag, and M.R. Rosner, *Insulin-degrading enzyme is differentially expressed and developmentally regulated in various rat tissues.* Endocrinology, 1993. **132**(2): p. 604-11.
173. Bulloj, A., et al., *Insulin-degrading enzyme sorting in exosomes: a secretory pathway for a key brain amyloid-beta degrading protease.* J Alzheimers Dis, 2010. **19**(1): p. 79-95.
174. Tamboli, I.Y., et al., *Statins promote the degradation of extracellular amyloid {beta}-peptide by microglia via stimulation of exosome-associated insulin-degrading enzyme (IDE) secretion.* J Biol Chem, 2010. **285**(48): p. 37405-14.
175. Pascoe, L., et al., *Common variants of the novel type 2 diabetes genes CDKAL1 and HHEX/IDE are associated with decreased pancreatic beta-cell function.* Diabetes, 2007. **56**(12): p. 3101-4.
176. Ghosh, S., et al., *The Finland-United States investigation of non-insulin-dependent diabetes mellitus genetics (FUSION) study. I. An autosomal genome scan for genes that predispose to type 2 diabetes.* Am J Hum Genet, 2000. **67**(5): p. 1174-85.
177. Sladek, R., et al., *A genome-wide association study identifies novel risk loci for type 2 diabetes.* Nature, 2007. **445**(7130): p. 881-5.
178. Flannick, J., et al., *Loss-of-function mutations in SLC30A8 protect against type 2 diabetes.* Nat Genet, 2014. **46**(4): p. 357-63.
179. Fakhrai-Rad, H., et al., *Insulin-degrading enzyme identified as a candidate diabetes susceptibility gene in GK rats.* Hum Mol Genet, 2000. **9**(14): p. 2149-58.

180. Standl, E. and H.J. Kolb, *Insulin degrading enzyme activity and insulin binding of erythrocytes in normal subjects and Type 2 (non-insulin-dependent) diabetic patients.* Diabetologia, 1984. **27**(1): p. 17-22.
181. Snehalatha, C., et al., *Immunoreactive insulin and insulin degrading enzymes in erythrocytes. A preliminary report.* J Assoc Physicians India, 1990. **38**(8): p. 558-61.
182. Fawcett, J., et al., *Insulin metabolism in human adipocytes from subcutaneous and visceral depots.* Biochemical and Biophysical Research Communications, 2010. **402**(4): p. 762-766.
183. Steneberg, P., et al., *The type 2 diabetes-associated gene ide is required for insulin secretion and suppression of alpha-synuclein levels in beta-cells.* Diabetes, 2013. **62**(6): p. 2004-14.
184. Pivovarova, O., et al., *Modulation of insulin degrading enzyme activity and liver cell proliferation.* Cell Cycle, 2015. **14**(14): p. 2293-300.
185. Pivovarova, O., et al., *Glucose inhibits the insulin-induced activation of the insulin-degrading enzyme in HepG2 cells.* Diabetologia, 2009. **52**(8): p. 1656-64.
186. Mirsky, I.A. and G. Perisutti, *Effect of insulinase-inhibitor on hypoglycemic action of insulin.* Science, 1955. **122**(3169): p. 559-60.
187. Bennett, R.G., F.G. Hamel, and W.C. Duckworth, *An insulin-degrading enzyme inhibitor decreases amylin degradation, increases amylin-induced cytotoxicity, and increases amyloid formation in insulinoma cell cultures.* Diabetes, 2003. **52**(9): p. 2315-20.
188. Leissring, M.A., et al., *Designed inhibitors of insulin-degrading enzyme regulate the catabolism and activity of insulin.* PLoS One, 2010. **5**(5): p. e10504.
189. Charton, J., et al., *Imidazole-derived 2-[N-carbamoylmethyl-alkylamino]acetic acids, substrate-dependent modulators of insulin-degrading enzyme in amyloid-beta hydrolysis.* Eur J Med Chem, 2014. **79**: p. 184-93.
190. Deprez-Poulain, R., et al., *Catalytic site inhibition of insulin-degrading enzyme by a small molecule induces glucose intolerance in mice.* Nat Commun, 2015. **6**: p. 8250.
191. Durham, T.B., et al., *Dual Exosite-binding Inhibitors of Insulin-degrading Enzyme Challenge Its Role as the Primary Mediator of Insulin Clearance in Vivo.* J Biol Chem, 2015. **290**(33): p. 20044-59.
192. Farris, W., et al., *Insulin-degrading enzyme regulates the levels of insulin, amyloid beta-protein, and the beta-amyloid precursor protein intracellular domain in vivo.* Proc Natl Acad Sci U S A, 2003. **100**(7): p. 4162-7.
193. Abdul-Hay, S.O., et al., *Deletion of insulin-degrading enzyme elicits antipodal, age-dependent effects on glucose and insulin tolerance.* PLoS One, 2011. **6**(6): p. e20818.

194. McLellan, M.A., N.A. Rosenthal, and A.R. Pinto, *Cre-loxP-Mediated Recombination: General Principles and Experimental Considerations.* Curr Protoc Mouse Biol, 2017. **7**(1): p. 1-12.
195. Herrera, P.L., L. Orci, and J.D. Vassalli, *Two transgenic approaches to define the cell lineages in endocrine pancreas development.* Mol Cell Endocrinol, 1998. **140**(1-2): p. 45-50.
196. *pGreenPuro™ shRNA Cloning and Expression Lentivector User Manual* S. Biosciencies, Editor 2008.
197. *National Center for Biotechnology Information. PubChem Substance Database; SID=24848008, https://pubchem.ncbi.nlm.nih.gov/substance/24848008.*, Jan. 7, 2019.
198. Moon, J.S. and K.C. Won, *Pancreatic alpha-Cell Dysfunction in Type 2 Diabetes: Old Kids on the Block.* Diabetes Metab J, 2015. **39**(1): p. 1-9.
199. Henquin, J.-C. and M. Nenquin, *Immaturity of insulin secretion by pancreatic islets isolated from one human neonate.* Journal of diabetes investigation, 2018. **9**(2): p. 270-273.
200. Wheeler, T.J. and P.C. Hinkle, *Kinetic properties of the reconstituted glucose transporter from human erythrocytes.* J Biol Chem, 1981. **256**(17): p. 8907-14.
201. Tal, M., et al., *Glucose transporter isotypes switch in T-antigen-transformed pancreatic β cells growing in culture and in mice*. Vol. 12. 1992. 422-32.
202. Thorens, B., et al., *The loss of GLUT2 expression by glucose-unresponsive beta cells of db/db mice is reversible and is induced by the diabetic environment.* J Clin Invest, 1992. **90**(1): p. 77-85.
203. Guillam, M.T., et al., *Early diabetes and abnormal postnatal pancreatic islet development in mice lacking Glut-2.* Nat Genet, 1997. **17**(3): p. 327-30.
204. Guillam, M.T., P. Dupraz, and B. Thorens, *Glucose uptake, utilization, and signaling in GLUT2-null islets.* Diabetes, 2000. **49**(9): p. 1485-91.
205. Maeda, Y., et al., *Glucose transporter gene expression in rat conceptus during early organogenesis and exposure to insulin-induced hypoglycemic serum.* Acta Diabetol, 1993. **30**(2): p. 73-8.
206. Butler, A.E., et al., *Beta-cell deficit and increased beta-cell apoptosis in humans with type 2 diabetes.* Diabetes, 2003. **52**(1): p. 102-10.
207. Tomita, T., *Apoptosis in pancreatic β-islet cells in Type 2 diabetes.* Bosn J Basic Med Sci, 2016. **16**(3): p. 162-79.
208. Dor, Y. and B. Glaser, *beta-cell dedifferentiation and type 2 diabetes.* N Engl J Med, 2013. **368**(6): p. 572-3.
209. Cinti, F., et al., *Evidence of beta-Cell Dedifferentiation in Human Type 2 Diabetes.* J Clin Endocrinol Metab, 2016. **101**(3): p. 1044-54.
210. Thorel, F., et al., *Conversion of adult pancreatic alpha-cells to beta-cells after extreme beta-cell loss.* Nature, 2010. **464**(7292): p. 1149-54.
211. Chera, S., et al., *Diabetes recovery by age-dependent conversion of pancreatic delta-cells into insulin producers.* Nature, 2014. **514**(7523): p. 503-7.

212. Hunter, C.S. and R.W. Stein, *Evidence for Loss in Identity, De-Differentiation, and Trans-Differentiation of Islet β-Cells in Type 2 Diabetes.* Front Genet, 2017. **8**: p. 35.
213. Reaven, G.M., et al., *Documentation of hyperglucagonemia throughout the day in nonobese and obese patients with noninsulin-dependent diabetes mellitus.* J Clin Endocrinol Metab, 1987. **64**(1): p. 106-10.
214. Wise, J.K., R. Hendler, and P. Felig, *Obesity: evidence of decreased secretion of glucagon.* Science, 1972. **178**(4060): p. 513-4.
215. Weir, G.C. and S. Bonner-Weir, *Five stages of evolving beta-cell dysfunction during progression to diabetes.* Diabetes, 2004. **53 Suppl 3**: p. S16-21.
216. Yoon, K.H., et al., *Selective beta-cell loss and alpha-cell expansion in patients with type 2 diabetes mellitus in Korea.* J Clin Endocrinol Metab, 2003. **88**(5): p. 2300-8.
217. Maclean, N. and R.F. Ogilvie, *Quantitative estimation of the pancreatic islet tissue in diabetic subjects.* Diabetes, 1955. **4**(5): p. 367-76.
218. Garabadu, D. and S. Krishnamurthy, *Metformin attenuates hepatic insulin resistance in type-2 diabetic rats through PI3K/Akt/GLUT-4 signalling independent to bicuculline-sensitive GABAA receptor stimulation.* Pharm Biol, 2017. **55**(1): p. 722-728.
219. Marselli, L., et al., *Pancreatic Islets from Type 2 Diabetic Patients Have Functional Defects and Increased Apoptosis That Are Ameliorated by Metformin.* The Journal of Clinical Endocrinology & Metabolism, 2004. **89**(11): p. 5535-5541.
220. Patane, G., et al., *Metformin restores insulin secretion altered by chronic exposure to free fatty acids or high glucose: a direct metformin effect on pancreatic beta-cells.* Diabetes, 2000. **49**(5): p. 735-40.
221. Zhao, L., et al., *Insulin-degrading enzyme as a downstream target of insulin receptor signaling cascade: implications for Alzheimer's disease intervention.* J Neurosci, 2004. **24**(49): p. 11120-6.
222. Grarup, N., et al., *Studies of association of variants near the HHEX, CDKN2A/B, and IGF2BP2 genes with type 2 diabetes and impaired insulin release in 10,705 Danish subjects: validation and extension of genome-wide association studies.* Diabetes, 2007. **56**(12): p. 3105-11.
223. Uchizono, Y., et al., *The balance between proinsulin biosynthesis and insulin secretion: where can imbalance lead?* Diabetes Obes Metab, 2007. **9 Suppl 2**: p. 56-66.
224. Schnell, A.H., I. Swenne, and L.A. Borg, *Lysosomes and pancreatic islet function. A quantitative estimation of crinophagy in the mouse pancreatic B-cell.* Cell Tissue Res, 1988. **252**(1): p. 9-15.
225. Orci, L., et al., *Insulin, not C-peptide (proinsulin), is present in crinophagic bodies of the pancreatic B-cell.* J Cell Biol, 1984. **98**(1): p. 222-8.
226. WC, D., *Insulin degrading enzyme.* The Handbook of Experimental Pharmacology. Springer-Verlag Press, Berlin, vol 92:143–165, 1990.